Functional Characteristics of Dental Pulp Mesenchymal Stem Cells

Yvonne Wai Yee Pang

A thesis submitted to University College London

for the degree of

DOCTOR OF ENGINEERING

February 2015

The Advanced Centre for Biochemical Engineering
Department of Biochemical Engineering
University College London
Bernard Katz Building
Gordon Street
London WC1H 0AH, UK

Declaration

'I, Yvonne Wai Yee Pang confirm that the work presented in this thesis is my own. Where information has been derived from other sources, I confirm that this has been indicated in the thesis.'

……………………………………………….

Abstract

Mesenchymal stem cells (MSCs) in many adult tissues provide cell sources to sustain tissue growth and/or repair *in vivo*, yet MSCs are mainly studied based on their *in vitro* characteristics. One emerging population of such MSCs are from dental pulp mesenchymal tissue, termed dental pulp stem cells (DPSCs). For instance, the continuously growing rodent incisor model has recently provided the first *in vivo* evidence that the *in vivo* identities of MSCs are of multiple origins including from perivascular niches. However, little is known about the molecular mechanisms underlying MSC response to injury *in vivo*, including that in the context of tooth repair. We therefore compared processes involved in recruiting stem cells during injury repair, particularly cell migration of pulp cells isolated from distinct anatomical locations. We found pulp cells from the region containing putative stem cells showed the highest migration capacity and their migration ability could be stimulated by activating Wnt activity *in vitro*. Furthermore, following *in vivo* tooth injury on transgenic mice, Wnt/β-catenin was also found up-regulated close to the injury site, possibly regulating injury repair via promoting perivascular-associated stem cell accumulation in close proximity to the injury site. In addition, analysis of a novel injury experimental model- the incisor tip, that undergoes constant attrition/repair through natural feeding, confirmed that this rapid incisal tip repair is also facilitated by perivascular stem cells, similar to other experimental injury models, but at a far more striking level. Thus, future work will utilise this novel model to investigate regulatory mechanisms including Wnt signalling in mediating mesenchymal tissue repair. Taken together, we demonstrated that the Wnt pathway may play a crucial role in regulating MSCs during incisor injury repair *in vitro* and *in vivo*. Also, the naturally existing "incisal tip niche" is potentially a unique model for new insights into mesenchymal tissue repair *in vivo*.

Acknowledgements

Firstly, I would like to thank my supervisors Professor Paul Sharpe and Dr. Ivan Wall for their patience in guiding and supporting me throughout my EngD. Thank you both for giving me the opportunity to work on this exciting project and for teaching me so much over the past 4 years. Special thanks to Dr. Andrea Mantesso for her encouragement and helping set up the initial stages of my project and my sincere thanks go to Professor Chris Mason for inspiring me to enter the field of regenerative medicine and for his continuing support and advice. Thank you to Professor Agi Grigoriadis for his cell culture guidance and to Dr. Isabelle Miletich for her invaluable practical tips while I worked in CFD2 and for letting me borrow your coplin jars and hybridization boxes to name but a few. I'd also like to thank Dr. Eileen Gentleman for her kind assistance with the Raman microspectroscopy work.

I wish to thank Angela and Rebecca for your wonderful friendship and never failing to put a smile on my face whenever I pass the office, and also for putting up with my countless requests for colour printing and for all those tasty biscuits! Special thanks to Dr. Chris Healy, Dr. Alasdair Edgar, Martin Chaperlin and Alex Huhn for their great technical support. My heartfelt thanks go to Dr. Wenny An, Dr. Ana Angelova and Dr. Tian Yu, your continuous encouragement has been invaluable and I hope that I will become great researchers as you all are.

To all present and past CFD2 members: Samantha, Abi, Mona, Maiko, Katsu, Felipe, Lucyene, Sandra, Finn, Doris, Long Long, Abbas, Sarah and Thantrira, thank you for helping me at various stages of my project and making the lab a happier place to work. To my write up buddies Lara, Sana and Dalea I can finally join you in post-thesis life. Thank you to John, Leanne, Owen and Iwan with whom I've shared this EngD journey with as well as the Silverstone racetrack while running a half marathon. Go Team Regenmed!

I am immensely grateful to Nish and Jif who have been sisters to me since joining CFD and have supported me every step of the way. I cannot thank you both enough and hope we can have a reunion soon? Thank you to Lucy and Mel for keeping me sane and for listening to me talk about dental stem cells and growing teeth during our monthly dinners.

Thank you to the EPSRC and the UK Stem Cell Foundation for funding my project, and to the KCL Dental Institute and UCL Doctoral School for funding my attendance to some unforgettable conferences including the TMD in Berlin, ISSCR in Japan and ECI in San Diego.

My warmest thank you goes to Edd, I am forever indebted to you for your unwavering support throughout this EngD journey that we have shared. Your love, friendship and belief in me have made these past few years so much easier and I couldn't have done it without you.

I am most grateful to my parents for their great sacrifices in providing me with so many opportunities in my life and for their endless patience, support and love. Thank you for putting up with a stressed out daughter and thank you to my brother who has always been there for me and it is to my family that I dedicate this thesis.

Table of contents

List of figures

List of tables

List of abbreviations

αMEM	alpha Minimum Essential Medium
αSMA	alpha smooth muscle actin
APC	Adenomatous polyposis coli
ASC	Adult stem cell
AXIN2	Axis inhibition protein 2
BATGAL	β-catenin activated transgene β-galactosidase
BBR	Boehringer blocking reagent
BCIP	5-Bromo-4-chloro-3-indolyl-phosphate
BLASTN	Basic local assignment search tool for nucleotides
BM	Bone marrow
BMMSC	Bone marrow mesenchymal stem cell
BMP	Bone morphogenetic protein
BrdU	Bromodeoxyuridine
BSA	Bovine serum albumin
BSP	Bonesialoprotein
CAP	Cementum-derived attachment protein
CBFA1	Core-binding factor alpha 1
CCR	Chemokine (C-C motif) receptor
CFU-Fs	Colony forming unit fibroblasts
CK1	Casein kinase I
CL	Cervical loop
c-MET	Mesenchymal-epithelial transition factor
c-myc	Myelocytomatosis viral oncogene homolog
Cre	Cre recombinase
CXCR	C-X-C chemokine receptor

DEPC	Diethyl pyrocarbonate
DFSC	Dental follicle stem cells
DIG	Digoxygenin
Dkk	Dickopf
DMSO	Dimethyl sulfoxide
DPSC	Dental pulp stem cell
DSH	Dishevelled
DSPP	Dentine sialophosphoprotein
E	Embryonic day
ECM	Extracellular matrix
ECM	Extracellular matrix
EDTA	Ethylenediaminetetraacetic acid
ERM	Epithelial rests of Malassez
ERT	Estrogen receptor hormone-binding domain tamoxifen
ESC	Embryonic stem cell
FACS	Fluorescence activated cell sorting
FBS	Fetal bovine serum
FGF	Fibroblast growth factor
FZD	Frizzled
GFAP	Glial fibrillary acidic protein
GSC	Gingival stem cells
GSK3β	Glycogen synthase Kinase 3 beta
GvHD	Graft vs host disease
H&E	Haematoxylin and Eosin
HA/TCP	Hydroxyapatite /tricalcium phosphate
HERS	Hertwig's epithelial root sheath
HSC	Hematopoeitic stem cell

IB	Incisor body
IEE	Inner enamel epithelium
IGF-2	Insulin growth factor-2
IL-2	Interleukin-2
IMS	Industrial methylated spirit
iPSC	Induced pluripotent stem cell
Klf4	Krueppel-like factor 4
LB	Luria-Bertani
LDL	Low density lipoprotein
LEF	Lymphoid enhancing factor
LRC	Label retaining cells
LRP	LDL receptor related protein
MABT	Maleic acid buffer containing Tween 20
MCP-1	monocyte chemotactic protein-1
MSC	Mesenchymal stem cell
MTT	3-(4,5-Dimethylthiazol-2-yl)-2,5-Diphenyltetrazolium Bromide
NBT	4-nitro blue tetrazolium chloride
NCBI	National centre for biotechnology information
NG2	Neural/glial antigen 2
NGF	Nerve growth factor
NK	Natural killer
NOD	Non-obese diabetic
NTMT	NaCl +Tris-HCl + Magnesium chloride + Tween buffer
OCN	Osteocalcin
OCT	Optimal cutting temperature
OCT3/4	Octomer binding
OEE	Outer enamel epithelium

P	Postnatal day
PDFGβ	Platelet derived growth factor beta
PDGF	Platelet derived growth factor
PDGFR	Platelet derived growth factor receptor
PDL	Periodontal ligament
PDLSC	Periodontal ligament stem cells
PFA	Paraformaldehyde
PTC1	Patched homolog 1
R26R	Rosa 26 R
RT	Room temperature
SC	Stem cell
SCAP	Stem cells from the apical papilla
SCID	Severe combined immunodeficiency
SDF	Stromal-derived factor
SEM	Standard error of the mean
SHED	Stem cells from human exfoliated deciduous teeth
Shh	Sonic hedgehog
SOX2	Sex determining region Y-box2
Spry	Sprouty
SSC	saline-sodium citrate
TA	Transit amplifying
TCF	T-cell factor
TGFβ	Transforming growth factor beta
TNF	Tumour necrosis factor
TOPGAL	TCF optimal promoter β-galactosidase
VEGF	Vascular epidermal growth factor
WNT	Wingless-int

1. Introduction

1.1 Tooth development

1.1.1 The dental pulp and the structure of the tooth

The tooth is an organ that can be broadly divided into two segments; the crown, which projects into the oral cavity and is encased by a protective layer of enamel, and the root, which is embedded in the alveolar bone of the jaw. Dentine, which forms the majority of the tooth mainly consists of the mineral hydroxylapatite and is produced by odontoblasts that are derived from neural-crest- (ecto) mesenchyme cells. The dental pulp is the soft, fibrous connective tissue that lies within the central cavity of the tooth and is enclosed by the dentine. This crucial tissue maintains tooth vitality by supplying nutrients via blood vessels and feeling via sensory nerve fibres. Importantly, the pulp tissue is also a reservoir of dentine-producing odontoblasts that line the pulp-dentine border as a layer of columnar-shaped, polarised cells capable of dentine-matrix deposition under both physiological and pathological conditions (Goldberg and Smith, 2004). At the root, the continuous layer of dentine is covered by cementum and the periodontal ligament (PDL) fibres support and connect the tooth to the alveolar bones (Figure 1.1). All of the tissues that surround and support the tooth are collectively termed the periodontium (Young, 2006)
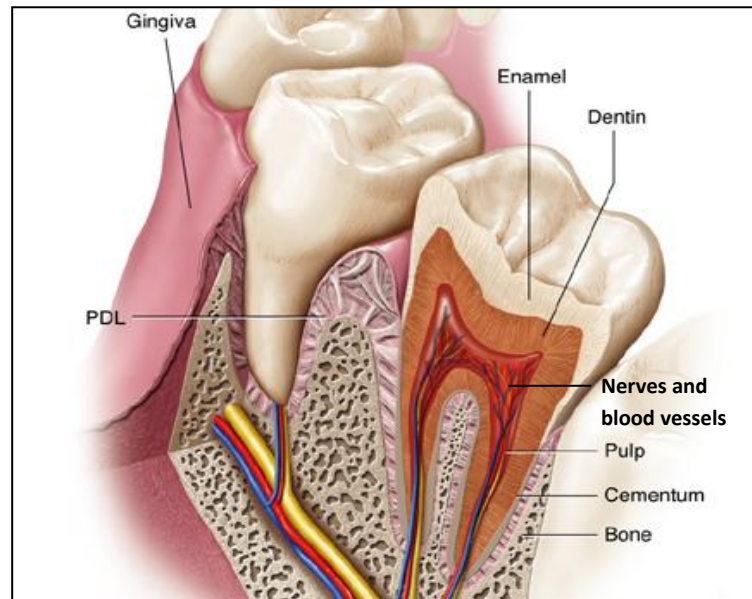
Figure 1.1 The tooth structure
The odontoblasts are dentine-producing cells housed within the dental pulp tissue that occupies the central cavity of the tooth and is protected by the surrounding layer of dentine. At the crown, enamel covers the dentine while cementum covers the root part of the dentine and allows periodontal ligament (PDL) attachment to secure the teeth to the alveolar bones (Image adapted from Cate, 1998).

1.1.2 Tooth development

Tooth development or odontogenesis involves a series of tightly regulated, sequential epithelial and mesenchymal interactions during early embryogenesis (Thesleff and Nieminen, 1996). The resulting ectodermal organ, the tooth, is a complex structure that consists of two specialised hard tissues, including the enamel which is the hardest substance in the human body, and dentine which forms part of the soft-hard tissue interface at the root, which anchors to the bone via the periodontal ligament complex. Its development is analogous to other ectodermal structures such as hair, skin, sweat glands and salivary glands (Pispa and Thesleff, 2003) and forms from the reiterative crosstalk between the odontogenic oral epithelium, that gives rise to the enamel-forming ameloblasts, and the underlying cranial neural crest-derived mesenchymal cells that form

the rest of the dental tissues, including the dental pulp, dentine-producing odontoblasts and periodontal ligament (Tucker and Sharpe, 2004).

Specification of the dental field where the tooth later develops occurs prior to the first morphological indication of tooth development, a local thickening of the oral epithelium (Neubuser et al., 1997). The resulting thickened dental epithelium termed the dental lamina occurs at approximately embryonic day E11.5 in mice and at approximately 7 weeks into human embryonic development. Subsequent invagination into the underlying mesenchyme results in an epithelial "bud" while the surrounding mesenchyme simultaneously condenses around it (E12.5-E13.5-bud stage). Further invagination and folding of the epithelium around the condensing mesenchyme, leads to the formation of a "cap" structure (E14-cap stage). Accompanying this process is the development of the enamel knot transient signalling centre which appears at the tip of the late bud and marks the onset of tooth crown development and determination of tooth shape. At this stage, the peripheral cells of the dental papilla and those surrounding the enamel organ proliferate to form the dental follicle or sac (Avery, 2001). The development of a "bell" shaped tooth germ then follows at E16 (bell stage) and eventually the invaginated epithelium completely encloses the condensed mesenchyme, referred to as the "dental papilla" (Miletich and Sharpe, 2003). At the late bell stage (E18), cyto-differentiation occurs where the epithelia-derived ameloblasts and mesenchyme-derived odontoblasts differentiate terminally along the epithelium-mesenchymal interface and deposit enamel and dentine, respectively (Thesleff and Nieminen, 1996; Tucker and Sharpe, 2004; Zhang et al., 2005b). It is from the dental papilla in which the future dental pulp tissue arises and becomes richly vascularised during the bell stage to deliver nutrition and oxygen to support the tooth-forming cells (Avery, 2001; Nanci, 2008) (Figure 1.2 A and B).
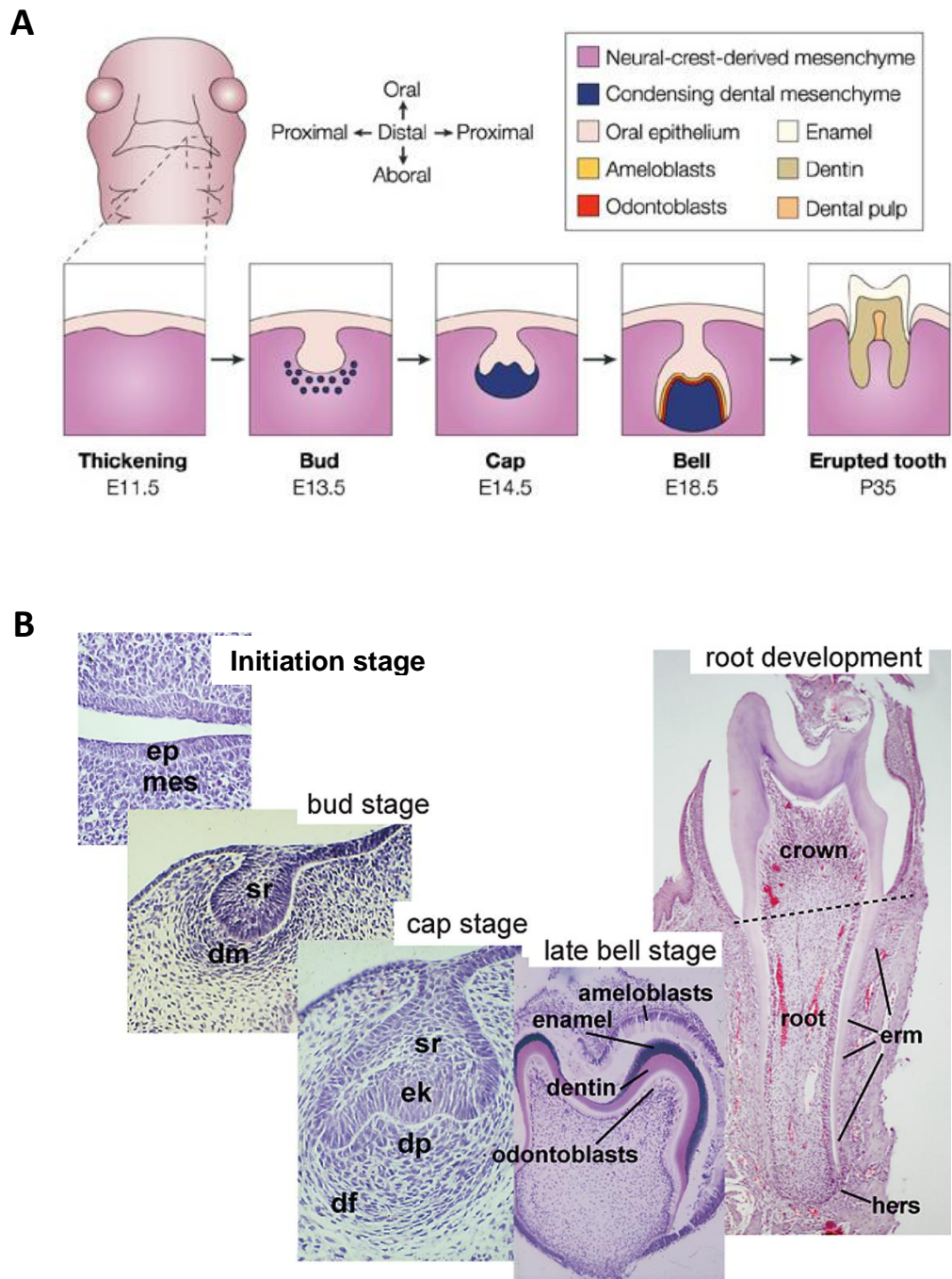
Figure 1.2 Tooth morphogenesis stages

A: Frontal view of an embryonic head at E11.5. The enlargement of the boxed region represents the mandibular molar site of development and the stages of tooth development are indicated following the arrows. The tooth germ is formed from the oral epithelium and neural-crest-derived mesenchyme (Tucker and Sharpe, 2004). B: Important stages of tooth development are shown histologically. The initial stages of development focus on crown formation. Root development is initiated only once this has been accomplished. At the bell stage, the epithelium-derived ameloblasts and odontoblasts originating from the mesenchyme deposit the enamel and dentine, respectively. At the root, ameloblasts and enamel are missing which is covered instead by the softer dentin and cementum. Abbreviations: Ep: epithelium, mes: mesenchyme, sr: stellate reticulum, dm: dental mesenchyme, dp: dental papilla, df: dental follicle, ek: enamel knot; erm: epithelial cell rests of malassez, hers: hertwig's epithelial root sheath (adapted from (Thesleff and Tummers, 2008)).

During the cap and bell stages, the leading edge of the invaginating epithelial cells enveloping the underlying dental mesenchyme is known as the cervical loop, with the cells located at the dental papilla-epithelium interface termed the inner enamel epithelium (IEE) and those facing the dental follicle termed the outer enamel epithelium (OEE). In humans, when crown formation is almost completed, the IEE and OEE undergo proliferation from the cervical loop of the enamel organ to form a double layer of cells known as Hertwig's epithelial root sheath (HERS) (Nanci, 2008). HERS acts as a structural divider at this point where the dental papilla lies within the bell shaped tooth germ while the dental follicle consists of the rest of the surrounding neural crest-derived mesenchyme. Under the guidance of HERS, tooth root development commences. Though HERS is crucial to the development of the tooth roots, uncertainty remains over its specific roles (Diekwisch, 2001; Huang and Chai, 2012; Zeichner-David et al., 2003). It appears that HERS participates along multiple stages during root development including the establishment of root number, cementogenesis, PDL formation and dentinogenesis of the root (Huang and Chai, 2012). One striking feature of HERS in mammals is their transient nature. After inducing the dental papilla, cells adjacent to the IEE become odontoblasts and initiate root dentine formation, the HERS structure becomes "perforated" allowing the mesenchymal dental follicle cells to penetrate into the epithelial layer and invade the newly generated root dentine surface (Diekwisch, 2001). As the root elongates, more dental follicle cells invade through HERS onto the root surface to form the cementoblasts and generate the cementum. Eventually, HERS disintegrates and the remnants of this transient structure become known as the epithelial rests of Malassez (ERM) (Luan et al., 2006a).

To perform its physiological function, the teeth need to establish occlusal contacts with opposing teeth, which is fulfilled in the final stage of tooth development, eruption into the oral cavity. Following root formation, this process begins with movement in the axial direction until the occlusal surface of the tooth is parallel to the occlusal plane of the

mouth. At this point, the ameloblasts are still covering the enamel and reduced enamel epithelium, which are the remnants of the enamel organs (Nanci, 2008). When the crown passes through the overlaying bone and approaches the soft tissue, the reduced enamel epithelium and oral epithelium combine to form a dense mass of epithelial cells where the central cells within the mass collapse to form an epithelial channel for the tooth to erupt. During eruption, the cells of the reduced epithelium degenerate and as the enamel becomes exposed, the ameloblasts are lost forever, while the dentine-producing odontoblasts remain on the periphery of the dental pulp to support this crucial tissue located in the tooth core that provides and maintains tooth vitality throughout life (Nanci, 2008).

Tooth development is evidently an intricate physiological process thus, not surprisingly requires the orchestration of many different signalling pathways. Paracrine signalling molecules belonging to several conserved families mediate these dynamic interactions and are used reiteratively as tooth morphogenesis progresses. These include the Transforming growth factor β (TGFβ), Fibroblast growth factor (FGF), Hedgehog, Wnt and Tumour Necrosis Factor (TNF) family of proteins (Thesleff, 2003). Other modulators of these signalling pathways such as inhibitors of BMPs (Follistatin and Ectodin/Sostdc1) and FGFs (such as Sprouty) are also required for the correct development of tooth shape, number and the production of optimal hard tissue, therefore highlighting the significance of regulatory control during odontogenesis (Thesleff and Tummers, 2009).

1.1.3 The human and mouse dentition

The mouse dentition is very much a simplification of the human form (Figure 1.3). The main difference is that in mice, only two different tooth types exists: the incisors and the molars, which are separated by a toothless gap known as the diastema in both jaws (Tucker and Sharpe, 2004). Humans on the other hand have additional canine and premolar teeth as well as a second dentition, meaning that they possess a set of deciduous teeth that are replaced by a permanent set upon adulthood. Nevertheless, the mouse dentition is a valuable model to study odontogenesis since it contains unique, continuously growing incisor teeth that undergo constant remodelling, thus allows all stages of odontogenesis including amelogenesis and dentinogenesis to be examined when observing a single tooth from the apical to the incisal end (Harada and Ohshima, 2004; Ohshima et al., 2005).
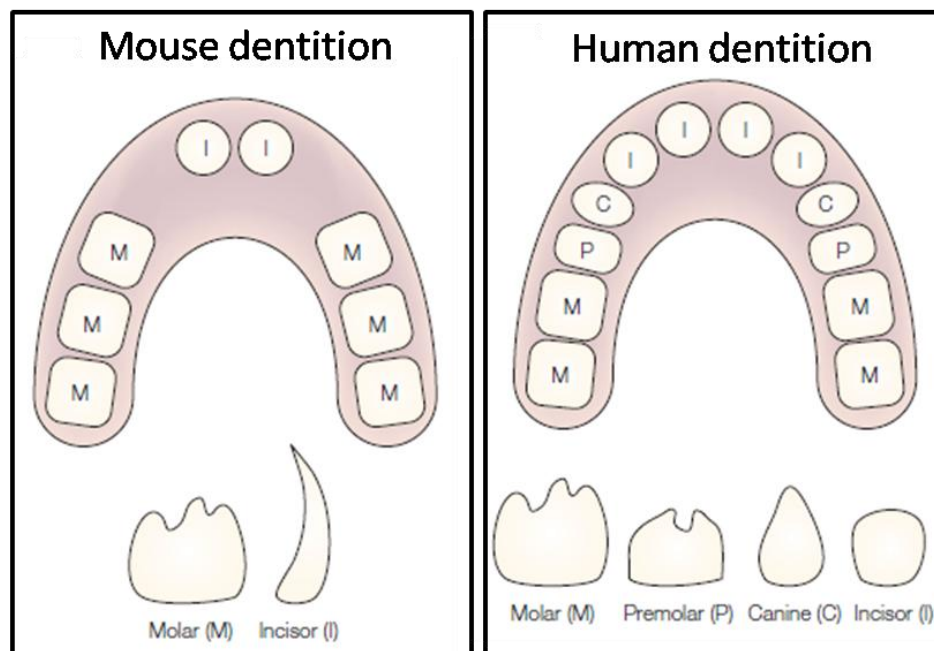
Figure 1.3 Schematic representation of the mouse and human dentition
In mice, the incisors and molars are separated by a gap known as the diastema. The human dentition is much more complex with 4 different types of teeth where canines and premolar teeth are present unlike in mice (adapted from (Tucker and Sharpe, 2004)).

1.1.4 The continuously growing rodent incisor

In common with other rodents such as rats, rabbits and guinea pigs, mice have 2 sets of continuously growing maxillary and mandibular incisors. Its development is initiated at E12, a little later than the molars, which begin developing from the oral ectoderm at E11.5 (Neubüser et al., 1997). At early stages, incisor and molar development are identical, however upon reaching the cap stage, the incisor tooth bud rotates anteroposteriorly resulting in a horizontal alignment to the long axis of the mandible (Figure 1.4). As development progresses to the bell stage (E16), the ameloblast-producing labial (facing the lip) epithelium elongates further than the lingual (facing the tongue) epithelium to form a distinctive structure termed the "cervical loop". This is the junctional zone where the inner enamel epithelium meets the external enamel epithelium at the edge of the enamel organ (Nanci, 2008)
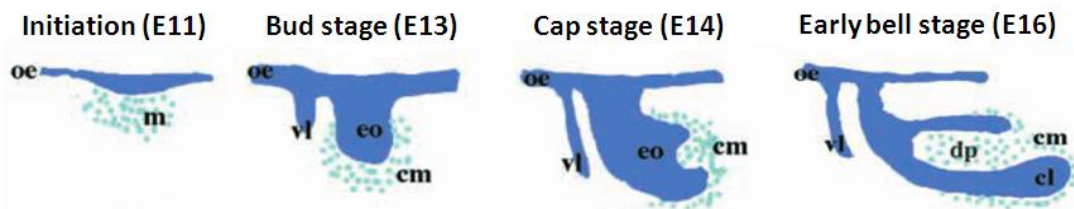
Figure 1.4 A schematic of mouse incisor development

Initiation of the incisor occurs at E11 followed by the bud (E13), cap (E14) and early bell stage (E16). The initial stages of morphogenesis are similar in all teeth. In comparison to molar tooth development, the incisors differs at E14 (cap stage) where the developing germ rotates anteroposteriorly becoming parallel to the long axis of the incisors (E16, early bell stage). At early bell stage (E16), the cervical loop is seen at the apical end of the labial epithelium. Only the labial epithelium gives rise to the enamel- forming ameloblasts. Epithelium: dark blue; dental mesenchyme: light blue dots. Abbreviations, cl: cervical loop; cm: condensed mesenchyme, d: dentine, dp: dental papilla, eo: enamel organ; m: mesenchyme, vl: vestibular lamina (adapted from (Harada et al., 2002)).

Interestingly, the labial and lingual epithelia noticeably differ in size with the lingual side being much thinner than that of the labial (Figure 1.5A). Star-shaped stellate reticulum cells reside at the heart of the labial cervical loop (Figure 1.5C), while the lingual cervical loop is thin and contains few stellate reticulum cells. Enamel is deposited exclusively by ameloblasts that differentiate along the labial aspect of the mouse incisor, thus visibly covers only the labial surface of the tooth (Figure 1.5B). In contrast, the lingual surface is enamel-free and directly borders the dentine layer. Therefore, the lingual and labial surfaces can be recognised as morphologically and functionally analogous to the non-continuously growing molar root and crown, respectively (Harada and Ohshima, 2004; Ohshima et al., 2005).

It is the larger, labial cervical loop containing the specialised arrangement of a central core of star-shaped stellate reticulum cells, surrounded by a basal layer of epithelial cells that possess the epithelial stem cells to support continuous incisor growth (Figure 1.5C). This structure is maintained throughout life in teeth that undergo continuous growth and eruption, never forming HERS and ERM and consequently remain rootless or "open rooted". In contrast, in non-continuously growing teeth such as mouse molars and all human teeth as described previously in section 1.1.2, the cervical loop undertakes structural modifications upon root formation resulting in HERS and ERM components (Figure 1.4D) (Thesleff and Tummers, 2008; Tummers and Thesleff, 2003).
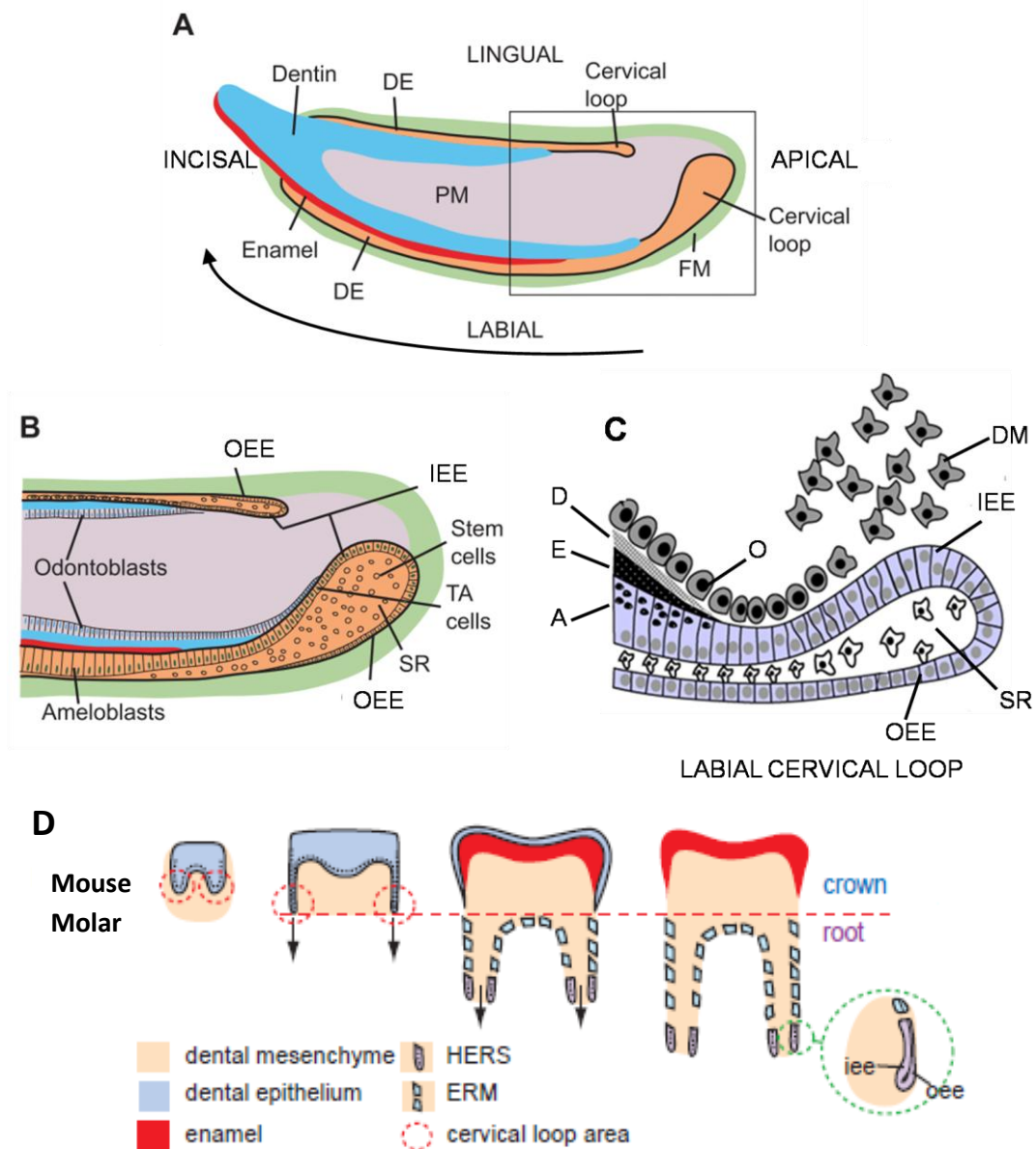
Figure 1.5 Schematics of the mouse incisor and molars

A: Basic overall organization of the incisor tooth. Growth occurs from the cervical (apical) to the incisal end indicated by the arrow. B: Enlargement of boxed region in A showing the individual cell types that comprise the lingual and labial cervical loops. Stem cells reside within stellate reticulum, core of the cervical loop. Arrow indicates the direction of incisor growth. D: Cross sectional view of mouse molar development. The mouse molar crown fate of the cervical loop is lost and switches to root indicated by the missing stellate reticulum. Upon completion of root formation the mouse molar has no functional cervical loop epithelium unlike the continuously growing mouse incisor, where the cervical loop continues to generate crown. Colour coding is as follows: enamel (red), dentin (blue), epithelium (orange), and follicular mesenchyme (green). Abbreviations: A: ameloblasts, D: dentine, DE: dental epithelium, E: enamel, ERM: epithelial cell rests of Malassez, HERS: Hertwig's epithelial root sheath, DM: dental mesenchyme, FM: follicle mesenchyme, IEE: inner enamel epithelium, O: odontoblasts, OEE: outer enamel epithelium, PM: papilla mesenchyme, SR: stellate reticulum, TA: transit amplifying (adapted from (Wang et al., 2007) and (Tummers and Thesleff, 2003)).

This region is odontogenically significant, as reports have identified an epithelial stem cell niche at the apical end of the labial cervical loop, the control of which is governed by mesenchymal molecular cues adjacent to the inner enamel epithelium (Harada et al., 1999; Harada et al., 2002; Wang et al., 2007). Mesenchymal FGF signalling was found to regulate the perpetual growth of the mouse incisor in conjunction with epithelial Notch signalling, ensuring epithelial stem cell progeny survival and proliferation. More specifically, it was demonstrated using both *in vitro* and *in-vivo* loss of function techniques including FGF10 bead implantation experiments, *Ffg10*-deficient mice and anti-FGF10 neutralizing antibodies, that mesenchymal FGF10 is indispensible to support the maintenance of the self-renewing epithelial stem cells responsible for growth at the cervical end (Harada et al., 1999; Harada et al., 2002). In the early *in vitro* experiments, culture of the mouse incisors with their cervical loops mechanically excised resulted in stunted epithelium that underwent differentiation into ameloblasts. However, when the differentiated region of epithelium was removed instead, the intact cervical loop generated new epithelium differentiating into secretory ameloblasts, indicating the presence of a primitive cell population capable of regenerating the dental epithelium (Harada et al., 1999). Moreover, slowly dividing putative stem cells were also identified among the peripheral stellate reticulum cells close to the basal epithelium inside the cervical loop region using BrdU (5-bromo-2'deoxyuridine) labelling followed by a 7 day chase period. Interestingly, a short 3 hour chase period revealed a region of rapidly dividing BrdU positive cells throughout the inner enamel epithelium zone suggestive of a region of "transit-amplifying" cells (Harada et al., 1999). The cells within the cervical loop therefore fulfil key criteria in the definition of a stem cell which is that they should regenerate themselves and also produce transit amplifying cells that divide and differentiate (Alonso and Fuchs, 2003). A following report indicated that FGF10-null mice developed morphologically hypoplastic labial cervical loops. In addition, loss of function *in vitro* studies using cultured incisor explants with neutralizing

anti-FGF10 antibody caused apoptosis and destruction of the cervical loop, which was subsequently rescued upon addition of human FGF10 protein. Altogether, this provides evidence that FGF10 is a key survival factor in maintaining the stem cell compartment of developing mouse incisor tooth germs (Harada et al., 2002). Another FGF signal (FGF3) is also implicated in the maintenance of the epithelial stem cell niche. The mesenchyme around the lingual cervical loop expresses FGF10, while the labial cervical loop receives signals from both FGF3 and FGF10. Thus, the differences in structure of the lingual and labial cervical loops may be attributed to this asymmetric FGF3 expression in the incisor mesenchyme (Wang et al., 2007). This FGF3 expression was found to be modulated by an integrated gene regulatory network between Activin, BMP, FGF and Follistatin (a TGFβ inhibitor). FGF3 signals promote stem cell proliferation and BMP4 represses Fgf3 expression, while the repressive effect of BMP4 is in turn inhibited by Activin. Follistatin was shown to antagonize the activity of Activin indicating differences between the levels of Activin and Follistatin expression contribute to the distinctive asymmetry of rodent incisors (Wang et al., 2007). A further study also demonstrated that sprouty (*Spry*) genes, which encode intracellular antagonists of the FGF signalling pathway, are critical for ensuring the essential asymmetry in enamel deposition for normal incisor shape and function. The loss of Spry4 leads to an ectopic epithelial-mesenchymal FGF signalling loop on the lingual side and the formation of ectopic ameloblasts by the stem cells resulting in "tusk-like" adult incisors (Klein et al., 2008).

Extensive reports have elucidated the role and regulation of the epithelial stem cell niche in the continuously growing rodent incisor (Harada and Ohshima, 2004). Yet the precise location and regulation of the mesenchymal stem cells (MSCs) in the cervical end of the incisor remains unclear. However, two other possible niches alongside the epithelial stem cell niche have been identified, a perivascular niche (pericyte cells) and MSCs of a non-pericyte source reveal dual origins of MSCs present for maintaining homeostasis and tissue repair of the pulp counterpart (Feng et al., 2011). Very recently, a third niche originating from the neurovascular bundle has also been identified to support MSC homeostasis in the adult mouse incisor (Zhao et al., 2014).

1.2 Mesenchymal stem cells

The basic definition of a stem cell is one that can undergo self renewal and multi-lineage differentiation (Morrison et al., 1997). Their role is to provide a supply of cells either for maintenance or repair of injured tissues. Stem cell studies broadly refer to three types. Embryonic stem (ES) cells, first reported in 1981 are derived from the inner cell mass of the blastocyst stage of the embryo and are pluripotent meaning that they can form all cell types of the body thus are described as most "primitive" and "plastic" (Evans and Kaufman, 1981). Adult stem cells (ASCs) are multipotent cells present post-natally and function to repair tissue and sustain continuous growth in many adult tissues including those of the hair and gut (Alonso and Fuchs, 2003). The third group of stem cells are generated from ASCs genetically reprogrammed using pluripotency associated genes specifically Octomer-binding transcription factor 3/4 (Oct3/4), (sex determining region Y)-box2 (Sox2), Krueppel-like factor 4 (Klf4) and myelocytomatosis viral oncogene homolog (c-myc) to generate induced pluripotent stem cells (iPSCs) (Takahashi and Yamanaka, 2006). Unlike ES cells,

where its harvesting procedure requires the destruction of human embryos, utilisation of IPSCs circumvents this controversy. However, there are concerns associated with the retrovirus gene transfer method in that random gene insertion could increase the risk of tumour formation and since some of the reprogramming factors are oncogenic, this is a further important consideration (Okita and Yamanaka, 2011).

Adult stem cells naturally exist in the body as a safeguard mechanism that activates upon injury to repair damaged tissues. Thus, they have great appeal as a practical source for a broad range of clinical applications. An important group of ACSs are the mesenchymal stem cells (MSCs), present in the majority of connective tissue in the body. The most studied and well characterised of which are the bone marrow mesenchymal stem cells (BMMSCs). This population was first described in 1970 by Friedenstein et al. as colony forming unit fibroblast cells (CFU-Fs) generated in monolayer cultures of guinea pig bone marrow (Friedenstein et al., 1970). These clonogenic cells have plastic adherent properties that could be expanded *in vitro* and were later shown to be "multipotent" populations that could differentiate along the now considered gold standard criteria of tri-lineage potential; meaning that MSCs should have the capacity to undergo osteogenic, chondrogenic and apidogenic differentiation (Pittenger et al., 1999).

MSCs can be isolated from many different adult tissue types, however they are typically heterogeneous in nature with varying proliferation and differentiation potentials (Kolf et al., 2007). Cell surface markers have been used in an attempt to identify and purify MSCs and in 2006 the Mesenchymal and Tissue Stem Cell Committee of the International Society for Cellular Therapy provided the scientific community with a standard set of "minimal" criteria to define human MSCs. Essentially, these cells must be plastic-adherent when cultured *in vitro*, contain over 95% CD105+, CD73+ and CD90+ cells, lack expression of CD45, CD34, CD14 or CD11b, CD79a or CD19 and HLA class II and finally they must have the

capacity to differentiate into osteoblasts, adipocytes and chondroblasts under standard *in vitro* differentiating conditions (Dominici et al., 2006). Nevertheless, there remains no formal consensus on which markers are appropriate to exclusively isolate MSCs as different groups largely employ a diverse collection of markers. Among these, Stro-1 is considered the most recognized putative MSC marker and together with negative selection against glycophorin-A (an erythroid lineage marker), CFU-Fs enrichment was observed in harvested bone marrow cells (Gronthos et al., 2003; Simmons and Torok-Storb, 1991). Crucially, Stro-1 expression is not exclusive to MSCs and there is also no equivalent Stro-1 marker in mice. In addition, the use of Stro-1 is limited to human MSCs at early passages as its expression is lost during culture expansion (Shi et al., 2002). Thus, defining the phenotype of MSCs from animal models solely based on the expression of markers is complicated and not necessarily the most reliable method.

Further to their roles in the regulation of tooth development, FGFs and Wnts among other growth factors have been implicated in the maintenance of "stemness" in MSCs. Unlike ESCs which have unlimited self renewal capacity and can be expanded indefinitely *in vitro*, MSCs have shorter lifespan in culture. The addition of FGF2 was shown to prolong MSC viability *in vitro* allowing expansion while retaining multilineage potential (Tsutsumi et al., 2001). Since *in vitro* expansion of MSCs is a vital pre-requisite for their use in future autologous therapies with a typical average loss of 0.5-1 billion cardiomyocyte cells in the human left ventricle after a heart attack (Murray et al.,2006) this is an important consideration in the efforts for successful clinical translation. More recently, FGF8 has been demonstrated to induce dopaminergic neuron formation in human BMMSCs, when supplemented together with SHH (Funk and Alexanian, 2013). Numerous reports suggest that Wnts play a critical role in regulating stem cells and cancer (Reya and Clevers, 2005). Wnt3a in particular has been demonstrated to maintain undifferentiated human adult MSCs while inhibiting osteogenic differentiation (Boland et al., 2004). Furthermore, in rat

BMMSCs, Wnt3a is a promoter of MSC migration (Shang et al., 2007). These studies highlight chemical genetics as an important approach to understanding the control of MSCs that will undoubtedly aid in unravelling tissue regeneration pathways to further the field of regenerative medicine.

1.2.1 Immunomodulation by MSCs

A major advantage of using MSCs in future clinical therapies is their immunomodulatory properties. They have been shown to possess immunosuppressive function both *in vitro* and *in vivo* and mainly act through secretion of molecules that are either induced or upregulated via cross-talk with immune cells (Ghannam et al., 2010). Both CD4+ and CD8+ T-lymphocyte proliferation is suppressed by MSCs, while Interleukin-2 (IL-2)-induced proliferation of resting Natural Killer (NK) cells is also inhibited (Spaggiari et al., 2006). Since the anti-proliferative, immunomodulatory and anti-inflammatory effects of MSCs have become clear, their regenerative capabilities are now not the exclusive driving force behind their study. Excitingly, MSCs as potential therapeutic agents to treat rejection after allogeneic transplantation such as graft-vs-host disease (GvHD) has been demonstrated *in vivo* studies with BMMSCs. In 2002, using a baboon skin graft model, it was shown that *in vitro* expanded donor or third-party BMMSCs are immuosuppressive and prolonged the rejection of histoincompatible skin grafts (Bartholomew et al., 2002). While in human trials, remarkable clinical response has been observed. BMMSCs were found to reverse grade acute IV GvHD of the gut and liver of a leukaemia patient suffering from rejection after a blood stem cell transplant (Le Blanc et al., 2004). In addition, multiple patients suffering from other cancers including myeloma and solid tumours revealed complete eradication of acute GvHD in six of eight patients (Ringden et al., 2006). Though the specific mechanisms

through which MSC immunomodulation operates warrant further investigation, encouraging data indicate comparable therapeutic effects between allogeneic and autologous MSCs (Hare et al., 2012).

1.2.2 The MSC niche

The concept of a stem cell "niche" was pioneered by Schofield in 1978. In the study, decreased proliferative potential in hematopoietic stem cells (HSCs) of the spleen was observed in comparison to HSCs derived from the bone marrow. This led to the important hypothesis whereby stem cells are associated with other complementing cells which in turn determine their behaviour. Since the HSCs of the spleen were no longer associated with their "niche" that supports ongoing stem cell activity, the cells effectively mature and lose their stem cell identity (Schofield, 1978). As such, the niche functions to balance the production of stem cells and progenitor cells to maintain growth and repair in adults tissues. They do so from within specialised and complex microenvironments consisting of stem cells (SCs), non-SCs, extracellular matrices and molecular signals that regulate stem cell behaviour in a highly dynamic system (Becerra et al., 2011; Scadden, 2006; Voog and Jones, 2010). Overall, in order to maintain the crucial balance between homeostasis and repair, the stem cells must remain undifferentiated and respond to certain cues that can travel into the niche to signal the stem cells that their differentiation potential is required for the regeneration or repopulation of a tissue (Kolf et al., 2007).

Extensive research into MSCs has been largely based upon their behaviour in an entirely non-native context; that is *in vitro*. Therefore, it is important to take into consideration that the removal of these cells from their natural environment or "niche" almost certainly

causes alterations to their phenotype and behaviour depending on their *in vivo* or *in vitro* setting (Augello et al., 2010). Thus, to truly harness these potentially powerful cells for future regenerative medicines, *in vivo* identification of MSCs is vital and one aspect of determining their function is to define their topography *in situ* in various organs.

Stem cell niches have been identified in many different tissue types including the hair follicle (Fuchs et al., 2004), intestine (Barker, 2014) and in the tooth (Sloan and Waddington, 2009). In teeth, they reside within specific anatomic locations of the dental pulp where the microenvironment regulates how the dental pulp stem cell population contributes to tissue maintenance, repair and regeneration (Mitsiadis et al., 2011). To date, there have been 6 sources of stem cells harvested from dental tissue-related niches and in order to provide a greater understanding of stem cell function and aid development of future MSC-based therapies, an important avenue to investigate would be to evaluate the stem cell niche in healthy vs diseased or damaged tissues. Increasing knowledge of the differences between their underlying mechanisms will enable better replication of natural tissue repair and enhance the efficiency of this process. One area of great interest is the migration of stem cells.

1.2.3 Stem cell homing

The homing effect of stem cells towards sites of injury is another important stem cell niche-related paradigm (Augello et al., 2010). During the tissue repair process, cells local to the wound may differentiate and carry out repair to the best of their ability, but often these cells are post-mitotic, thus are unable to provide the numbers required for successful regeneration of the tissue. Hence, signalling to recruit stem/progenitor cells to home

towards the site of injury, proliferate and differentiate into the necessary cell type to replenish the lost population is required. Not only are the signals that maintain the stem cells within the niche essential, the signals which cause them to exit the niche are equally important to fully appreciate the dynamic function of the niche.

The recruitment of stem/progenitor cells residing within neighbouring healthy tissues to an injury site is facilitated by cell homing factors. Stromal-derived factor 1 is among those found to regulate MSC migration together with its receptor CXCR4 (Shi et al., 2007; Son et al., 2006). They appear particularly important in regulating MSC homing for cardiac repair since this protein is upregulated in numerous myocardial infarction models as well as in ischemic cardiac patients (Ghadge et al., 2011).

There are two types of cell homing, the first is defined as cell movement via the blood circulatory system until the cell is arrested by microvascular endothelial cells in a target organ, while the second is more appropriate to describe the movement of local stem cell homing. This type of "homing mode" is known as interstitial movement whereby the stem cells recognize and follow extravascular guidance cues independently of blood flow (Laird et al., 2008). Interestingly, even without injury, MSCs have the innate capacity to home towards bone marrow and lung tissue (Francois et al., 2006). However, during tissue damage, this cell homing pattern was altered. This was demonstrated in mice when either subjected to total body irradiation or local irradiation at specific sites which produced enhanced engraftment of injected MSCs into more organs and in greater numbers than in non-irradiated animals (Francois et al., 2006). Later in 2008, a study in mice overexpressing MCP-1 (a chemokine) showed that BMMSCs systemically infused into these animals preferentially migrated towards their hearts, in comparison to wild-type mice, where migration towards the organ was negligible (Belema-Bedada et al., 2008). This correlated with other reports demonstrating MSC homing towards bone marrow (Devine et al., 2001;

Morikawa et al., 2009; Sackstein et al., 2008). Although many of the MSC homing studies discussed above involve systemic delivery of MSCs and their engraftment potential, alternative therapeutic approaches other than to use MSCs as direct replenishment of cell units to restore the lost tissue should be explored. One example is endogenous cell homing which permits cell populations already present in a patient's body, including stem/progenitor cells to be actively recruited to sites of injury. In teeth, Kim et al. showed that endogenous cell homing can be achieved without the need for exogenous cell transplantation. Their experimental model using endodontically treated human incisors implanted *in vivo,* in the dorsum of mice for 3 weeks, showed that upon delivery of bFGF and/or vascular endothelial growth factor (VEGF), re-cellularized and revascularized connective tissue that integrated to native dentinal wall in root canals was achieved. Furthermore, the addition of platelet-derived growth factor (PDGF), basal infusion of nerve growth factor (NGF) and BMP7 resulted in complete filling of the root canal with dental pulp-like tissue (Kim et al., 2010). While in the continuously growing mouse incisor model, labelled MSCs from the cervical loop pulp can also home towards the injured site (Feng et al., 2011). In the liver, in response to injury, BMMSCs were shown to mobilise into the circulatory system and were recruited into the injured liver under the direction of chemokine (C-C motif) receptor (CCR)9, chemokine (C-X-C motif) receptor (CXCR)4 and mesenchymal-epithelial transition factor (c-MET) chemoattraction signals (Chen et al., 2010). Such studies demonstrate the potential of endogenous MSC recruitment and subsequent repair of injured tissues. However, critical to the implementation of MSCs in routine clinical practice would be to enable the direction of MSC migration with high efficiency, whether therapeutically infused or actively mobilised from tissue-resident populations (Chen et al., 2011).

1.3 Dental stem cells

Paradoxically, although teeth are non-essential for life and thus not considered a major target for regenerative medicine research compared to neural or cardiac diseases, for example, this very fact makes teeth ideal for testing new cell-based treatments (Volponi et al., 2010). The accessibility of teeth circumvents the need for major surgery and naturally lost or surgically removed teeth provide multiple opportunities throughout life to isolate a variety of dental stem cell populations. Furthermore, dental disease is a widespread public health problem that affects the quality of life of humans from young to old age and is associated with heart disease (DeStefano et al., 1993) as well as diabetes (Lamster et al., 2008). In addition to using dental stem cells for tooth repair, restoration and regeneration, significantly, they may also have a purpose for non-dental uses, such as developing stem cell-based therapies for major life-threatening diseases.

1.3.1 Dental pulp stem cells

The capacity of dental pulp cells to respond to damage caused by pathological conditions such as carious lesions and restorative processes such as cavity preparation has been well documented (About et al., 2000; Robertson et al., 1997; Smith et al., 1995b; Smith et al., 1994). Replenishment of the odontoblast population appears to originate from progenitor cell populations that reside in the deeper pulp. These cells are capable of self renewal and can migrate after noxious stimuli and differentiate into odontoblasts (Fitzgerald et al., 1990; Smith and Lesot, 2001). When dental tissue is moderately damaged, the tertiary dentin secreted by the odontoblasts becomes reactionary. On the other hand, during deep cavity

preparation the odontoblasts are destroyed which leads to the influx of pericytes or mesenchymal cells into the dental pulp. These cells exhibit odontoblastic properties, and can replace the necrotic odontoblasts and secrete reparative dentin (Smith et al., 1995b; Tziafas, 1995). This suggests that the niche in which the cells normally reside, along with the local environment, are important for cell identity.

In 2000, Gronthos et al. first reported the identification of stem cells from adult human dental pulp. This population of DPSCs from permanent third molars was characterized by their high proliferation and high frequency of colony-forming cells compared with BMMSCs. While both cell types shared similar immunophenotype *in vitro*, functional studies showed that DPSCs produced only sporadic, but densely calcified nodules with no adipogenesis whereas BMSCs routinely calcified throughout the adherent cell layer with lipid-laden clusters of adipocytes (Gronthos et al., 2000). Additional *in vivo* transplantation into immunocompromised mice demonstrated the ability of DPSCs to generate functional dental tissue in the form of dentin/pulp-like complexes. Further characterization revealed that DPSCs were also capable of differentiating into adipoctyes, as measured by the formation of characteristic oil red O-positive lipid-containing clusters (Gronthos et al., 2002) as well as osteoblasts and endotheliocytes (d'Aquino et al., 2007). In addition, differentiation into neural-like cells was observed as they were found to express markers of neuronal precursors and glial cells such as nestin and glial fibrillary acid protein (GFAP) respectively (Wislet-Gendebien et al., 2003). This evidence suggests that DPSCs may have a broader capacity for differentiation than originally proposed and may reflect their developmental origin.

1.3.2 Stem cells from human exfoliated deciduous teeth

One of the most convenient and easily accessible sources are stem cells from human exfoliated deciduous teeth (SHED). In 2003, Miura et al. identified a population of highly proliferative, multipotent, clonogenic cells from the remnant pulp of teeth that are naturally lost during childhood. SHED demonstrated the capacity to differentiate into a range of cell types including neural cells, adipocytes and odontoblasts (Miura et al., 2003). *In vivo* transplantation of SHED have demonstrated induction of bone formation and generated dentine (Miura et al., 2003; Sakai et al., 2010; Shi et al., 2005) . In addition they promote neuronal survival in mouse brain and express neural markers. The expression of neuronal and glial cell markers implies that SHEDs may be related to the neural crest-cell origin of the dental pulp. In contrast to DPSCs, SHED exhibited higher proliferation rates, increased population doublings, osteoinductive capacity *in vivo* and an ability to form sphere-like clusters (Miura et al., 2003). Furthermore, SHED lack the capacity to reconstitute a complete dentin-pulp-like complex thus, supports the notion that this cell population is unique and distinct from DPSCs. This could be attributed to their difference in developmental timeframe. Since SHED cells are at an earlier stage they likely represent a more immature stem cell population. Current *in vivo* data suggests SHED have greater capacity for mineralisation than DPSCs (Wang et al., 2012) .

1.3.3 Periodontal ligament stem cells

The periodontal ligament (PDL) is a fibrous layer derived from the dental follicle that contains specialised connective tissue which functions to maintain and restrict teeth within the jaw. It is located between the cementum and the inner wall of the alveolar bone socket and regulates periodontal homeostasis by providing nourishment to the teeth (Nanci, 2008). It has long been recognized to contain a population of progenitor cells (McCulloch, 1985). More recently Seo et al., (2004) revealed that dental stem cells from human periodontal ligament (PDLSCs) were capable of differentiating along multilineages to produce cementoblast-like cells and adipocytes. In this study, the PDLSCs extracted from human third molars by single colony selection were characterised as STRO-1/CD146 positive (Seo et al., 2004). Moreover, during *in vivo* studies, cementum/PDL-like structures formed along with dense collagen fibres similar to Sharpey's fibres showing their potential to regenerate PDL attachment, which is critical for development of a functional tooth. It was also demonstrated that the tissue regeneration capacity is maintained even after recovery from frozen human tissue (Seo et al., 2005). These findings were confirmed by expression of STRO-1, single-colony-strain generation, multipotent differentiation, cementum/periodontal-ligament-like tissue regeneration and a normal diploid karyotype, all characteristics of normal PDLSC (Seo et al., 2005). Moreover, when PDLSCs were co-transplanted with human apical papilla stem cells (SCAP), using a hydroxyapatite /tricalcium phosphate (HA/TCP) carrier into the tooth sockets of miniature pigs, construction of the root/periodontal complex was successfully formed and were even capable of supporting a porcelain crown allowing normal tooth function (Sonoyama et al., 2006). Taken together, these results suggest cryopreserved PDL from extracted teeth may be viable for future therapeutic purposes.

Regeneration of mineralized tissue and periodontal ligament has been achieved using ovine PDLSC transplanted into non-obese diabetic (NOD) and severe combined immunodeficiency (SCID) mice (Gronthos et al., 2006). The PDLSCs were derived from ovine periodontal ligament using immunomagnetic bead selection, based on expression of the mesenchymal stem cell-associated antigen CD106 (vascular cell adhesion molecule 1). The CD106+ cells were able to form adherent clonogenic clusters of fibroblast-like cells with high proliferative capacity *in vitro* and expressed a phenotype (CD44+, CD166+, CBFA-1+,collagen-I+, bone sialoprotein+) corresponding with human-derived PDLSCs (Gronthos et al., 2006). Periodontal ligament is able to withstand mechanical forces of stress and tension similar to that of a tendon. Not surprisingly, a tendon-specific transcription marker called scleraxis was found to be expressed at much higher levels in PDLSCs than in DPSCs or BMSCs. Therefore, PDLSCs are considered as a unique population of adult MSCs different from pulp tissue or bone marrow (Shi et al., 2005).

1.3.4 Root apical papilla stem cells

Located in the root foramen area of the tooth exists another unique population of dental stem cells known as stem cells from the root apical papilla (SCAP). The loosely attached "apical cell-rich" zone of the apical papilla tissue is only present during root development before the tooth erupts into the oral cavity (Huang et al., 2008). This means that routine third molar extraction procedures represent unique opportunities to harvest yet another dental stem cell population.

In 2006, Sonoyama et al., demonstrated that SCAP have capacity to differentiate into odontoblasts and adipocytes and display higher proliferative potential compared with DPSCs when measured by bromodeoxyuridine (BrdU) uptake (Sonoyama et al., 2006).

When co-transplanted with PDLSCs into tooth sockets of miniature pigs, dentin and periodontal ligament was formed. These findings suggest that this population of cells could be suitable for cell-based regeneration therapies using a combination of autologous SCAP/PDLSCs together with artificial dental crown (Sonoyama et al., 2006). Moreover SCAP appear to be a source of primary odontoblasts responsible for the formation of root dentin (Sonoyama et al., 2006), whereas DPSCs are possibly the source of replacement odontoblasts that produce dentin (Gronthos et al., 2000).

Most human tissue at the developing stage is not clinically available for stem cell isolation. However, the root apical papilla is accessible in dental clinical practice via extracted wisdom teeth. As these teeth develop later in life in comparison with other tooth types, access to a still-developing tissue similar to those in embryonic development is achievable. Since there are four wisdom teeth present in adults with the possibility of each one of their roots yielding one apical papilla, this poses an opportunity for banking these dental stem cells for future autologous use. However, the success of this will depend on their survival under freeze-thawing conditions.

1.3.5 Dental follicle stem cells

The dental follicle is a loose ectomesenchyme derived connective tissue sac surrounding the enamel organ and the dental papilla of the developing tooth germ prior to eruption (Ten Cate, 1998). It is believed to contain progenitors for cementoblasts, PDL and osteoblasts. The dental follicle cells form the PDL by differentiation into the PDL fibroblasts which secrete collagen and interact with fibres on the surfaces of adjacent bone and cementum. The differentiation capacity of bovine dental follicle cells (BDFCs) has been determined *in vivo* when cementoblast formation was observed after their transplantation

into SCID mice (Handa et al., 2002a; Handa et al., 2002b). In these studies, monoclonal antibody (3G9) against cementum-derived attachment protein (CAP) was used as a marker molecule for cementoblasts. Previous research demonstrated that CAP promotes attachment of dental follicle cells and its expression is limited to cementum matrix and cementoblasts during cementogenesis, illustrating its suitability as a marker for cementoblasts (Saito et al., 2001).

Dental follicle progenitor cells isolated from the follicular sacs of human third molars were characterized by their rapid attachment in culture and expression of putative stem cell markers Nestin and Notch-1 (Morsczeck et al., 2005). In comparison with BM cells, PDL cells and osteoblasts, precursor cells from human dental follicles expressed higher levels of insulin-like growth factor-2 (IGF-2). Furthermore, after induction, the cells were able to form compact calcified nodules or appeared as plain membrane structures *in vitro*. When transplanted in immunocompromised mice, bone sialoprotein (BSP) and osteocalcin (OCN) were expressed differentially, without any indication of cementum or bone formation (Morsczeck et al., 2005). Further analysis has demonstrated heterogeneity amongst cell populations in developing follicles as *in vitro* studies revealed that several cloned dental follicle cell lines under the same culture conditions had different activities of alkaline phosphatase and different capacities for differentiation. The differentiation pathways characterized included periodontal ligament-type lineage, cementoblastic or alveolar bone osteoblastic lineage (Luan et al., 2006b). Transplantation of a clone of porcine dental follicle cells into SCID mice demonstrated variation in BSP, OCN and periostin expression under the effect of collagen 1 matrix, which is postulated to facilitate the mineralization process during the crown-formation stage (Tsuchiya et al., 2008). Once the mechanisms that drive dental follicle cell differentiation are unravelled, in future, it may not be necessary to obtain PDL cells from extracted teeth (Mantesso and Sharpe, 2009).

1.3.6 Gingival stem cells

Among the most important elements of the periodontium is the gingival tissue, which has demonstrated remarkable wound healing and regenerative capacity. Of the two tissue types isolated from the gingiva, the fibroblast population are a heteregeneous mix of cells that contribute to the wound healing process by responding to different growth factors and secreting certain extra cellular matrix proteins (Phipps et al., 1997; Schor et al., 1996; Zhang et al., 2009), while its oral epithelium counterpart has shown remarkable promise for the treatment of ocular disorders (Chen et al., 2012; Nakamura et al., 2004; Nakamura et al., 2003). Progenitor cells and multipotent MSC subpopulations have been isolated and characterised from gingival fibroblasts (Fournier et al., 2010; Hsu et al., 2012; Mitrano et al., 2010). The straightforward isolation of gingival fibroblasts makes them a very practical source of dental stem cells and they have also been recently reprogrammed to form IPSC lines (Wada et al., 2011).
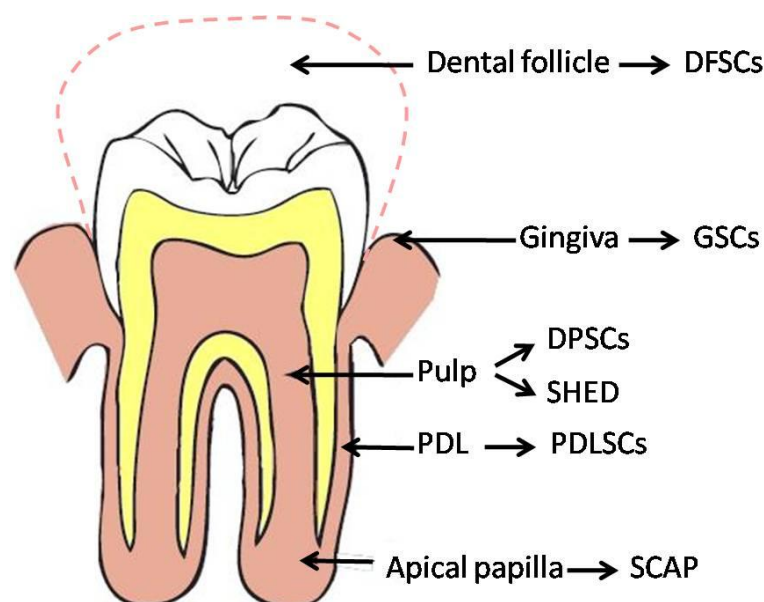
Figure 1.6 Summary of dental stem cell sources
DPSC: dental pulp stem cell; PDL: periodontal ligament; PDLSC: periodontal ligament stem cell; SCAP: Stem cells from the apical papilla; SHED: Stem cells from exfoliated deciduous teeth; DFSCs: dental follicle stem cells; GSCs: gingival stem cells (adapted from (Huang, 2009)).

1.4 Pericytes

Pericytes are known as mural or Rouget cells that are located along the abluminal endothelial wall of microvessels including arterioles, capillaries and venules (Bergers and Song, 2005; Crisan et al., 2009; da Silva Meirelles et al., 2008). These morphologically distinct cells are embedded within the basement membranes of microvasculature and possess cell bodies with prominent nuclei in relation to the cytoplasm, from which long processes extend and physically contact and communicate with endothelial cells lining the inner vessel wall (Allt and Lawrenson, 2001). Together, pericytes and endothelial cells synergistically contribute to the function and maintenance of blood vessels via soluble factors and physical interactions (Armulik et al., 2005).

1.4.1 The perivascular niche

Efforts to trace the identity of tissue-resident MSCs have consistently suggested their close association with vasculature (Corselli et al., 2010). In 2009, a study on equine adipose tissue revealed that MSC frequency positively correlates with higher blood vessel density (da Silva Meirelles et al., 2009) while in bone marrow, the quantity of MSCs (CFU-F) per nucleated marrow cell decreased with age, corresponding to the reduction in vascular density in older individuals (Caplan, 2009). Furthermore, perivascular cell markers are also expressed by MSCs including NG2, Stro-1, αSMA, Thy-1, V-CAM1 and PDGFβ (da Silva Meirelles et al., 2008). Based on the expression of a combination of markers (CD146, NG2 and PDGFR-β) and the absence of hematopoietic, endothelial and myogenic markers, vascular pericytes from multiple human organs have been identified (Crisan et al., 2008a). On the basis of this evidence, MSCs seem likely to reside within widespread "perivascular niches" along microvessels throughout the body. The proximity to vessels would allow

pericytes rapid access into the bloodstream to replace cells lost due to physiological turnover or repair of local tissue injury (da Silva Meirelles et al., 2008).

Other evidence to suggest the relationship between MSCs and pericytes is their common multipotent feature. Pericytes have long been suggested as progenitors for tissue repair (Richardson et al., 1982). Using thermally injured fat pads of rats, cells local to the wound appeared liberated from their anatomical site and 5 days post injury, adipocytes together with neo-vascularisation was observed; demonstrating the capacity of pericytes to differentiate into adipocytes during the wound healing process (Richardson et al., 1982). Later on, generation of bone and cartilage was also observed using labelled perivascular cells during periosteal bone healing and in grafted perichondrium respectively (Diaz-Flores et al., 1992a; Diaz-Flores et al., 1992b). Roles for pericytes as progenitors for neural and muscle lineages has also been suggested (Dore-Duffy et al., 2006; Meyrick and Reid, 1978). While both *in vitro* and *in vivo* experiments have shown that in addition to their clonal osteogenic, chondrogenic and adipogenic potential, which fulfils a key MSC criteria, pericytes retain myogenicity regardless of whether they are isolated from human muscle or non-muscle tissues (Crisan et al., 2008b). Furthermore, it was recently shown that cultured human perivascular cells transplanted *in vivo*, enhanced cardiac improvement post-infarction in mice (Chen et al., 2013).

In further support of the perivascular/MSC niche concept, in common with MSCs, pericytes natively express markers CD44, CD73 and CD90, possibly reflecting their developmental affiliation. Furthermore, cultures of MSC-like cells have been generated from cells isolated with pericyte-specific markers CD146 and PDGFR from human endometrium and were shown to be phenotypically and functionally similar to MSCs (Schwab and Gargett, 2007).

Classic label retaining cell (LRC) assays have been used to identify stem/progenitor cells based on the retention of nucleotide label incorporated into the DNA of cells during DNA

synthesis in slowly proliferating stem cells (Lajtha, 1979; Potten et al., 1979). In the PDL of mouse molars, slowly cycling stem cells were identified using 3H-thymidine pulse experiments followed by radioautographic analaysis. Cells located in close proximity to blood vessels (<10μm) were label retaining (slow-cycling) while proliferating cells that lost their labelling upon cell division were detected at distances further than 10μm from blood vessel walls. This evidence supports the notion that slowly dividing populations of progenitor cells are resident in perivascular locations (McCulloch, 1985). Other congruent recent data from murine endometrium indicates the presence of perivascular BrdU LRCs (after a 12 week chase period) positive for α-SMA and lacking expression of CD31 or CD45 assuring pericyte origin (Chan and Gargett, 2006). Taken together, these results provide evidence in support of the hypothesis that pericytes are possibly *in vivo* native cells of the well characterised *ex vivo* MSCs (Augello et al., 2010).

1.4.2 Perivascular cells of the dental pulp

To date, all pioneering studies in search of dental pulp stem cell populations have presented consistent expression of pericyte/perivascular markers (Gronthos et al., 2000; Miura et al., 2003; Sonoyama et al., 2006). Immunoselection of perivascular cells from human dental pulp based on positive expression of pericyte markers and negative expression of endothelial cells have demonstrated that isolated fractions generated 7 fold greater CFU-Fs than unfractionated dental pulp cells (Shi and Gronthos, 2003). Moreover, in comparison to BMMSCs, FACS sorted subfractions of CD146 positive clonogenic dental pulp cells contained a larger proportion (63%) of pericyte-associated cell surface antigen (3G5) positive cells, while in bone marrow only a minority were positive for 3G5. Subsequent *in vivo* transplantation of these cells demonstrated the capacity to regenerate

bone marrow and dental pulp microenvironments (Shi and Gronthos, 2003). These findings may correspond to a common ontogeny between dental pulp tissue and pericytes originating from neural crest derived cells (Chai et al., 2000) and suggest DPSCs reside within perivascular niches inside the dental pulp.

Further *in vivo* tooth damage LRC studies on extracted human immature third molars drilled to artificially produce pulp cavities demonstrated localised labelling of perivascular cells surrounding blood vessels after 1 day of BrdU uptake. When collected 2 or 4 weeks post BrdU labelling, the labelled perivascular cells had proliferated, migrated and were observed restricted to the cavity area only, suggesting that the progenitor/stem cell niche resides predominantly in perivascular regions from which they migrate to the site of injury (Tecles et al., 2005). While in another study involving rat molar odontoblast injury, pericytes both nearby and distant from the injury were shown to be activated by the Notch signalling pathway, known to be important for controlling stem cell fate (Lovschall et al., 2005). In recent years, EphB/ephrin-B molecules have also revealed important roles in signalling DPSC in tooth maintenance and their receptor/ligand expression within the perivascular sites demonstrated involvement in response to tooth damage (Arthur et al., 2009; Stokowski et al., 2007). While in the continuously growing mouse incisor model, LRC studies have identified slowly dividing pulp mesenchymal cells close to the epithelial stem cell niche (Lapthanasupkul et al., 2012; Seidel et al., 2004) and perivascular MSCs have been identified using cre-mediated genetic lineage tracing of pericytes (Feng et al., 2011). Using the NG2creER;Rosa26R pericyte reporter line mice, pericytes were shown to differentiate into odontoblasts during tooth growth and in response to damage *in vivo*. However, in both cases, pericyte contribution did not account for all of the cell differentiation since only 15% of the newly formed odontoblasts were pericyte derived. This suggested that an additional source of non-pericyte derived MSC cells coexists with those that are of pericyte origin (Feng et al 2011). In their odontoblast injury study, using

Dil labelling in different regions of the mouse incisor pulp to identify any responses to tooth damage, cells labelled in the cervical area migrated to the damaged area after 2 days, while in the absence of damage, the cells remained quiescent. This provides evidence that a distinct population of MSCs are resident close to the cervical end of the incisor (Feng et al., 2011). Taken together, the role of the perivascular niche may be to maintain the DPSCs in their functional state and pericyte contribution to MSC-derived mesenchymal cells in any given tissue is variable and may be dependent on the extent of the vascularity.

1.5 Dental stem cells for injury repair

Inside the pulp chamber of teeth, compact nonhematopoietic fibrous tissue is permeated by a microvascular network that is entombed by mineralized dentine (Shi and Gronthos, 2003). Together they form the dentine-pulp complex which displays a remarkable and entirely natural, albeit limited regenerative potential in response to injury (reviewed by (Sloan and Smith, 2007; Sloan and Waddington, 2009). Following primary dentinogenesis during tooth formation, the post-mitotic odontoblasts remain functional in that they retain their ability to respond to mild injury, such as attrition or early caries, whereby surviving odontoblasts up-regulate secretory activity resulting in the formation of "reactionary dentine" without other pulp cell involvement (Smith et al., 1994). However, damage of greater intensity that result in odontoblast death requires cell renewal by a new generation of odontoblast-like cells differentiated from a local progenitor population resident in the pulp and this process is termed "reparative dentinogenesis" (Smith et al., 1995a). Endogenous dentine extracellular matrix components were capable of stimulating odontoblasts to secrete reactionary dentine when implanted into unexposed cavities in ferret teeth for 14 days (Smith et al., 1994). The absence of odontoblast death confirmed

that reactionary dentinogenesis can arise from interactions between existing odontoblasts and appropriate molecular stimuli in contrast to the reparative process, where a whole new cascade of biological events such as proliferation, chemotaxis, cell migration and finally terminating in cytodifferentiation are necessary to provide a new generation of odontoblast-like cells prior to matrix secretion (Smith et al., 1995a). Underpinning these reparative/regenerative processes are several important bioactive molecules that signal and regulate tertiary dentine production and are sequestered within the dentine matrix. In particular, members of the TGF-β family including TGF-β1, β3 and BMP-7 have been shown *in vitro* to stimulate odontoblast secretions (Sloan et al., 2000; Sloan and Smith, 1999). Using cultured rat incisor tooth slices, it was shown that TGF-β_1 and TGF-β_3 soaked beads stimulated predentine secretion at the bead application site (Sloan and Smith, 1999). While BMP-7 soaked beads similarly led to increased extracellular matrix secretion by the odontoblasts located at the site of application (Sloan et al., 2000). During reparative dentinogenesis, ECM components released local to the site of injury are likely to provide chemotactic stimuli for pulp cell recruitment of those within the immediate vicinity of the damage but also progenitors resident in quiescent niches in other areas of the pulp. Knowledge of the underlying mechanisms by which pulp cell recruitment occurs holds exciting possibilities in the development of therapeutic strategies to target endogenous dental pulp stem cells for regenerative dentistry. However, vital to this will be understanding the niches in which the progenitors reside in order to exploit their function by either maximising recruitment or even influencing specific populations recruited for greater specificity to tissue response. One possible population are the perivascular stem/progenitor cells in light of the local angiogenic response common to all wound repair sites (Sloan and Smith, 2007). Pulp cell mobilization has been demonstrated to involve bi-directional EphB/EphrinB interactions and suggest a role for perivascular DPSC attachment and migration to maintain these cells within their stem cell niche under steady state

conditions (Stokowski et al., 2007). A follow up study by the same group using the tooth injury model showed in the presence of ephrin-B1-Fc fusion protein, not only were perivascular BrdU positive cells retained at the injury site, but colony forming capacity was also increased both in size and number suggestive of a role in restricting mobilization of DPSCs from the perivascular niche and/or increase in proliferation and growth (Arthur et al., 2009). Moreover, reverse signalling in the presence of EphB2-Fc revealed enhanced mineralization capacity, which may be associated with the stimulation of odontogenic differentiation (Arthur et al., 2009). The potential role of other signalling molecules SDF1, bFGF, and BMP7 could play in the migration of dental stem/progenitor was recently investigated. Using 3D migration assays, bFGF and SDF1 enhanced migration while BMP7 had little effect, most likely because the latter induced odontoblastic/osteoblastic differentiation of dental pulp cells (Suzuki et al., 2011). Migration of DPSCs from specific dental pulp niches in response to injury and the underlying mechanisms that regulate this process involves a diverse range of signalling pathways and therefore remains an area of ongoing enquiry. A useful model would be to investigate repair responses in healthy vs damaged tissues in a continuously growing organ where a readily active pool of stem cells provides an opportunity to study the delicate balance between maintenance and repair, such as the continuously growing rodent incisor.

1.5.1 Wnt signalling and injury repair

Wnt proteins belong to the large family of secreted ligands that activate several receptor mediated pathways and plays a fundamental role in diverse embryonic developmental and cellular processes such as embryonic induction, generation of cell polarity and specification of cell fate (Cadigan and Nusse, 1997; Logan and Nusse, 2004). This pathway is also essential for morphogenesis and homeostasis of several oral organs including teeth, taste buds, salivary glands and oral mucosa (Yang and Liu 2013) (Liu and Millar, 2010). The importance of this signalling pathway is not limited to influencing embryogenesis, in adults, the maintenance of stem cells for tissue homeostasis is also Wnt regulated and its disruption is linked to diseases such as cancer (Moon et al., 2004; Nusse, 2008; Reya and Clevers, 2005).

At the cell membrane, the Wnt signalling cascade begins when the Wnt family protein interacts with its receptor Frizzled (FZD) and LDL receptor related protein (LRP) family of co-receptors. Upon Wnt receptor activation, several different pathways can be activated, among these, the most extensively studied is the canonical, also known as the β-catenin pathway. In the absence of Wnt, β-catenin, a component of intercellular adhesion junctions is recruited to the "destruction complex" consisting of adenomatous polyposis coli (APC) and Axin proteins, which phosphorylate β-catenin by casein kinase I (CK1) followed by glycogen synthase kinase 3β (GSK3β). This results in ubiquitination and protease-mediated degradation of β-catenin (Moon et al., 2004).

When the β-catenin pathway is activated, interaction of FZD with the cytoplasmic dishevelled (DSH) protein results in phosphorylation of DSH and the inhibition of GSK3β, causing the inactivation of the destruction complex. This allows the stabilization of cytoplasmic β-catenin and its subsequent translocation and accumulation in the nucleus

where it interacts with T-cell factor (TCF) and lymphoid enhancer-binding protein (LEF) transcription factors to activate the transcription of downstream Wnt target genes (Figure 1.7).
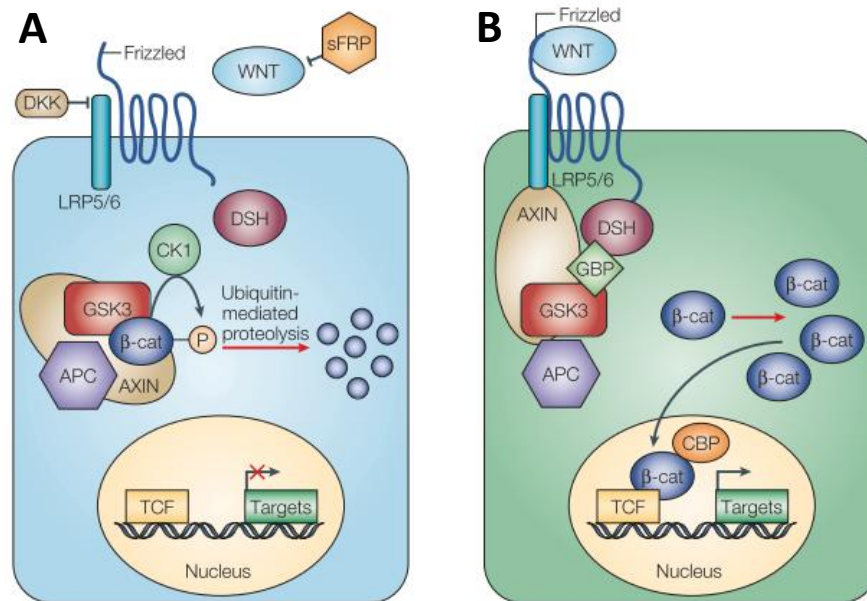
Figure 1.7 Schematic of WNT/β-catenin signalling
In the absence of active WNT (a), β-catenin is degraded, and prospective target genes are in a repressed state. If WNT signalling (b) is active, β-catenin degradation is reduced. As β-catenin accumulates, it enters the nucleus, binds to T-cell factor (TCF)- and lymphoid enhancer- binding protein (LEF)-family transcription factors and activates transcription. The components shown are described in more detail in the text; additional pathway components are described on web sites that are linked to the main text. APC, adenomatous polyposis coli; β-cat, β-catenin; CBP, CREB-binding protein; CK, casein kinase; DKK, Dickkopf; DSH, Dishevelled; GBP, GSK3- binding protein; GSK, glycogen synthase kinase; LRP, LDL- receptor-related protein; P, phosphorylation; sFRP, secreted Frizzled-related protein; TCF, T-cell factor (Moon et al., 2004).

Wnt signalling is known to be elevated during injury to mammalian and some aquatic species. Injury is thought to trigger the upregulation of the endogenous Wnt pathway and is implicated in the subsequent healing of the wound. Growing evidence implicates the Wnt pathways as essential to stimulate the recruitment of stem/progenitor cells for tissue regeneration and repair (Whyte et al., 2012). In animals capable of regeneration for example zebrafish and axolotls, inhibition of Wnt signalling disrupts or impairs dorsal fin, retinal and limb regenerative capacity respectively (Gurley et al., 2008; Kawakami et al., 2006; Ramachandran et al., 2011). Blocking Wnt is thought to disrupt the recruitment of stem/progenitor cells to the site of injury and in skin it was shown in mice that inhibition of this pathway resulted in the prevention of effective healing of the epidermis as hair and sweat gland was absent. Interestingly, overexpression of Wnt ligand (Wnt-7a) in the epidermis promoted hair follicle neogenesis, a key criteria of functioning skin (Ito et al., 2007). Both hair and teeth are derivatives of the ectoderm and share common developmental regulation of sequential and reciprocal interactions between the epithelium and mesenchyme (Pispa and Thesleff, 2003). Thus, unsurprisingly, Wnt signalling has been shown to play an integral role during odontogenesis and several Wnt genes are broadly expressed in the oral and dental epithelium (Sarkar and Sharpe, 1999). Targeted inactivation of lymphoid enhancer factor-1 (LEF-1), a nuclear mediator of Wnt signalling, leads to the arrest of tooth development at the bud stage (Kratochwil et al., 2002; Sasaki et al., 2005; van Genderen et al., 1994). More recently, expression of Axin2 has also indicated a role for canonical Wnt signalling in the development of the crown and root during both pre- and postnatal tooth development (Lohi et al., 2010). In terms of dental tissue repair, Yamashiro and colleagues demonstrated that Wnt10a is specifically expressed in the odontoblast cells in mouse molars and co-localises with dentin sialophosphoprotein (DSPP)(Yamashiro et al., 2007). This tooth specific non-collagenous matrix protein regulates dentine mineralisation and is secreted in fully differentiated

odontoblasts (Arana-Chavez and Massa, 2004). Thus indicating that Wnt plays a role in regulating dentine mineralisation in the mature secretory odontoblasts and further evidence of specific Wnt10a expression in epithelial secondary enamel knots reveals a potential link between tooth morphogenesis and differentiation of odontoblasts that is Wnt associated (Yamashiro et al., 2007). Other research implicating the importance of Wnt signalling in dentinogenesis derives from data showing that the inhibition of mesenchymal Wnt/ β-catenin by Dickkopf-related protein 1 (Dkk1) (a potent antagonist of the pathway) over-expression in mice leads to impaired post-natal mandibular molar dentine formation (Han et al., 2011). Collectively, these data suggest Wnt/ β-catenin signalling originating from the pulp mesenchyme is key to the formation of dentine, thus local modulation of this pathway could provide therapeutic benefits and enable effective tooth regeneration (Yang and Liu, 2013). However, to date, little is known about the *in-vivo* response during tooth damage in terms of Wnt signalling, thus future work focusing on this will yield further clues to the mechanisms and interplay with other cellular processes important for tooth repair. In order to monitor the Wnt/ β-catenin signalling activity *in vivo*, mouse reporter lines should be used. At present, several reporter lines have been developed to follow canonical Wnt signalling activity, the TCF Optimal Promoter (TOP)-β-galatosidase (TOPGAL) reporter line allows the detection of β-catenin/TCF complexes as does the β-catenin Activated Transgene (BAT)-β-galatosidase (BATGAL) reporter (DasGupta and Fuchs, 1999; Maretto et al., 2003). While the Axin2[LacZ] reporter line is considered the most accurate readout for canonical Wnt signalling because the *lacZ* reporter gene is knocked into the *Axin2* locus and therefore is under control of the Axin2 promoter, which is a direct transcriptional target of Wnt/ β-catenin signalling (Lustig et al., 2002). Axin2 also known as Conductin or Axil, is a homolog of Axin within the cytoplasm and forms part of the destruction complex thus forms a negative feedback loop in the pathway (Jho et al., 2002). Interestingly a study comparing the lungs of the three described Wnt reporter mouse lines

revealed that the optimal choice of Wnt reporter line is based upon whether an up- or downregulation of Wnt activity is being evaluated. However, Alam and colleagues concluded that the Axin2^{LacZ} mouse line is most robust for the detection of Wnt signalling especially in the context of injury (Al Alam et al., 2011).

1.6 Aim of the research project

MSCs are a population of cells resident in adult stromal tissues responsible for tissue growth and/or repair, whose biology has mainly been studied *in vitro*. The rodent incisor is a continuously growing organ and provides an excellent model to study MSC contributions to both growth and repair. Previous reports have demonstrated a role for pericytes during injury repair of the mouse incisor and that growth is supported by the MSCs that reside in a niche at the cervical end of the tooth. Interestingly, the MSCs responsible for growth also have the capacity to respond to injury. Based on this, the hypothesis was that mesenchymal pulp cells from different anatomical regions of the incisor display varying stemness and *in vitro* characterization of these cells was conducted initially. Since cell migration is a process believed to be involved in effective injury repair, the cell migration capacity of the pulp cells was analysed to address the question of what molecular mechanisms underlie stem cell recruitment.

The properties of MSCs *in vitro* alone cannot accurately reflect the *in vivo* response to injury. Given that canonical Wnt signalling plays crucial roles in tooth development, postnatal dentinogenesis as well as stem cell regulation, this signalling pathway was hypothesised to be involved in tooth injury and repair. Experimental *in vivo* damage experiments were conducted to address this, using both wild type and a Wnt reporter mouse line. Since pericytes have already been described to contribute to incisor tooth repair, it is likely that the pericytes are a candidate population to respond to injury

response cues such as Wnt signals therefore, lineage tracing of the pericytes in the context of *in vivo* tooth damage in molars was also investigated.

From a different perspective of studying the mouse incisor, we examined the incisal tips. The lifelong growth of these teeth is counterbalanced by attrition at the tip via feeding and gnawing. This therefore provides an opportunity to analyse an alternative form of constant, natural tooth damage in situ. The tip is distant from the cervical loop which is where most of the stem cell population for growth is located, so we hypothesised that the population responsible for its maintenance would likely be of a different origin such as the pericyte population. Using this unique injury model designed by nature, mesenchymal tissue organ repair was mimicked and confirmed a pericyte role for a proposed "incisal tip niche".

2. Materials and methods

2.1 Reagents and solutions

2.1.1 *In vitro* cell culture

Alcian blue	Sigma, A5268
Alizarin Red S	Sigma, A5533
AlphaMEM medium	Lonza, BE02-002F
Antibiotic-antimycotic solution	Sigma, A5955
Ascorbic acid	Sigma, 49752
Dulbecco's phosphate buffered saline	Sigma, D8537
Fetal bovine serum	Lonza, DE14-801F
Oil Red O	Sigma, O0625
STEMPRO adipogenesis kit	Gibco, A10070-01
STEMPRO chondrogenesis kit	GIbco, A10071-01
STEMPRO osteogenesis kit	Gibco, A10072-01
TryplE Express	Gibco, 12563-011
FGF8	R&D Systems, 423-F8
BFGF	R&D Systems, 233-FB
BMP4	R&D Systems, 314-BP
WNT3A	R&D Systems, 1324-WN

2.1.2 Tissue processing

DePex mounting medium	BDH, 360294H
Diethyl pyrocarbonate (DEPC)	Sigma, D5758
Ehrlich's Haematoxylin	Solmedia, HST003
Eosin, aqueouos solution (0.5% Eosin Y in distilled H_2O)	Riedel-de Haën, 32617
Ethanol	VWR, 101077Y
Ethylenediaminetetraacetic acid (EDTA)	VWR, 20302.293
Formic acid, 98%	Fisher, F/1850/PB17
Histoclear	National Diagnostics, HS-202
Neomount mounting medium	Merck, 1090160500
Paraformaldehyde	Sigma, P6148
Ultraplast Polyisobutylene Histological Wax	Solmedia, WAX060

2.1.3 β-galactosidase staining

1,2,3,4 -Tetrahydronaphthalene	Sigma, 429325
5-bromo-4-chloro-3-indolyl-β-D-galactopyranoside (X-Gal)	Fermentas, R0404
Eosin, Alcoholic Solution (in Ethanol)	
0.25% Eosin Y disodium salt	Riedel-de Haën, 32617
21% Distilled H_2O	

0.5%ml Glacial Acetic Acid   VWR, 20104.334

Glutaraldehyde   MERCK, 1042390250

IGEPAL CA-630 (NP-40)   Sigma, I3021

Magnesium chloride ($MgCl_2$)   Fisher, BP214-500

Methanol   Fisher, M/4056/PB17

Nuclear Fast Red (in H_2O)

    0.2% Nuclear Fast Red   Sigma, 60700

    10% Aluminum potassium sulfate   Fisher, A/2400/53

Phosphate buffered saline (PBS)   Fisher, BP-665-1

Potassium ferricyanide ($K_3[Fe(CN)_6]$)   BDH,102044D

Potassium ferrocyanide ($K_4[Fe(CN)_6]$)   BDH, 102054F

Propan-2-ol (isopropanol)   AcorsOrganics, 389710025

Sodium deoxycholate   Sigma, D6750

Trizma® base   (Tris base)   Sigma, T1503

2.1.4 Molecular biology techniques

5-alpha Competent E. Coli cells   New Eng Biolabs,C2988J

Ampicillin Sodium Salts (50 mg/ml)   Sigma, A9518

Fast Plasmid® Mini   Eppendorf AG, 955150601

Luria-Bertani (LB) broth

1% Tryptone	Oxoid, LP0042
1% NaCl	BDH, 102415K
0.5% Yeast	Oxoid, LP0021

Luria-Bertani (LB) agar

1% Tryptone	Oxoid, LP0042
1% NaCl	BDH, 102415K
0.5% Yeast	Oxoid, LP0042
1.5% Agar	Oxoid, LP0011

QIAGEN Plasmid Maxi Kit	QIAGEN, 12163
QIAquick® Gel Extraction Kit	QIAGEN, 28706
Restriction enzymes and buffers	Promega

2.1.5 In-situ hybridization

Polymerase enzymes	Promega
Acetic anhydride	BDH, 100022M
Anti-Digoxigenin-AP Fab fragments	Roche, 11093274910
BCIP (5-Bromo-4-chloro-3-indolyl-phosphate)	Roche, 11383221001

Boehringer Blocking Reagent	Roche, 11096176001
CHAPS	Sigma, C3023
50x Denhardt's	
1% (w/v) Ficoll 400	Sigma, F4375
1% (w/v) Polyvinylpyrrolidone	BDH, 436032C
1% (w/v) Bovine Serum Albumin	Sigma, A9647
50% Dextran sulphate	Chemicon, 0702051849
DIG RNA labelling Mix (10X)	Roche, 11277073910
DL-Dithiothreitol (DTT)	MP Biomedicals, 100597
Formamide	Merck, K36952408
Glycine	Sigma, G7403
Heparin lithium salt, from Porcine Interstinal mucosa	Sigma, H08078
IGEPAL CA-630	Sigma, I3021
NBT (4-Nitro blue tetrazolium chloride)	Roche, 11383213001
Polyvinyl alcohol	BDH, 297914D
Proteinase K	Sigma, P2308
SDS (Sodium dodecyl sulfate)	Severn, 30-33-50
SigmaSpin™Post-Reaction Clean-Up Column	Sigma, 5059
TEA (Triethanolamine)	BDH, 103704U

Triton® X-100 (Iso-Octylphenoxypolyethoxyethanol)   BDH, 306324N

tRNA (RNA from yeast)   Roche, 109223

Tween-20   Sigma, P7949

Table 1. Details of plasmids used for making probes

Gene	Vector	Size of insert	Digestion enzyme to linearise plasmid DNA	Polymerase enzyme to generate antisense probe
Axin2		2.5kb	XbaI	T7
Ptc1	pBluescript	1kb	BamHI	T3

2.1.6 *In-vivo* administered chemicals

Tamoxifen   Sigma, T5648

Corn oil   Sigma, C8267

Tetracycline   Sigma, T4062

EMLA anaesthetic   Centaur, 21190516

Hynorm   Centaur, 30209036

Hynovel   Centaur, 23191407

Buprenorphine   Centaur,30276871

2.2 *In-vitro* experimental procedures

2.2.1 Primary rat dental pulp cell culture

Dental pulps from five day old wistar rat pups were used for all *in vitro* experiments. The animals were sacrificed by cervical dislocation followed by decapitation. Using sterile tweezers, both mandibular and maxillary incisors were carefully dissected out in cold sterile 1XPBS supplemented with antibiotic-antimycotic solution. The dental pulp was then extracted by squeezing the tooth gently to withdraw the whole pulp mesenchyme. The tissue was then divided into the cervical loop and incisor body regions by removing a small section of the central region of the pulp to ensure two distinct populations (Figure 2.1). After washing with sterile 1XPBS, the dissected tissues were minced into fine pieces and digested with TrypLE Select by incubating at 37°C. Digestion was monitored every 10-15 minutes by aspirating and resuspending the tissue until the solution became cloudy and individual pieces of tissue was no longer observed. The cells were centrifuged at 1200rpm for 5 minutes followed by removal of the supernatant and resuspension in expansion medium consisting of Alpha Minimum Essential Medium (αMEM) supplemented with 15% fetal bovine serum, 1% antibiotic-antimycotic and 0.1% 0.1M L-ascorbic acid. The resuspended cells were then filtered through a 70µm cell strainer to obtain single cell suspensions.
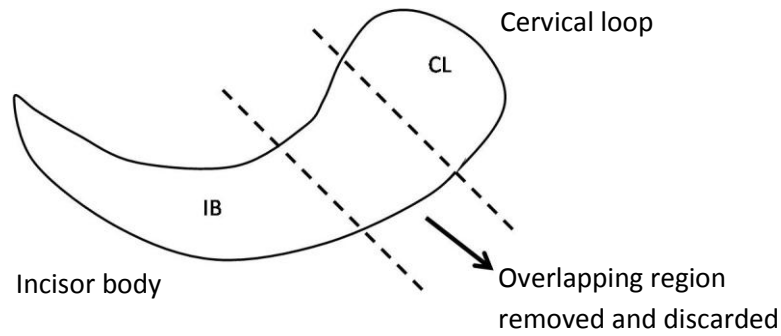
Figure 2.1 Schematic of the rat incisor pulp
After extraction of the intact dental pulp, and removal of the dental epithelium, the overlapping region between the cervical loop and the incisor body was removed to ensure two distinct populations of cells. In this experimental work, where the text refers to "cervical loop" and "incisor body" cells, unless otherwise stated, this refers to mesenchyme derived pulp cells only. Abbeviations CL: cervical loop, IB: incisor body.

2.2.2 Growth curve

Cervical loop and incisor body cells were seeded into 3, 6 well plates at a density of 1×10^4 cells per well and cultured in αMEM expansion medium at 37^oC , 5% CO_2. Media was replaced every 2-3 days and cells were counted in triplicate by trypan blue exclusion at days 3, 6, 9, 12, 15 and 18 after seeding. The mean and standard deviation were calculated.

2.2.3 Differentiation experiments

2.2.3.1 Osteogenic differentiation

Cells were seeded into 24 well plate wells at 5×10^3 cells/cm^2 with αMEM and incubated at 37^oC, 5% CO2 , in a humidified atmosphere for 4 days before replacing with osteogenesis differentiation medium (Gibco-Invitrogen, Paisley, UK) supplemented with 1% antibiotic-

antimycotic. Media was replaced every 3 days and the osteogenic cultures were fixed and processed for 0.2% Alizarin Red S staining after 9 days to visualise calcium deposition.

2.2.3.2 Chondrogenic differentiation

Micromass cultures were generated by seeding 5μL droplets of 80,000 cells in the centre of 24 well plate wells and incubating at 37°C for 2 hours under humidified conditions. After allowing the cells to attach, warmed chondrogenesis media (Gibco-Invitrogen, Paisley, UK) supplemented with 1% antibiotic-antimycotic was added to the wells taking care to avoid disturbing the cell micromass. Cultures were refed every 2-3 days, after 16 days the chondrogenic pellets were processed for Alcian blue staining. For alcian blue staining the cells were washed with PBS twice and fixed in 4% paraformaldehyde for 30 minutes. Alcian blue solution was prepared first (0.5% Alcian blue in 95% ethanol) then, cells were washed twice with 0.1M HCl before incubating overnight with a 4:1 solution of alcian blue (4:1 0.1M HCl to Alcian blue) at room temperature. Cells were washed with 70% ethanol before observing for the presence of blue staining demonstrating synthesis of proteoglycans.

2.2.3.3 Adipogenic differentiation

Cells were seeded at a density of $1x10^4$ cells/cm^2 into 24 well plate wells and cultured in αMEM for 4 days in 37°C, 5% CO_2, under humidified conditions before replacing with adipogenic differentiation medium (Gibco-Invitrogen, Paisley, UK) supplemented with 1% antibiotic-antimycotic. The cultures were refed every 3-4 days. After 3 weeks in culture, the cells were washed and fixed as previously described. Oil red O working solution was prepared by diluting 30mL of stock stain (0.5g Oil Red O dissolved in 100mL isopropanol using gentle heat from a water bath) with 20mL distilled water. After leaving to stand for

10 minutes, the solution was filtered and used immediately. Cells were washed in distilled water for a few minutes, rinsed in 60% isopropanol, stained with freshly prepared Oil Red O working solution for 10 minutes, rinsed in 60% isopropanol again. Cells were rinsed with distilled water and observed for the presence of red stained lipid droplets.

2.2.4 CFU Assay

Colony forming assays were performed by seeding 10^3 cells/well into 6 well culture plates in αMEM expansion medium. Medium was changed every 3 days and after 2 weeks the wells were stained directly with crystal violet (0.5% in 2% ethanol) to visualise colony formation. Whole 6 well plates were scanned in an Epson 1200U photo scanner and colonies were quantified using Image J software where >50 cells was classed as a colony.

2.2.5 Scratch migration assay

The cells were seeded with αMEM medium at a density of $6x10^4$ cells/ well into 12 well plates and cultured until confluent. After reaching confluency a wound was created by scraping a channel into the monolayer in each well using the P100 pipette tip. Images were taken daily until closure of the gap. Wound areas were measured using Image J software and the rate of wound closure was calculated.

2.2.6 Transswell migration assay

Prior to seeding, the lower surface of the transwell membranes were coated with collagen type I (10μg/mL) for 1 hour inside a 37°C, 5% CO_2 humidified tissue culture incubator. Dental pulp cells were seeded in triplicate onto the upper surface of the transwell membrane in migration buffer (2mM $CaCl_2$, 1mM $MgCl_2$, 0.2mM $MnCl_2$ and 0.5% BSA) at a density of 2.5x10^4 cells/ well. The bottom wells were filled with the same migration medium with 10ng/mL FGF8b, 100ng/mL bFGF, 100ng/mL BMP4, 100ng/mL Wnt3a or without growth factors and the 24 well plate was subsequently incubated at 37°C for 24 hours. For analysis, the media within the transwells was discarded and the upper surface of the membrane was scrubbed with a cotton swab to remove the non migrated cells (Figure 2.2). After washing briefly in 1X PBS, the whole membrane was then fixed in 4% PFA for 15 minutes at room temperature followed by staining in 0.5% crystal violet in 2% ethanol. Excess staining was gently rinsed off with tap water and the inserts were air dried overnight at room temperature. To quantify cell migration, 18 random microscopic fields were chosen for analysis and images were taken on a Zeiss microscope with the AxioCam HRC (Zeiss) using the Axiovision software.
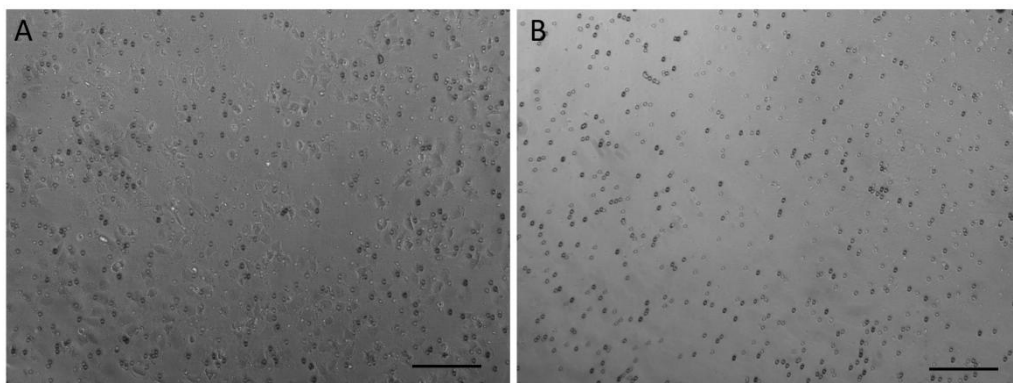
Figure 2.2 Non-migrated cell removal in transwell assay
To verify the efficiency in removal of the non-migrated cells on the upper surface of the membrane, images were taken before and after scrubbing with the cotton bud. Non-migrated cells are visible prior to cell removal (A) and are entirely removed following the scrubbing process (B). Scale bars represent 300μm.

2.2.7 MTT Assay

Cells were seeded in triplicate at a density of 5×10^3 cells/well (100µL) into a 96 well plate with migration medium containing growth factors as described in section 2.2.6. Triplicate wells without growth factors were used as controls. After a 24 hour incubation period at 37^oC, the medium was removed and replaced with 25µL of MTT (5mg/mL) followed by incubation for 4 hours at 37^oC to allow the cells to metabolise MTT and yield purple formazan crystals. All media was removed from each well and the cells were then lysed with 100µL of extraction buffer (20% SDS in 50% dimethyl formamide) per well. The plate was then swirled gently before reading absorbance at 570nm using a spectrophotometer plate reader.

2.2.8 Scratch migration towards dentine

Cells were seeded into 10mm x 35mm cell culture dishes (Greiner, CELLSTAR) using αMEM expansion medium cultured until 100% confluent. Once confluency was reached, cells were removed from half of the dish using a cell scraper (Sarstedt) and twice rinsed in PBS to remove any remaining floating cells. After replacing each well with fresh αMEM, the cell free zone was dried by tilting the plate to expose it to air, taking care to avoid drying the wound edge. Using collagen II solution (BD Biosciences) a single piece of fresh dentine approximately $2mm^2$ isolated from the lower incisor was attached to the cell free area 2mm from the scratch wound edge before carefully returning the plate to a horizontal position (Figure 2.3). Images of the wound edge were taken daily using the Nikon Eclipse TS100 microscope to track cell movement.
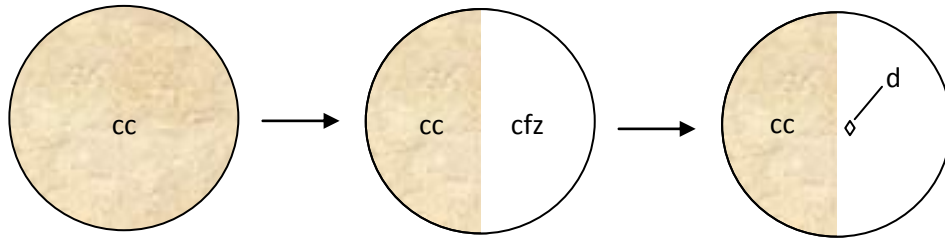
Figure 2.3 Schematic of the scratch wound dentine assay
Half the well of a confluent monolayer of cells was scraped to achieve a cell free zone in which freshly dissected dentine was adhered to using collagen. Abbreviations, cc: confluent cells, cfz: cell free zone, d: dentine.

2.3 Collection of neonatal and adult mouse tissues

All animal experiments were approved by the UK Home Office. Mouse colonies of wild type CD1 and transgenic mice were maintained with the assistance of Mr Alex Huhn. Neonatal and adult tissues were collected following the Home Office schedule one specification. For postnatal pups, the day the litter was born was assigned as postnatal day 0 (P0). Cervical dislocation was performed to sacrifice the animals followed by decapitation and the heads were collected in ice-cold 1XPBS.

2.4 Tissue processing

2.4.1 Fixation, decalcification and dehydration of mouse tissue

Mandibles and maxillae of postnatal mice were carefully dissected in cold 1XPBS and subsequently fixed overnight in 4% paraformaldehyde (PFA) at 4°C. The P5 tissues were decalcified in 10% EDTA pH8.0 at 4°C for 1-2 weeks. For adult tissues, depending on the subsequent processing steps, the samples were either decalcified for 3-5 weeks with

Morse's Solution (10% sodium citrate, 22.5% formic acid) at room temperature on a shaker or decalcified in 10% EDTA pH7.4 at $4^{\circ}C$ for 4-6 weeks. All decalcifying solutions were changed every other day. Following fixation or decalcification, tissues were washed thoroughly with 1X nuclease- free PBS to eliminate residual fixative or decalcification solution.

2.4.2 Paraffin wax embedding

After decalcification, the samples were then dehydrated through a series of ascending ethanol concentrations (30%, 50%, 70%) the duration of each step was 6 hours – overnight per change and then subsequent further processing was conducted with the Leica ASP300 Tissue Processor (Table 2). After the long incubation stage in Ultraplast wax, mandibles and maxillae were embedded sagittally using stainless steel moulds. Wax blocks were stored at room temperature until sectioned.

Table 2. Tissue processing protocol

Solution	P5 tissue	Adult tissue
70% IMS	30 min	3 hours
90% IMS	2 hours	3 hours
4 x 100% IMS	2 hours each	3 hours each
3 x Xylene	2 hours each	3 hours each
3 x Ultraplast wax	2 hours each	4 hours each

2.4.3 Tissue sectioning and mounting

Wax blocks were initially trimmed to remove excess wax and then sectioned using a microtome (Leica RM2245) to produce wax ribbons 7 μm in thickness. Consecutive sections were mounted onto glass slides (Superfrost®Plus, VWR™) to achieve a series of slides each with a set of similar serial sections.

2.4.4 Haematoxylin and eosin staining

To view the general cell morphology, sections were stained with haematoxylin and eosin (H&E). Haematoxylin stains the nuclei blue while cytoplasm, connective tissue and other extracellular structures are stained pink or red by eosin. Selected sections were deparaffinized with 2 x 10 minute histoclear washes followed by rehydration through a graded series of 2 minute ethanol washes (100%, 90%, 70% and 50%). Afterwards, sections were washed for 10 minutes in distilled water before submersion in Erhlich's Haematoxylin for 10 minutes. Excess haematoxylin was removed by washing the sections under running water for 10 minutes. Next, the sections were rinsed briefly in distilled water and then immersed in acid alcohol (0.5% HCl, 70% ethanol) for 15 seconds. The sections were then stained with 0.5% aqueous Eosin for 2 minutes and washed in distilled water before dehydration through a series of ethanol washes (70%, 90% and two 100%) for 2 minutes each. After clearing in two changes of histoclear, the sections were coverslipped with Neomount® under the fume hood. Sections were viewed in brightfield using the Zeiss microscope (Axioskope 2 plus) and captured with an AxioCam HRC using Axiovision software.

2.4.5 Aniline blue staining

The slides were placed into two histoclear washes 10 minutes each, followed by rehydration in descending ethanol washes (100%, 90%, 70%, 50%) all at 2 minutes each, after a 2 minute deionised water wash the slides were stained with Ehrlich's haematoxylin for 10 minutes. Afterwards, the sections were washed gently in running water for 10 minutes and rinsed in deionised water before staining in 2.5% aniline blue for 2 minutes. Following this, the slides were rinsed briefly in deionised water and then submerged in 1% acetic acid for 5 minutes followed by another deionised water rinse. The slides were dehydrated with 90% ethanol (1 minute) and two 100% ethanol washes at 5 minutes each. Before coverslipping, with neomount the slides were cleared in two 5 minute washes with histoclear and subsequently left to dry overnight at room temperature in a fume hood.

2.5 β-galactosidase staining for LacZ activity

2.5.1 Whole mount β-galactosidase staining

To visualise lacZ activity in the lacZ reporter mice samples used in this work, whole mount β-galactosidase staining was performed. After dissection, the samples (mandibles or incisors) were washed several times in 1XPBS followed by fixation in 1%PFA: 0.2% glutaraldehyde in 1XPBS solution at 4oC overnight. After fixation, to remove any remaining fixative, the samples were washed in 1XPBS three times followed immediately by incubation in x-gal staining solution (Table 3) in a 37°C oven and protected from light. After 24 hours when adequate blue staining had developed, the samples were rinsed in 1XPBS

three times for 5 minutes each to stop the reaction followed by a post-fix step in 4% PFA

for 1 hour at room temperature.

Table 3. Reagents in X-gal staining solution

Components	Concentration
Tris HCl pH 7.3	10mM
Sodium deoxycholate	0.005%
IGEPAL	0.01%
$K_3Fe(CN)_6$	5mM
$K_4Fe(CN)_6$	5mM
$MgCl_2$	2mM
X-Gal	0.8 mg/ml
1x PBS	up to final volume

2.5.2 Preparation of samples for cryo-embedding and sectioning

Post-fixation, the whole mount x-gal stained samples were washed thoroughly in 1XPBS

three times for 10-15 minutes each to remove residual PFA. The tissues were then

decalcified as previously described in section 2.4.1 before rinsing in 1XPBS to remove any

remaining decalcification solution. In preparation for cryoembedding the samples were

dehydrated in 15% sucrose solution containing 2mM $MgCl_2$ at 4^oC overnight followed by a

further dehydration step in 30% sucrose solution with 2mM $MgCl_2$ again at 4^oC overnight.

Prior to embedding, the samples were placed into Peel-A-Way embedding molds and

covered in OCT medium for 1 hour before embedding in a sagittal orientation by

submerging the molds into a mixture of dry ice and 70% ethanol. The samples were stored in -80°C before sectioning using a cryostat (Bright OTF) into 12μm sections and mounting directly onto Superfrost®Plus glass slides before storing at -80°C until further processing.

2.5.3 Counterstaining of x-gal stained sections

To better visualise cell morphology of the unstained structures, the x-gal stained cryosections were counterstained with nuclear fast red. The slides were first removed from the -80°C freezer and allowed to equilibrate to room temperature for 15 minutes before washing in 1XPBS three times 5 minutes each to remove residual OCT embedding medium, followed by counterstaining in 0.2% nuclear fast red for approximately 1-3 minutes until adequate staining was achieved. The sections were subsequently dehydrated in 70%, 90% and two 100% ethanol washes followed by histoclear for 5 minutes twice and coverslipped with Neomount and left to air dry overnight at room temperature in a fume cupboard.

2.6 Molecular biology techniques

2.6.1 Plasmid DNA transformation to competent E coli cells

A 50μL aliquot of *NEB* 5-alpha competent *E.coli* cells was thawed on ice before adding approximately 1.0ng of plasmid DNA. After gentle mixing, the tube was placed on ice for 30minutes to aid DNA adherence to the bacterial cell membrane. The cells were subsequently heat shocked at 42°C for 45 seconds and placed on ice immediately for 2 minutes. Luria-Bertani (LB) medium (450μL) was added to the mixture and incubated for 1

hour at 37°C. LB- agar plates with 100µg/mL ampicillin were streaked with 30-50µL of the transformed cells and then inverted before placing in the 37°C oven to incubate overnight. Single cell colonies were confirmed the next morning and the plates were stored for up to one week at 4°C.

2.6.2 Amplification and isolation of plasmid DNA

A single colony was selected from the LB agar plate and inoculated into either 4mL of LB medium (mini-preparation) or 200mL of LB medium (maxi-preparation) along with 100µg/mL ampicillin. This starter culture was then incubated for 12-16h at 37°C while shaking at 250rpm. Following the manufacturer's instructions, plasmid DNA was isolated using the QIAprep Spin Miniprep kit (mini-preps) and the QIAGEN Plasmid Plus Maxi kit was used to isolate and purify large quantities of plasmid DNA obtained from the maxi cultures.

2.6.3 DNA Quantification and sequencing

Plasmid DNA concentration was determined using the *NanoDrop*® ND-1000 spectrophotometer by placing 1.5µL of the DNA sample onto the pedestal and measuring the absorbance at 260nm. Verification that the plasmid contained the gene of interest was achieved by sequencing the plasmid DNA (source bioscience, UK.). Using the Basic Local Alignment Search Tool for Nucleotides (BLASTN) the sequencing results obtained were queried on the National Centre for Biotechnology Information (NCBI) website.

2.6.4 Preparation of DIG-labelled RNA probes

2.6.4.1 Linearisation and purification of plasmid DNA

To generate the antisense probes, 10µg of plasmid DNA containing the specific gene sequence was linearised at the 5' end of the insert using the appropriate restriction enzyme in a reaction mixture as shown in Table 4. The linearization reaction mixture was incubated at 37°C for 3 hours. To confirm complete digestion, 1µL of the linearized DNA product (approx. 400ng of linearized DNA) and the equivalent quantity of non-linearised DNA along with a 1kb DNA ladder were loaded onto a 1% w/v agarose gel. Subsequent electrophoresis was performed at 100V for 30-45 minutes until clear separation of the bands was achieved and DNA was visualised with an UV transilluminator light (3UV transilluminator). The linearised plasmid DNA was then purified using the QIAquick Gel Extraction Kit following the manufacturer's instructions.

Table 4. Reagents used to linearise plasmid DNA (per reaction)

Reagents	Volume
Plasmid DNA	20 µg
Bovine serum albumin (10µg/µl)	0.5 µl
Restriction enzyme	2 U/ µg plasmid DNA
10x Buffer	5 µl
Nuclease-free H$_2$O	up to final volume (50 µl)

2.6.4.2 Synthesis of antisense DIG-labelled RNA probe

Antisense RNA probes were synthesised from each linearised plasmid by the addition of reagents detailed in Table 5. After thorough mixing, the reaction mixture was incubated at 37°C for 1 hour. Next, 1μL of the specific polymerase was added followed by further incubation at the same temperature for an additional hour. Afterwards, 1μL of the transcribed DNA was analyzed by gel electrophoresis to confirm successful transcription of the RNA probe. The DNA template was then removed by adding 2μL of RNase free DNase to the mixture and incubated at 37°C for 15 minutes. The synthesised RNA was subsequently purified using a SigmaSpin[TM]Post-Reaction Clean-Up Column following the manufacturer's instructions and stored at -80°C.

Table 5. Reagents used to transcribe a DIG-labelled RNA probe (per reaction)

Reagents	Volume
Linearised DNA	1μg
100mM dTT	4μL
5X Transcription Buffer	8μL
RNasin (40U/μL)	1μL
DIG RNA Nucleoside Labelling Mix	2μL
Polymerase enzyme (20U/μL)	1μL
Nuclease-free H_2O	Up to the final volume of 40μL

2.6.5 DIG *in situ* hybridization on paraffin sections

2.6.5.1 Deparaffinization and hybridization of probe

All glassware used in this protocol was baked overnight at 180°C prior to use. In addition, all the solutions used were DEPC-treated and autoclaved. Slides containing the wax sections were deparaffinized in two, 15 minute histoclear washes, followed by rehydration through descending ethanol washes (100%, 90%, 70%- 2 minutes twice each) and finally washed in RNase free H_2O (1minute, twice). After rehydration, the tissues were fixed in 4% paraformaldehyde in 1XPBS for 10 minutes at room temperature followed by washing in 1XPBS (5mins, twice). To permeabilise the tissues, the slides were incubated in 10μg/mL proteinase K in 1XPBS for 8 minutes followed by a 5 minute 1XPBS wash and refixation in 4% PFA for 5 minutes all at room temperature. After rinsing with 1XPBS for a further 5 minutes, the remaining positive charges in the tissue were removed by acetylation for 10 minutes at room temperature in a solution of 125μL acetic anhydride in 50mL 0.1M Triethanolamine made immediately before use. Afterwards the slides were washed with 1xPBS (5 minutes, three times) and dehydrated in 70% ethanol (5 minutes) and 95% ethanol (1 minute) before air drying until the tissues became white.

For hybridization, the hybridization box was pre-warmed with paper towel soaked in 50% formamide and water. Approximately 20-50ng of DIG-labelled RNA probe diluted into 1mL of hybridization solution (Table 6) was denatured by heating at 80°C for 2 minutes followed immediately by 2 minutes on ice before applying 300μL of probe to each slide. Glass coverslips were placed onto each slide to evenly spread the probe and prevent evaporation and then carefully placed inside the hybridization box. The hybridization box was subsequently sealed with tape to retain humidity and incubated overnight at 65°C in the

hybrisation oven where a 300mL beaker of water was placed inside to maintain a stable humidity level.

Table 6. Reagents within hybridisation solution

Reagents	Volume (mL)
Formamide	25
50% Dextran sulphate	10
50X Denhardt's solution	1
Yeast tRNA (10mg/mL)	1.25
5M NaCl (DEPC treated)	3
1M Tris HCL pH8	1
0.5M EDTA pH8	0.5
1M sodium phosphate monobasic	0.5
20% N-Lauroyl sarcosine sodium	2.5
Nuclease free H_2O	5.25

2.6.5.2 Post hybridization washes and signal detection

After hybridization, the glass coverslips were removed by submerging in pre-warmed 5X SSC solution. The slides were then placed into prewarmed high stringency wash for 30 minutes inside the 65°C oven to remove the unbound probe. This was followed by three, 10 minute washes in RNAse buffer (0.5M NaCl, 10mM Tris-HCL-pH7.5, 5mM EDTA-pH8 in dH2O) before treating the slides with RNAse buffer containing 20μg/mL RNaseA for 30 minutes at 37°C followed by a final 15 minute RNAse buffer wash. The high stringency wash at 65°C was repeated on the slides for 20 minutes twice and subsequently washed in

2x SSC and 0.1X SSC at 37°C both for 15 minutes each. A final MABT wash (100 mM maleic acid pH7.5, 150 mM NaCl, 0.1% Tween 20) at room temperature for 15 minutes was performed before the sections were blocked in blocking buffer containing 10% heat inactivated sheep serum and 2% BBR in MABT for 1 hour at room temperature. Finally, the sections were incubated in blocking buffer supplemented with a 1:5000 dilution of anti-digoxigenin antibody conjugated to alkaline phosphatase overnight at 4°C for probe detection. The following morning the antibody was removed with four, 15 minute washes in MABT at room temperature. The sections were then washed for 10 minutes twice in freshly made NTMT buffer (100mM NaCl, 100mM Tris-HCl pH9.5, 50mM MgCl$_2$, 0.1% Tween-20) supplemented with 0.5mg/mL levamisole to help reduce background alkaline phosphatase activity.

Color reaction was developed at room temperature in the dark by incubating the sections with 2.5 µl/ml NBT and 1.7 µl/ml BCIP in a colour development solution consisting of 50% Polyvinylalcohol, 100mM Tris-HCl pH 9.5, 100mM NaCl, 5mM MgCl$_2$ and 0.1% Tween-20. When sufficient colour had developed (blue-purple), the reaction was stopped by rinsing with 1X PBS for 2 minutes, post fixing in 4% PFA for 1 minute and a briefly rinsing in 1X PBS before counterstaining in 0.005% nuclear fast red for 1 minute. The slides were then dehydrated in a series of increasing ethanol washes (70%, 95%, 100%) for 2 minutes twice each before being air-dried and mounted with cover slips using DePex mounting medium.

2.7 In vivo experimental procedures

2.7.1 Tamoxifen administration

Adult NG2creERT; R26R and NestincreERT;R26R transgenic mice were given 3 intraperitonial injection of 4 mg tamoxifen (200µl of 20mg/ml tamoxifen in corn oil solution) per 30 g body weight over 3 weeks to activate the cre-expression in NG2/Nestin expressing cells. Following tamoxifen administration, the NG2 mice were then use for the *in vivo* molar damage experiments and the Nestin mice were used for incisor tip analysis. To visualise the cre-activated gene expression, staining for β-galactosidase (LacZ) activity previously described in 2.5 was performed.

2.7.2 Tetracycline administration

A single intraperitoneal injection of 41.6 nmol/g body weight of tetracycline hydrochloride was administered to adult CD1 mice before collection after 24 hours. The mandibles were dissected out and fixed overnight in 4% PFA at 4°C. The tissues were dehydrated in sucrose, embedded in OCT medium as detailed in 2.5.2 and sectioned (approximately 100µm) on the Bright OTF cryostat. Samples were imaged using a Leica SP5 laser-scanning confocal microscope with an ultraviolet laser (LD405 nm) and 405- to 488-nm excitation filter.

2.7.3 *In vivo* incisor tooth damage

All incisor tooth damage experiments were performed by Dr Andrea Mantesso. Lower mandibles of P5 wild type CD1 mice or Axin2$^{LacZ/+}$ mice were locally anaesthetized using emla anaesthetic cream. After approximately 10 minutes, an 18-gauge needle was used to pierce the right mandible resulting in tooth damage and left mandibles were used as controls. After 24 hours, the mice were sacrificed and the mandibles were fixed and processed as described in section 2.4.1. For the Axin2 samples, LacZ activity was

determined following section 2.5.1 and the wild type mice sampled were used for in situ hybridization as previously described.

2.7.4 *In vivo* molar tooth damage

All mice were anaesthetised and the damage procedure was performed by Mr Alex Huhn. For the anaesthetic, a 1:1:2 ratio of hypnorm: hynovel: ddH$_2$O was administered at 1µL per gram body weight. After the mice were unconscious, using a ball tip diamond burr connected to a high speed dental drill handpiece, the centre of the maxillary first molars were pierced to generate molar pulp damage. Post surgery, 10 µL per gram body weight of buprenorphine was administered the to the mice for pain relief and they were placed in 37°C for 1 hour to recover and at 30°C for 24 hours before returning to room temperature. Post surgery, the mice were fed on a mash (softened pellets) diet.

2.7.5 Raman microspectroscopy

Adult CD1 wild-type mouse incisors were sent to Dr. Molly M. Gentleman at the department of Materials Science and Engineering, Stony Brook University where her group kindly conducted the Raman microspectroscopy analysis after collecting Raman spectra from the incisor tips. Briefly, spectra were collected using a Renishaw InVia spectrometer with a 785nm diode laser connected to a Leica confocal microscope with a motorised stage. A 1800 line/mm grating was used in scanning mode (10 s/scan) to collect spectra (350 to 3200 Raman shift cm^{-1}) with approximately 1cm^{-1} resolution. Prior to each measurement, the system was calibrated for position and intensity using an internal silicon standard. All curve-fitting was completed using Renishaw's Wire software.

3. Results chapter I: Characteristics of dental pulp mesenchymal cells of the rat incisor

3.1 Introduction

Dental pulp stem cell populations reported in the literature are heteregeneous in nature and their *in vivo* properties remain poorly understood. Unlike human teeth which have limited regenerative potential, the continuously growing rodent incisor undergoes constant self-renewal. It was reported that an epithelial stem cell niche is present at the apical end where residing cells continually replenish those lost through constant wear (Harada et al., 1999). However, whether the mesenchymal niche supports this continuous growth still remains elusive.

Since both the epithelial and mesenchymal component of the mouse incisor is replenished synergistically, the first hypothesis is that in addition to the epithelial stem cells, rodent incisors must also possess MSCs that can sustain the growth of the connective tissue element. However, the precise *in vivo* identity of these mesenchymal stem/progenitor cells is largely unknown. This is the same case for other mesenchymal cells such as fibroblasts, the principal stromal cells of mesenchymal origin. These cells function to synthesise extracellular matrix in connective tissues and play major roles in wound healing (Chang et al., 2002). It was demonstrated that even within the same tissue, fibroblasts from different anatomical locations of the skin displayed distinct characteristics (Chang et al., 2002). Therefore, since heterogeneity and topographic variation exist within mesenchymal tissues, this leads to the second hypothesis of this chapter in that not all cells from the entire dental pulp have equal "stemness". To test both hypotheses, the continuously growing rat

incisor model was used to examine *in vitro*, pulp cells from two anatomically distinct sites associated with varied differentiation status.

3.2 *In vitro* comparison between pulp cells from two distinct anatomical locations

3.2.1 Cell proliferation

To examine the proliferation characteristics of cells isolated from different regions of the incisor, a growth curve was plotted for the cervical loop pulp (CL) and incisor body (IB) mesenchymal cells immediately after isolation (Figure 3.1A). Between day 0 and day 3 a lag period is apparent in both cell populations as shown by the reduction in cell number from the original seeding density of 1×10^4 cells/ well suggesting the cells adapting to the culture conditions. The IB cells exhibited the largest reduction, where only a small number of cells had attached in comparison to the CL cells (Figure 3.1B). Both cell types showed similar proliferation between days 3 to 6. From day 6 to 12, as the CL cells progressed through to exponential growth until the experimental end point, interestingly, proliferation remained relatively static in the IB cultures. Here, cell growth reaches a peak at day 12 and declines thereafter. This is reflected in cell culture images taken on the initial and final cell count days (Figure 3.1B).
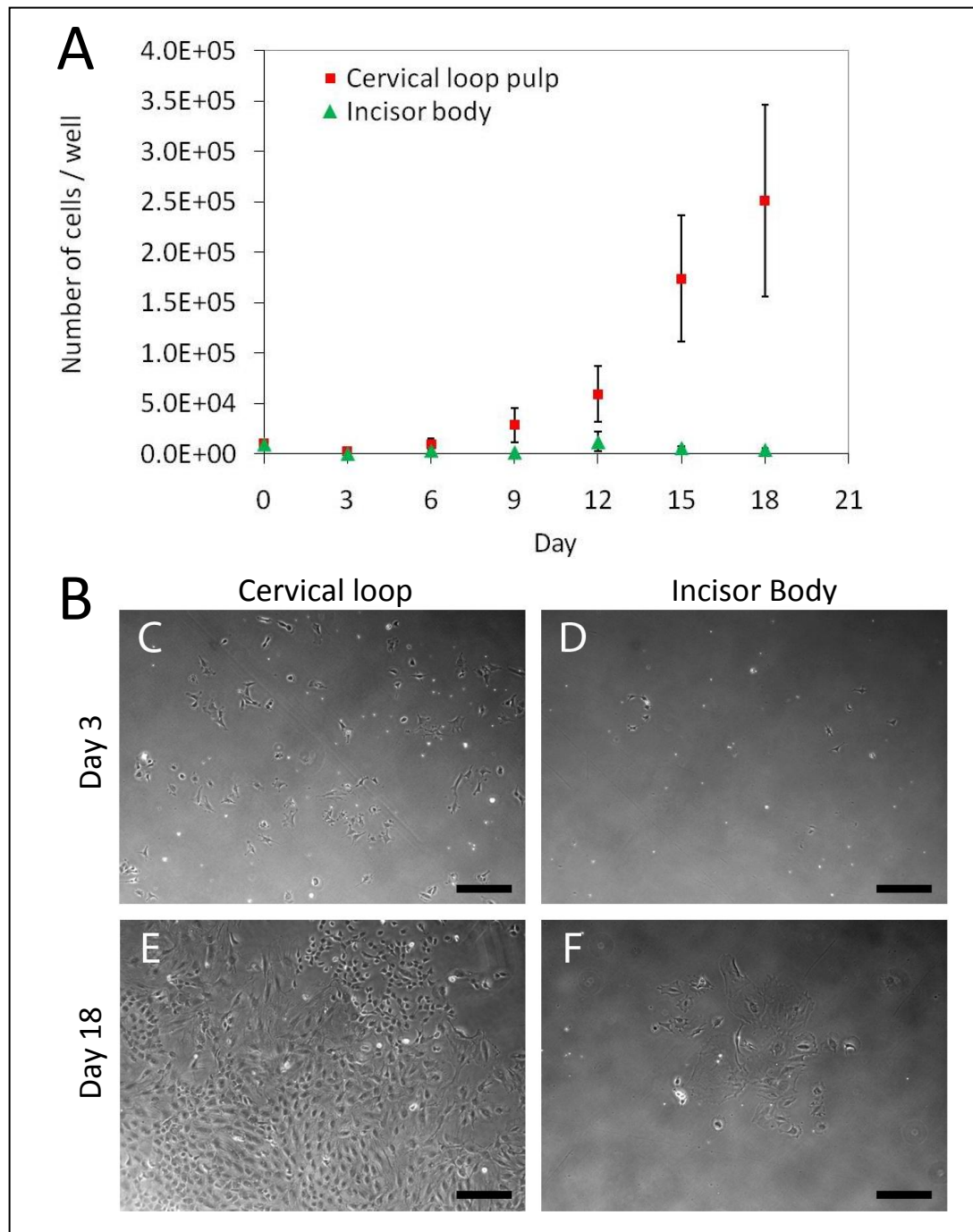
Figure 3.1 Growth curve of cervical loop and incisor body pulp cells.
Cells from two different anatomical locations, CL and IB were isolated and cultured on tissue culture plastic in 6 well plates. Cells counts were performed per well every 3 days using trypan blue exclusion. (A) The growth curve indicates a lag phase in both cultures until day 3. From day 6 there is a large increase in proliferation in the cervical loop cells, which enters exponential growth after day 12. Proliferation of the incisor body cells peaks at day 12 and declines thereafter. Values are mean ± s.d., n=3. (B) At day 3, attachment of cells is significantly greater in the cervical loop cultures (C) in comparison with the incisor body cells (D). By day 18, the cells have become enlarged, more elongated and compact (E, F). Images were taken using the Nikon Eclipse TS100 phase-contrast microscope. Scale bars indicate 300µm.

3.2.2 Differentiation capacity

Multilineage differentiation is another key *in vitro* characteristic of MSCs (Pittenger et al., 1999). To determine whether cells from the cervical loop pulp and incisor body regions are multipotent, each cell type was cultured in lineage-specific culture conditions. Under osteogenic conditions, the cervical loop cells showed the greatest formation of mineralized deposits with a few particular areas exhibiting dense mineralization shown by strong alizarin red staining after 9 days in culture (Figure 3.2A). Lack of alizarin red staining indicated little or no calcium deposition by the incisor body cells demonstrating their limited osteogenic capacity (Figure 3.2B). Chondrogenic differentiation in micromass cultures was induced by 7-8 cycles of induction and maintenance. After 16 days under chondrogenic conditions, the cells from the cervical loop had transformed morphologically, appearing less spindle-shaped and more compact and cuboidal. Moreover, a raised matrix-like layer was visible above the original micromass, which stained positive for alcian blue indicating the synthesis of proteoglycans (Figure 3.2C). The incisor body cells did not produce any matrix and were negative for alcian blue (Figure 3.2D). For adipogenic differentiation, the cells were cultured to around 70% confluency before inducing with adipogenic medium. Three weeks after initial induction, the appearance of lipid-laden cells was observed in both cervical loop and incisor body cultures and Oil red O staining confirmed the presence of adipocyte cells (Figure 3.2E). However, with cells from the incisor body, adipocyte differentiation was much more limited compared with the cervical loop cultures (Figure 3.2F).

The positive alcian blue and alizarin red staining together with the Oil red O stained adipocytes suggested that dental pulp cells from the cervical loop region have the ability to differentiate into fat, cartilage and bone. This indicates that a mesenchymal stem cell population may exist within this region of the continuously growing incisor. Although the

incisor body cells appeared to form adipocytes, their overall multilineage potential is more

restricted.
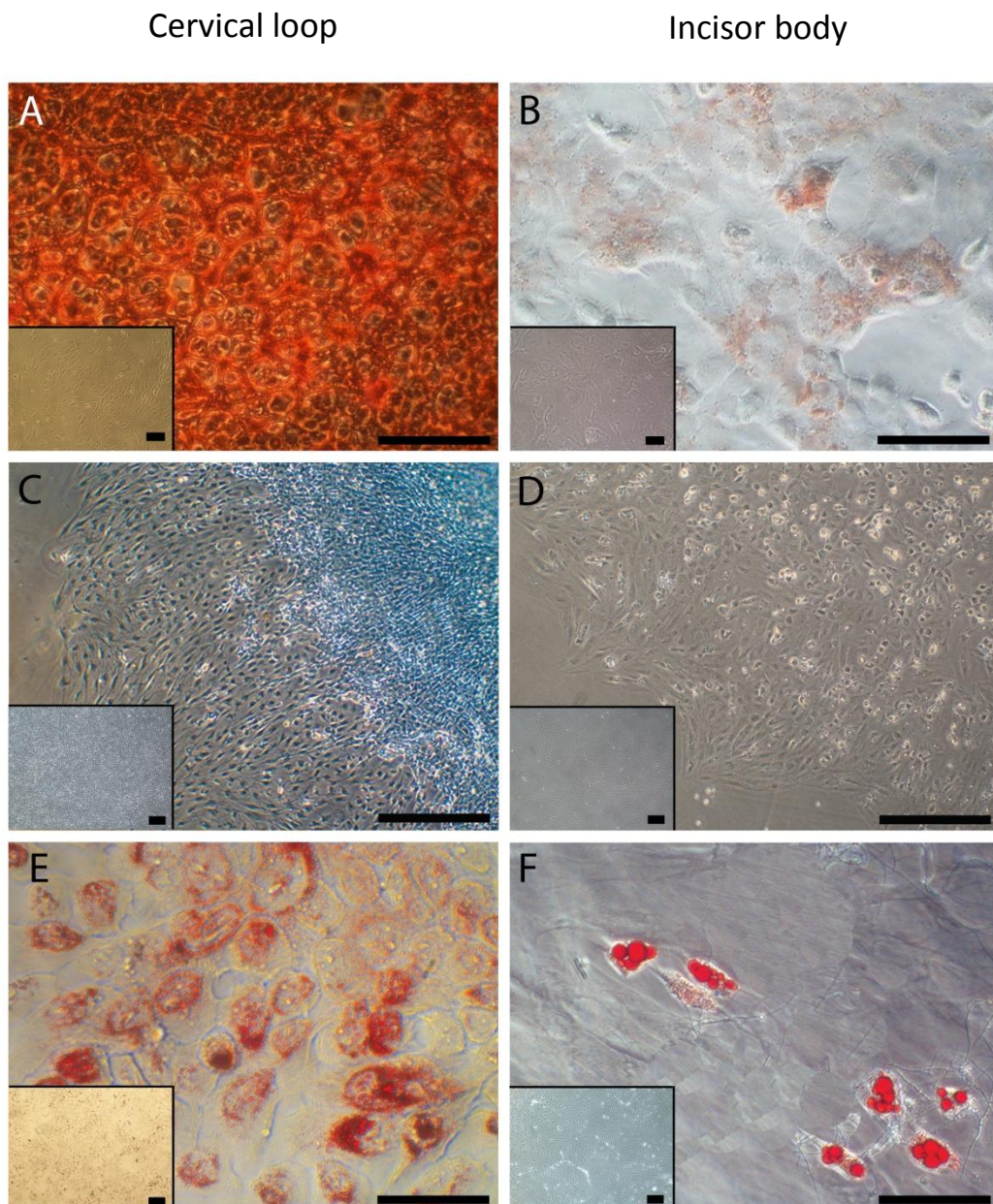
Figure 3.2 Multipotency of cervical loop and incisor body cells
Cervical loop and incisor body pulp cells cultured in osteogenic differentiation medium for 9 days stained with alizarin red, revealed intense calcium deposition by the cervical loop cells in comparison with the incisor body cultures (A, B). Under chondrogenic differentiation for 16 days in micromass culture, the cervical loop cells produced a matrix-like layer, positive for alcian blue that stains proteoglycan deposits indicative of functional chondrocytes. Conversely, incisor body cells were negative for alcian blue staining (C, D). After three weeks in adipogenic medium, characteristic lipid laden cells stained positively for Oil red O in cervical loop cultures while the incisor body cells appeared to have comparatively limited adipogenic potential (E, F). Inserted panels denote control cultures without differentiation medium. Scale bars represent 50µm in A,B,E,F and 500µm in C,D.

3.2.3 Colony forming capacity

Mesenchymal stem cells can be identified *in vitro* based on their ability to form adherent fibroblast-like colony forming units. Colony forming assays were performed on both cell populations to compare this characteristic (Section 2.2.4). During the colony-forming assay where over 50 cells were classed as a colony, in the cervical loop pulp cultures, fibroblast-like colonies (Figure 3.3A) as well as more morphologically compact colonies were observed after 14 days in culture (Figure 3.3C). Interestingly, the incisor body cells failed to form colonies (Figure 3.3B-D). To assess their colony forming ability, the plates were stained with crystal violet before counting. Crystal violet staining of the culture plates revealed many purple stained colonies, demonstrating the strong clonogenicity of cervical loop pulp cells (Figure 3.4A). Almost no colonies formed in the incisor body cultures, evident from the lack of purple staining in the incisor body wells indicating their deficiency in colony formation (Figure 3.4B). Quantification of this result indicated that on average, around 21.9 colonies were formed by cervical loop pulp cells compared to the 0.44 by the pulp body cells, this was greater to a highly significant extent where the $p=0.0007$ (Figure 3.4C).

Cervical loop   Incisor body
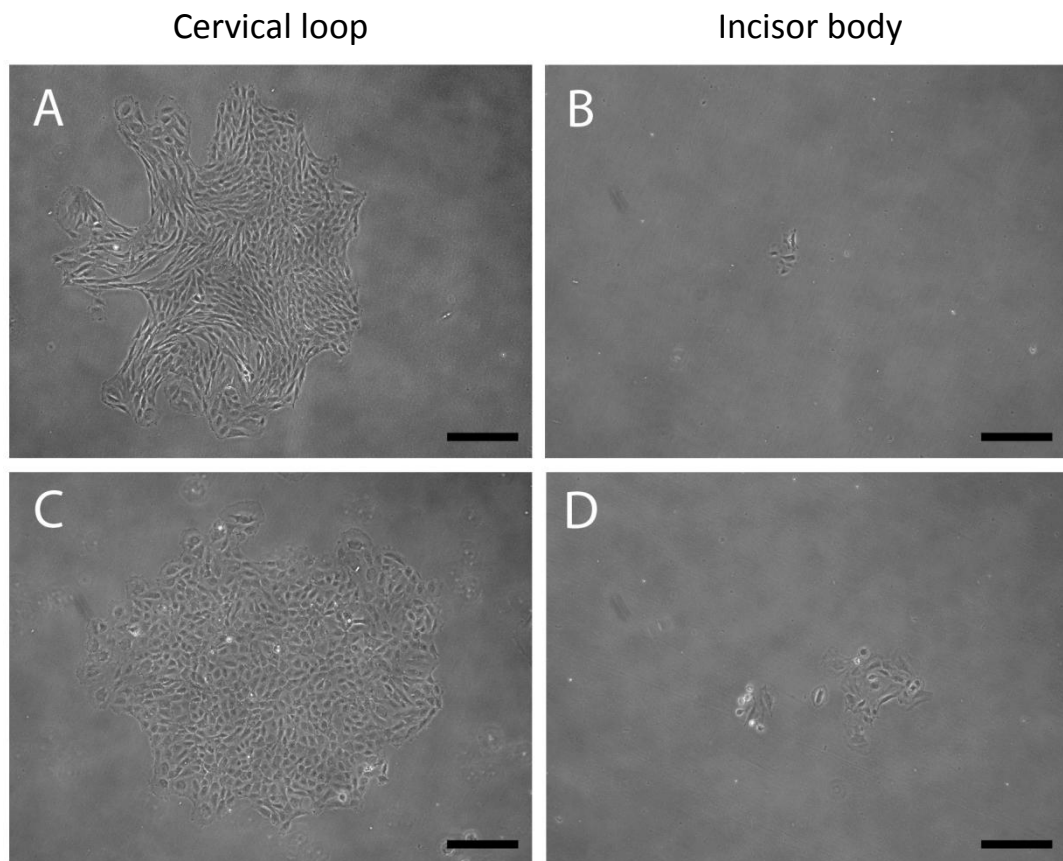
Figure 3.3 Morphology of cervical loop pulp and incisor body colonies

Distinctive colonies were observed in the cervical loop cultures 14 days after the initial cell seeding density of 10^3 cells per well in a 6 well plate. Morphological differences between colonies were visible where some developed more spindle-shaped appearance (A) compared to others that were compact (C). The incisor body cells fail to form colonies indicated by the sparsely attached cells (B,D). Scale bars indicate 300µm.
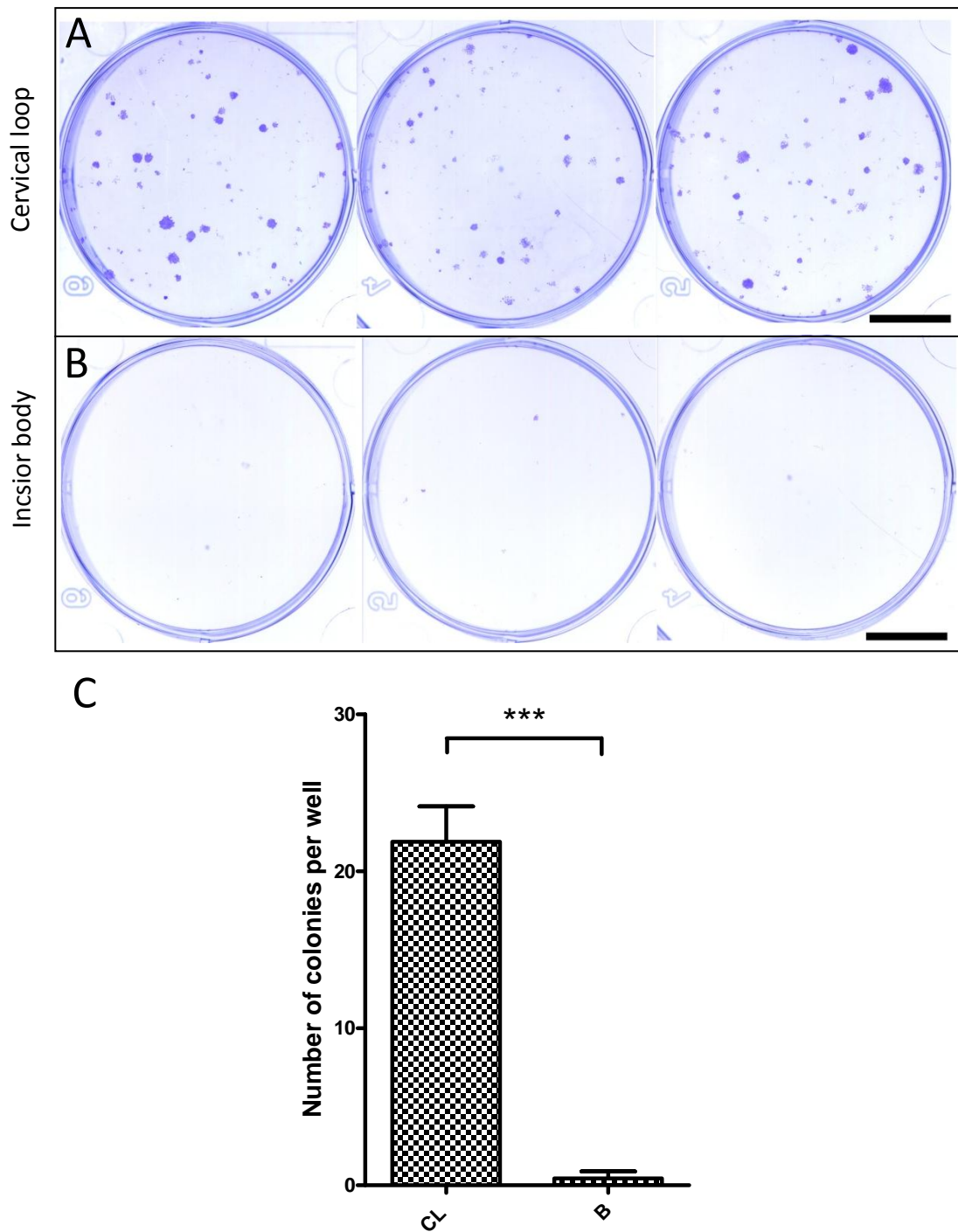
Figure 3.4 Colony forming capacity of cervical loop pulp and incisor body cells
Colony formation was examined by culturing the cells using a low initial seeding density of 10^3 cells per well of a 6 well plate. After a 14 day culture period, crystal violet staining allowed visualisation of the colonies determined as > 50 cells. Crystal violet stained plates indicated that cervical loop pulp cells were clonogenic (A), whereas incisor body cells lacked colony forming ability (B). Image J was used to quantify colony formation. Data was analysed by unpaired student's t test, *** indicates P≤0.001. Error bars indicate SD, n=3. Scale bars represent 1000µm in

3.3 Analysis of dental pulp cell migratory capacity

3.3.1 Scratch migration assay

A previous study by Feng *et al.* (2011) revealed that dental pulp cells from the mouse incisor located in the cervical loop region possessed the ability to undergo directed cell migration toward tissue damage. To confirm this property under *in vitro* conditions, a scratch wound assay was performed to assess the migratory capacity of the cells by observing the duration required for the cells to close the gap created by a scratch wound. The results indicated that both cell types were capable of migrating towards each other. However, the initial rate of wound space closure by the cervical loop cells was 25.4% per day compared to the incisor body cells which was 12.3% per day. The wound space generated in the cervical loop cultures closed fully by 4 days whereas the incisor body cultures which required 13 days (Figure 3.5 and 3.6). Again, this result reveals that the cervical loop cells are distinct in their behaviour compared to the incisor body cells. However, as this assay cannot explicitly determine that the scratch closure is due to migration alone and not proliferation, a more functional migration assay using transwell migration chambers was used to further investigate their *in vitro* migration properties.
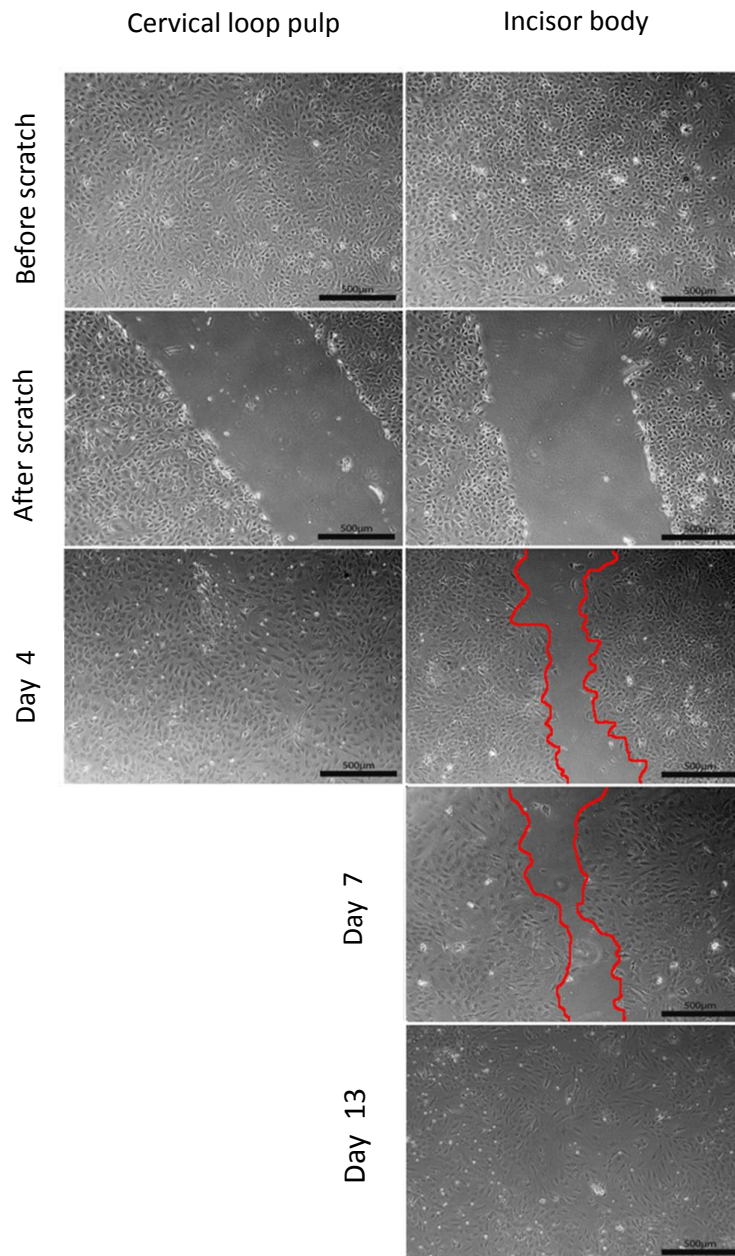
Figure 3.5 Scratch wound healing assay

The cell scratch assay revealed that complete wound closure was observed after 4 days in the cervical loop cell cultures. In comparison, the incisor body cells required 13 days to completely enclose the scraped area. Image J analysis was used to quantify percentage wound closure. Scale bars = 500μm for all panels. Data is representative of three independent experiments.
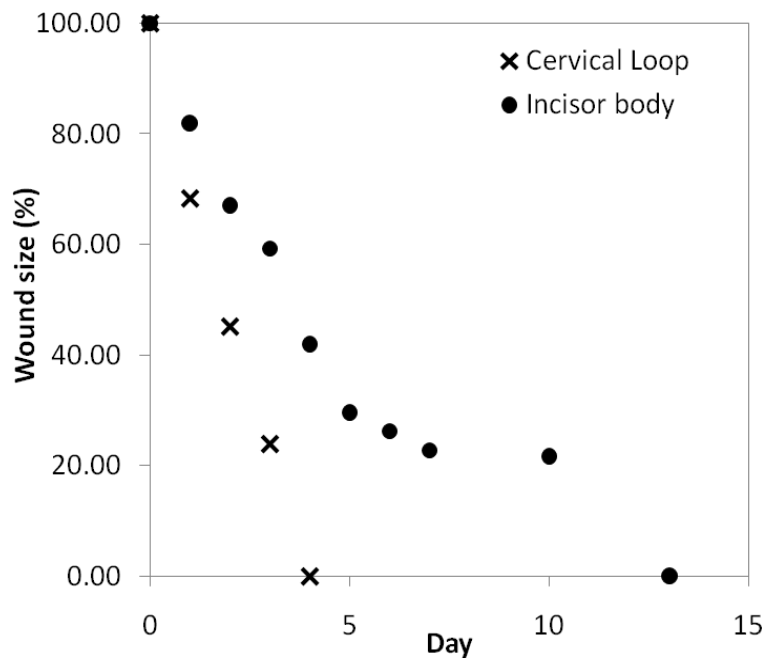
Figure 3.6 Percentage scratch wound closure
The rate of scratch wound closure by the cervical loop pulp cells is three times greater than the rate at which incisor body cells close the scratch. Data is representative of three independent experiments.

3.3.2 Transwell migration assay

The transwell assay also known as the Boyden chamber assay consists of two medium filled compartments separated by a microporous membrane that allows for the analysis of chemotaxis. During this assay, cells are seeded onto the upper side of the membrane which permits migration through the pores and into the lower well where chemotactic factors are present (Chen, 2005). Therefore, quantification of cell migration is achieved by counting the number of cells on the underside of membrane. Using 3μm pore sized transwell inserts, pulp cells that had migrated through the membrane were fixed and stained with crystal violet and subsequently counted. Many crystal violet stained cells were observed in the cervical loop cultures whereas migrated cells were scarce in the incisor

body experiments (Figure 3.7A). Subsequent quantification by counting 6 fields of view per transwell membrane revealed that on average, approximately 24 cervical loop cells migrated through the membrane per field of view compared to 8 incisor body cells per field of view. Therefore, cervical loop pulp cells appeared to have three times more migratory ability than the incisor body cells (Figure 3.7B).
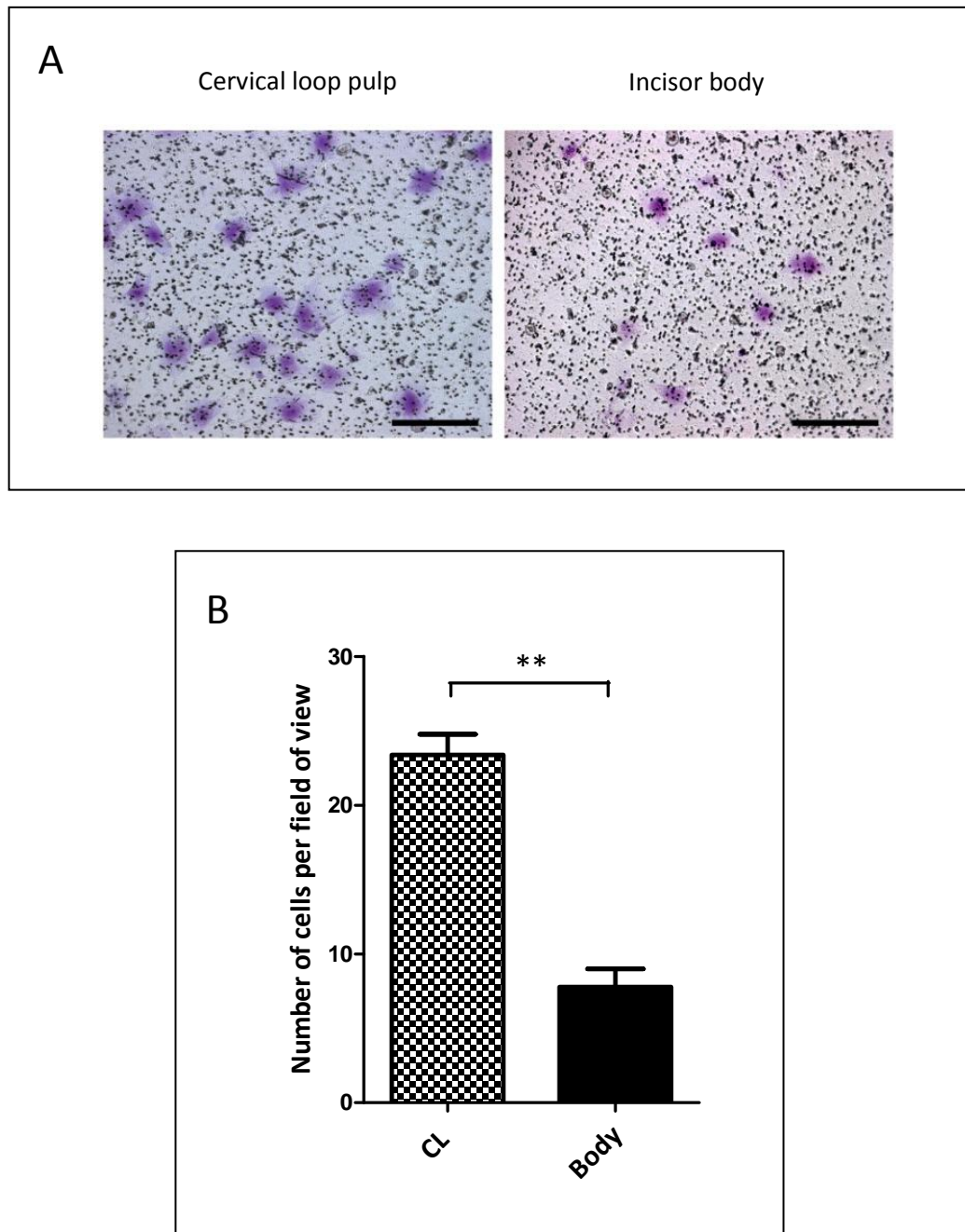
Figure 3.7 Transwell migration assay
(A) Crystal violet stained transwell membranes after a 24 hour migration period. Purple stained migrated cells were abundant in the incisor cervical loop cell cultures compared to the incisor body. Scale bars: 100µm (B) Quantification of the migrated cells confirmed almost three times as many cervical loop cells migrated through the 3µm pore sized transwells compared to the incisor body cultures. A total of 6 fields of view were counted and averaged per transwell. Data was analysed by unpaired student's t test, (**) indicates $p \leq 0.01$. Error bars represent SEM, n= 3.

3.3.3 Cell homing response to damaged dentine

On confirming the distinctive migration function of the cervical loop cells using both the scratch and transwell assays, this population was further examined to assess some of the potential mechanisms involved in the directed cell migration effect in response to incisor tooth damage observed by Feng *et al.* (2011).

Further to the scratch wound healing assay detailed in Figure 3.5, the assay was modified to determine whether cervical loop dental pulp mesenchymal cells *in vitro* respond to damaged dental tissue. To attempt to replicate chemotactic processes that occur during tooth damage, the original scratch migration assay detailed in section 3.3.1, was adapted to analyse migration towards a piece of damaged dentine. The rationale behind using dentine as a source of chemoattractants stems from reports indicating that during tooth development, members of the TGFβ family and other growth factors become sequestered within the dentine matrix (Cassidy et al., 1997; Finkelman et al., 1990). Furthermore, dentine chips formed as a result of operative debris can actually stimulate reparative dentineogenesis (Seltzer, 1999). This led to the reasoning that growth factors sequestered within the dentine may become released upon injury to the tooth and plays a role in the recruitment of cells involved in the repair process.

After generating a scratch wound by removing a section of the cell monolayer, a piece of damaged dentine was attached close to the wound edge and cell movement was traced by images taken every 24 hours (Figure 2.3). Three days after initiation of the "wound" where a straight leading edge was present (Figure 3.8C), there was a distinct protrusion of cells along the wound edge adjacent to the dentine compared with the cells located either side (Figure 3.8D). In the control experiments, using a collagen drop seeded the equivalent distance from the wound edge as the dentine piece marked by the dark spot, wound

repopulation was observed where cell movement of the entire leading edge was essentially parallel (Figure 3.8A,B). There was no marked protrusion of cells close to the collagen droplet indicating that the cell homing effect was attributed to the presence of the damaged dentine (Figure 3.8B).
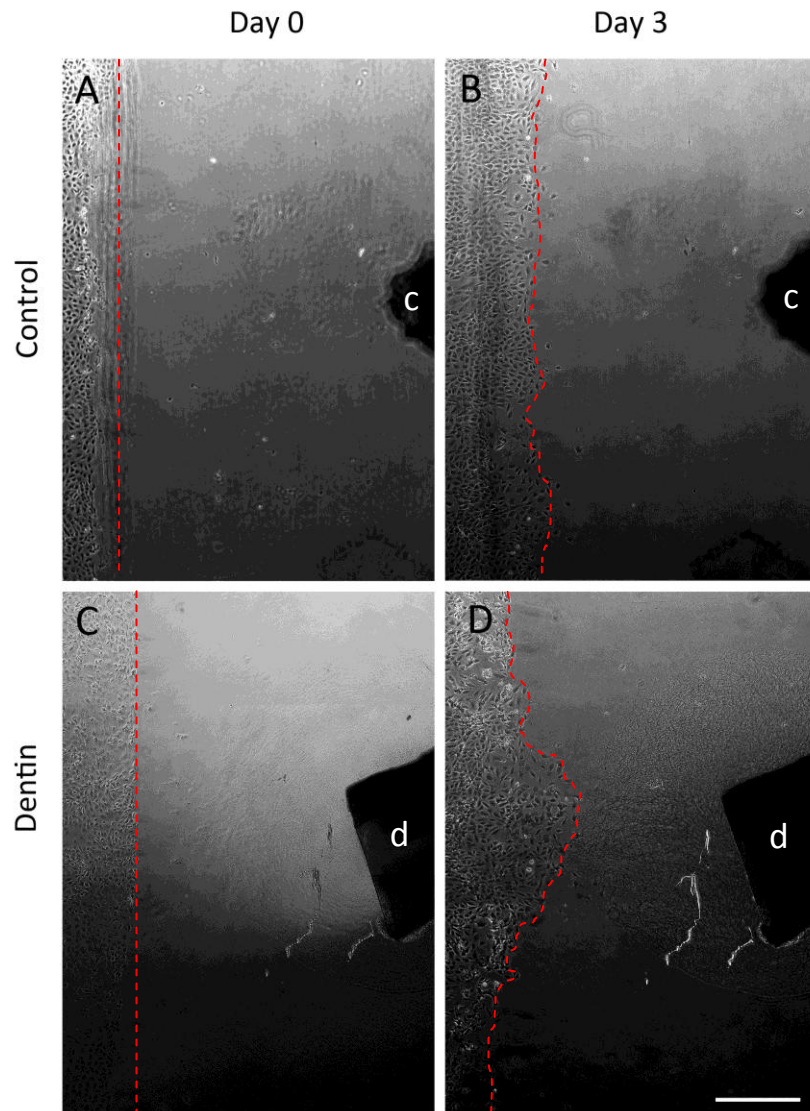
Figure 3.8 Cell homing of cervical loop pulp cells towards damaged dentine
Confluent cervical loop cells were scraped to provide a "cell free" zone where either a collagen droplet (A) or a piece of damaged dentine was attached (C). Tracing the leading of the cells revealed that after 3 days, these cells underwent directed cell migration towards the damaged dentine as shown by the protruding wound edge (D). In the control experiments, the wound edge moved in a parallel manner towards the collagen drop (B). Abbreviations d: dentine, c: collagen drop. Scale bar indicates 500μm. n=2

3.3.4 Transwell migration with stimulatory factors

From the observations in Figure 3.8, evidently, injury to the dentine triggers certain signals to be released to the surrounding cells which in turn respond by migrating towards the region where repair is necessary. To determine which signals the cervical loop pulp cells react to, the transwell assay was used together with different stimulatory factors as detailed in section 2.2.6. A variety of growth factors and proteins were selected as chemotactic factors because they are implicated in both tooth development and dentine repair. For example, in addition to TGF-β (Sloan and Smith, 1999), other proteins including recombinant BMPs were shown to mediate tooth repair by induction of dentine formation (Nakashima, 1994).

When the tooth is damaged, in order to repair the injury, it would be necessary to recapitulate certain processes during tooth morphogenesis. Thus, of the four key pathways involved in the regulation of tooth development, BMP, FGF and WNT signalling were selected for screening their effect on dental pulp cell migration. After a 24 hour migration period, all selected growth factors caused an increase in cell migration which was statistically significant from the control wells where no chemotactic factors were added (Figure 3.9).
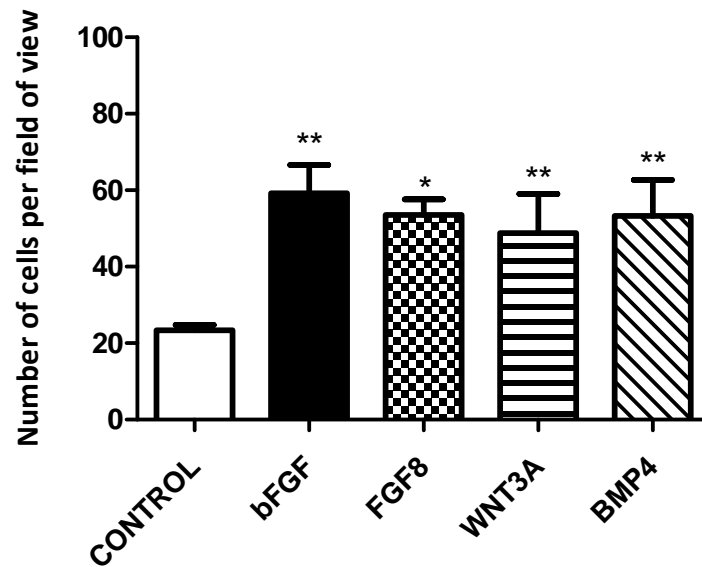
Figure 3.9 Transwell assay of cervical loop pulp cells with different stimulatory factors
Cervical loop pulp cell migration through 3μm pore sized transwells was enhanced by BFGF, FGF8, WNT3A and BMP4 as measured by counting the number of crystal violet stained migrated cells. Control wells contained cervical loop pulp cells without chemotactic factors. A statistically signifcant increase in migration was observed under all stimulatory conditions. Data was analysed by One-way ANOVA with post hoc Newman Keuls test; (*) and (**) indicate statistical significance at p <0.05 and p<0.01 respectively, relative to the control. Error bars represent SEM.

Since the results in 3.3.4 appeared to indicate that there was no significant differences between the chemotactic properties of each stimulatory factor, this lead to the reasoning that by not taking into account the proliferative effect of the factors, the migration result may have been masked, especially since FGFs have long been known as potent mitogens (Esch et al., 1985). The time course for this migration assay was 24 hours and although the doubling time for cervical loop cells calculated from Figure 3.1A was 46.5 hours, there is still the potential for enhanced proliferation due to the mitogenic effect of the growth

factors over the 24 hour migration period. Therefore, two different approaches were used to try and discount the proliferation effect.

The first method was to use mitomycin C to inhibit proliferation prior to seeding the cells into the transwells, with the premise that it may cause irreversible changes to the cells because of its potent DNA crosslinking effect (Section 3.3.5). The second approach discussed in Section 3.3.6 involves using a correction factor based on data derived from the MTT proliferation assay.

3.3.5 Transwell migration using mitomycin treated cells

The cervical loop pulp cells were treated with mitomycin C which is an anti-tumour antibiotic that inhibits DNA synthesis and nuclear division, therefore the true migration result should be observed. However, following exposure to mitomycin C and subsequently seeding the cells into the transwell assay, the results appeared skewed. Firstly, there was a noticeable decrease in overall cell migration (Figure 3.10) in comparison to the data achieved without addition of the anti-tumour antibiotic (Figure 3.9). Secondly, there was no significant difference in cell migration between the control wells and those with added growth factors, confirmed using a one way ANOVA test (Figure 3.10). This possibly suggests that the effect of mitomycin C was perhaps overly detrimental to the pulp cells. Mitomycin C is generally used on fibroblast cell lines to inactivate feeder cells required for the culture of human embryonic stem cells. These cells are more stable and robust whereas the cells used for these experiments were primary cell cultures and were perhaps be less able to withstand the noxious effect of the proliferation inhibitor.
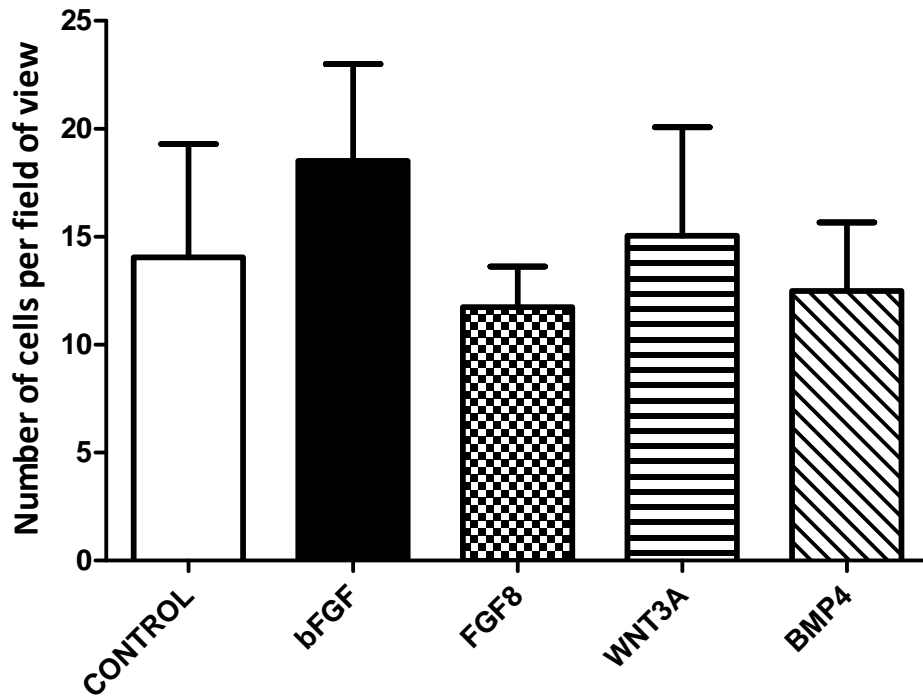
Figure 3.10 Transwell assay of cervical loop pulp cells with mitomycin
Prior to the growth factor transwell assay, the cervical loop pulp cells were treated with mitomycin C to eliminate any subsequent mitogenic effect the growth factors may produce on the cells. Treatment with the proliferation inhibitor was detrimental to the cells resulting in no significant difference between the controls and the growth factor treated wells. Data was analysed by One-way ANOVA with post hoc Newman Keuls test. Error bars represent SEM.

3.3.6 Transswell migration correction for proliferation

From the results in 3.3.5 it appears that the effect of mitomycin C has resulted in not only inhibition of cell proliferation but its toxicity may have also resulted in decreased migration caused by cell death owing to the sensitivity of primary pulp cell cultures as premised. In the alternative method, rather than directly inhibiting proliferation of the cells by adding mitomycin C, the data from section 3.3.4 was corrected to account for proliferation using a crude correction factor calculated by an MTT assay.

The MTT assay first described by Mosmann in 1983, tests the viability of cells through their mitochondrial enzymatic activity. Healthy cells cleave MTT, resulting in purple formazan crystals which can be quantified by spectrophotometric means. The level of formazan product generated is therefore directly proportional to the number of surviving cells. Using this assay, the proliferative effect of the growth factors on the cells was measured over a 24 hour time period (the same time period of the transwell assay), to determine the extent of proliferation caused by the growth factor. Analysis of the relative increase in proliferation compared to the control wells without the stimulatory factors allowed the extent of proliferation caused by the growth factor to be deduced and the generation of a rough correction factor by normalising the values to the controls.

The MTT assay revealed that as expected, the FGF family of growth factors had a definite proliferation effect on the cervical loop pulp cells. Although, this correction factor method is crude, nevertheless, following the correction of the results in Figure 3.8, the results now suggested that in fact, WNT3A had the greatest migratory effect on the cells followed by BMP4 which were statistically significant where $p=0.0042$ and $p=0.0177$ respectively (Figure 3.11).
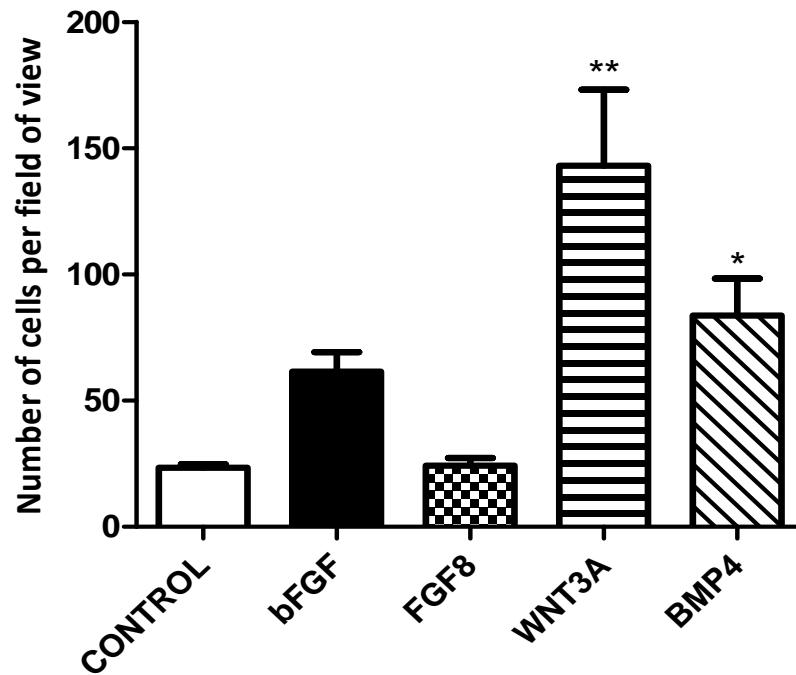
Figure 3.11 Transwell migration assay corrected for proliferation
A correction factor to account for proliferation was generated using the results from the MTT assay allowing the effect of proliferation by the growth factors to be calculated. Applying this correction factor to the results obtained in Figure 3.8 revealed that WNT3A and BMP4 significantly enhanced cervical loop pulp cell migration. Data was analysed by One-way ANOVA with post hoc Newman Keuls test. Error bars represent SEM. (*) and (**) indicate statistical significance at $p < 0.05$ and $p < 0.01$ respectively.

3.4 Discussion

To determine whether a mesenchymal stem cell niche exists in an anatomically defined region of the rat incisor, the responses of cells from two distinct regions of the pulp, the incisor body and the cervical loop were compared. Analysis of the proliferation potential of cells isolated from the two regions demonstrated that that cervical loop cells were highly proliferative in comparison to the incisor body cells, which displayed poor proliferative capacity.

Within a stem cell niche, there are a small number of "true" adult stem cells that are slowly dividing and have the capacity for infrequent, yet almost unlimited self-renewal. When these cells replicate, in addition to renewal of undifferentiated daughter stem cells, they also give rise to transit amplifying progeny. These transit amplifying progenitor cells are highly proliferative and display multipotent characteristics, differentiating along multiple mesenchymal lineages upon stimulation (Sloan and Waddington, 2009). Previous studies using rodent incisors identified the cervical loop epithelial stem cell niche responsible for continuously replenishing the enamel that is constantly worn down at the tip of the tooth (Harada et al., 1999; Harada et al., 2002). However, in order to maintain these teeth, which grow continuously throughout the life of the animal, they must possess stem cells that replenish both epithelial and mesenchymal compartments. The precise location of these MSCs remains elusive, though they have been postulated to also reside close to the cervical end of the incisor close to the cervical loops, since the growth and differentiation of the incisor always initiates at the apical end then extends towards the incisal end (Feng et al., 2011). Historically, label retaining studies using bromodeoxyuridine (BrdU) followed by a long chase period has been used to determine the location of putative stem cell niches in a range of different epithelial tissues including the hair follicle, skin epithelium

and intestinal crypts (Cotsarelis et al., 1990; Potten et al., 2002; Tumbar et al., 2004). In the mouse incisor, BrdU label retention identified slow cycling (label retaining) cells within the stellate reticulum of the labial cervical loops in cultured explants, indicating the location of the epithelial stem cell niche (Harada et al., 1999). More recently, in addition to the epithelial stem cell niches within the labial and lingual cervical loops, the possible location of the MSC niche was restricted to between the two loops indicated by BrdU pulse chase experiments (Seidel et al., 2004). Further evidence confirmed the presence of this MSC niche in the mouse incisor when BrdU labelling with a short chase period revealed rapidly dividing cells were also located close to the previously identified niche implicating a transit amplifying cell population (Lapthanasupkul et al., 2012). From the proliferation data, the highly proliferative cells isolated from the cervical loop region certainly fulfil the requirement to replenish the mesenchymal pulp cell population. In addition, the significant difference in the proliferative nature between the cervical loop and incisor body cell cultures could be attributed to the cell isolation approach. By separating the cell populations anatomically, the cervical loop cultures would most likely include the highly proliferative transit amplifying progenitor population. While the incisor body region of the pulp probably contained largely terminally differentiated cells and therefore did not propagate well in culture.

When markers have yet to be identified for specific stem cell populations, the BrdU method allows you to determine at least the location of stem cells, though label retention on its own does not verify "stemness" since cells that incorporate the BrdU and undergo cell cycle withdrawal and differentiation will also appear label retaining (Hsu and Fuchs, 2012). Therefore, it was also important to examine other mesenchymal stem cell properties of the located cell population to assess whether the cervical loop cell population meet certain criteria required for MSCs (Dominici et al., 2006).

To further characterize this population of highly proliferative cervical loop cells, differentiation experiments were performed. Multilineage differentiation is a well known and defining characteristic of MSC populations (Jiang *et al.*, 2002). Numerous reports have shown that human impacted third molars contain rich sources of dental pulp stem cells with multilineage potential (Gronthos *et al.*, 2002; Ikeda *et al.*, 2008; Seo *et al.*, 2004; Sonoyama *et al.*, 2006). This is also true for rat dental pulp cells which have been confirmed to differentiate into a variety of cell types including neural cells, adipocytes, myocytes, chondrocytes (Yang et al., 2007b), odontoblast-like cells (Zhang et al., 2005a) as well as osteoblasts (Yu et al., 2010). Consistent with previous studies on the multilineage capacity of rat incisor dental pulp cells (Zhang et al., 2005a) the results from this study confirmed the existence of a multilineage population. In addition, we reveal that dental pulp cells of multilineage potential are not homogeneously dispersed throughout the tissue, rather they exist in a defined anatomical location and reside in the cervical loop region of the pulp. *In vitro* comparisons between the two distinct dental pulp cell populations has never been performed before and, until now, no direct evidence for heterogeneity within the incisor pulp has been shown. More specifically, the cells from the cervical loop have strong osteogenic, chondrogenic and adipogenic potential while the incisor body cells appear to possess much more limited differentiation capacity. A possible explanation for the observed variability of the differential potency of the rat incisor pulp cells is that the main MSC niche resides in the cervical loop end. Therefore, in addition to resident stem cells this population would contain the transit amplifying population. The role of transit amplifying cells has been well characterised in the epidermis (Jensen and Watt, 2006; Jones and Watt, 1993). These progenitor cells are termed transit or "transiently" amplifying because their role is dynamic and influences the stem cell niche to regulate homeostatis of the tissue undergoing different physiological changes such as development and aging and pathological conditions, for example, injury and disease

respectively (Voog and Jones, 2010). Therefore, the heteregeneous combination of both the resident stem cells as well as the transit amplifying cell population would possess the greatest multipotent capacity. In contrast, the limited differentiation capacity of the incisor body cells but not entire lack of multipotency could be explained through the mixed origins of the rodent incisor tissue. This is perhaps unsurprising given that in the mouse incisor, there are dual origins of dental pulp cells (Feng et al., 2011). The incisor pulp body region possesses other much smaller stem cell niches including perivascular niches where a few isolated pericyte mesenchymal stem cells reside in a quiescent state prior to activation upon tooth injury or damage. Therefore, since only very few isolated pericytes are present within this region of the pulp, this represents a small minority of MSCs within the pulp and this restricted multilineage capacity would be reflected during *in vitro* culture under different multilineage conditions.

Evidence in the literature suggests that a distinct population of dental pulp mesenchymal cells located specifically in the apical dental mesenchyme possess cell homing capacity in response to damage (Feng et al., 2011). In this study using mouse incisors, upon damage to the tooth, mesenchymal cells close to the cervical opening migrated towards the site of injury. Cell labelling using 1,1'-dioctadecyl-3,3,3'3'-tetramethylindocarbocyanine perchlorate (diI) and tracking experiments demonstrated that directed migration did not occur for cells from non-cervical regions. These findings led us to investigate the migratory capacity of these cells *in vitro* using pulp cells from the cervical loop and comparing their migratory behaviour to cells isolated from the pulp body.

Scratch wound assays are classically used to study cell migration in a wound healing context and have been employed in previous studies using cultured skin fibroblasts (Wall et al., 2008) and bone marrow mesenchymal stem cells (Hao et al., 2009; Smith et al., 2010). In this method, a "wound" is created in a confluent plate of cells by scraping away a

specific area of the plate. Cell migration over time can then be monitored by imaging the cells to capture their movement towards the wounded area. Our results revealed that both cervical loop and incisor body pulp cells have inherent migratory ability but the wound closure period for cervical loop cells was much shorter at 4 days compared with 13 days for the incisor body cells. The scratch wound assay was used as a simple, quick assessment of wound repopulation capacity. However, wound repopulation in these assays can be a combination of migration and proliferation. Therefore, a second assay using transwell inserts was used to quantitatively measure migration in isolation from proliferation of these cells. Using 3µm pore sized transwell inserts, cervical loop region pulp cells underwent significantly greater migration than the incisor body cells, supporting the enhanced wound repopulation observation and provides confirmation that the *in vitro* properties of the pulp cells reflected those observed by Feng et al (2011) in their incisor pulp damage culture experiment (Feng et al., 2011).

Cell migration is part of the tissue repair process involving a series of highly orchestrated sequence of events such as cell-cell and cell-matrix interactions (Midwood et al., 2004; Mutsaers et al., 1997) and MSC/progenitor mobilisation involves proliferation, cell homing (chemotaxis) and differentiation. Identities of factors that drive these processes *in vivo* are poorly understood. Prior to using *in vivo* models, we initially created a novel cell-to-tissue migration assay modified from the well known *in vitro* scratch assay (Liang et al., 2007), by examining the response of cervical loop pulp cells towards a piece of damaged dentine. Cervical loop pulp cells immediately adjacent to the wounded dentine responded by mobilising towards it indicating cell recruitment. This provides evidence that chemotactic molecules which would normally be sequestered within the dentine matrix are released after injury (Sloan and Smith, 1999).

To screen a range of possible chemotactic molecules and elucidate the possible signalling pathways involved in the recruitment of the cervical loop MSC population during tooth injury, cervical loop pulp cells were stimulated with a selection of growth factors using transwell migration assays. Initial results indicated the enhanced migratory effect of all the selected growth factors. However, when the proliferative effect of the stimulatory factors was taken into account and corrected accordingly, the data suggested that Wnt3a produced the greatest migratory effect. Wnt ligands and their receptors coordinate many critical cellular and physiological processes such as the control of differentiation, proliferation and patterning during embryologic development and postnatally, where they regulate adult tissue homeostasis through maintaining a delicate equilibrium between stem cell proliferation and differentiation. Wounding or injury is responsible for the activation of Wnt signalling and Wnt activity contributes to all subsequent stages of the wound healing process including the control of inflammation, programmed cell death and more interestingly, the mobilization of stem cell "reservoirs" close to the wound site (Whyte et al., 2012). Among its different functions, the β-catenin or canonical Wnt pathway is a major regulator of stem/progenitor cell maintenance, expansion, and lineage specification in both embryonic and adult tissues (Grigoryan et al. 2008). Wnt signalling has been shown to be necessary for tissue regeneration. In animals that naturally possess regenerative capacity, when Wnt signalling is inhibited, this leads to the cessation in their regenerative ability demonstrated in experiments with axolotl, xenopus and zebrafish (Kawakami et al., 2006; Ramachandran et al., 2011). Abundant data from regenerative retinal studies also suggests that Wnt signalling blockade results in the disruption of stem/ progenitor cell recruitment towards the wound site (Das et al., 2008; Denayer et al., 2008; Liu et al., 2007). In other mammalian organs where regenerative capacity is limited, Wnt activity is still required for the repair process since its inhibition leads to enhanced scar tissue formation after myocardial infarction (Chen et al., 2004) and following wounding to

the skin (Ito et al., 2007). In terms of wound healing, it is clear that Wnt signalling is elevated during the initial stages of the injury response as shown in a variety of models including bone fractures and lung injuries (Chen et al., 2007; Villar et al., 2011). Therefore, the enhanced migratory response of cervical loop pulp cells to Wnt3a in the transwell migration experiments is suggestive of the pulp stem/progenitor cell response towards the upregulation of Wnt activity during injury.

In summary, for the first time, the data from this chapter demonstrates that specific regions of the rat incisor pulp mesenchyme harbours cells with different behavioural characteristics. In combination with published data, findings from these *in vitro* experiments using the rat incisor dental pulp provides supporting evidence that both the rat and mouse incisor MSC niche is situated in the proximal end of the dental pulp mesenchyme and confirms the cervical loop pulp cell migratory response observed previously (Feng et al., 2011). To further examine the dental pulp cell response during tooth damage, we hypothesised that Wnt signalling possibly plays a role in the tooth damage/response mechanism and using *in vivo* models, this will be further investigated in the subsequent chapter.

4. Results chapter II: *In vivo* tooth damage response

Data from the *in vitro* studies in chapter 3 suggest that canonical Wnt activity is important for the migration of cells from the incisor cervical pulp, the putative region for stem/progenitor cells. This result is consistent with previous reports demonstrating the role of the canonical Wnt pathway in wound healing, in which cell recruitment and migration are important components, within a variety of different tissues including bone (Minear et al., 2010), skin (Cheon et al., 2006), heart (Aisagbonhi et al., 2011) and cartilage (Dell'Accio et al., 2006). Thus, it would be of great interest to further test the role of Wnt signalling during tooth repair *in vivo*.

Given that Wnt signalling is also crucial in regulating stem cell behaviour and fate in several other tissues (reviewed by (Nusse, 2008; Reya and Clevers, 2005), we hypothesised that the Wnt signalling pathway might also be important during *in vivo* tooth injury and repair via regulating the stem/progenitor cell population. We initially utilised *Axin2*^{LacZ} (or conductin^{LacZ}) transgenic mice containing the mutation that both abolishes endogenous *Axin2* gene function and expresses the LacZ reporter under the control of the endogenous *Axin2* promoter/enhancer regions (Lustig et al., 2002). Since *Axin2* forms part of the degradation complex and induces β-catenin degradation in a negative feedback loop, it is a direct downstream target of canonical Wnt signalling and is therefore, considered an accurate reporter (Al Alam et al., 2011; Barolo, 2006; Jho et al., 2002). *Axin2*$^{Lac/+}$ heterozygous mice was previously used as reporter mice for Wnt activities and *Axin2*$^{LacZ/LacZ}$ homozygotes for upregulation of Wnt activity in skeletal bone defect repair (Minear et al., 2010). Thus, *in vivo* tooth damage was performed on the *Axin2*$^{LacZ/+}$ and *Axin2*$^{LacZ/LacZ}$ mouse

incisors and molars to detect and enhance Wnt activities during injury response, respectively.

To further investigate the mechanism for Wnt signals in regulating important cell populations during tooth damage and repair, the response of a potential MSC population, the pericytes, to tooth injury *in vivo* was evaluated. *In vivo* injury was provoked in the teeth of a tamoxifen-inducible pericyte reporter mouse line (NG2creER;Rosa26R), in which pericytes and their derivatives are labelled indelibly following tamoxifen induction, thus allowing permanent tracing of pericyte lineage cells during injury response and repair (Feng et al., 2011). To summarize, this chapter progresses from the *in vitro* characterization of the dental pulp cells from the rat, into modelling *in vivo* tooth damage in the mouse and the results suggest that canonical Wnt signalling is a likely candidate to coordinate the tooth repair process via the mobilisation of MSC populations such as pericytes.

4.1 *In vivo* incisor damage

To investigate whether Wnt expression plays a role during tooth injury and repair, initially, *Axin2* expression in the damaged tooth of postnatal day 5 wild type mice was examined. Tooth damage was generated in the mouse incisor by piercing the tooth with a needle as detailed in section 2.7.3 and collected 24 hours post injury. The wound created by the needle is indicated by the arrows in Figure 4.1C and D. *Axin2* expression is observed in cervical loop mesenchymal regions of the incisor as well as in the presumptive molar root areas indicated in both the damaged teeth and non-damaged controls (Figure 4.1A and C). Interestingly, only the pulp cells in the region immediately surrounding the pulp damage show increased expression of *Axin2*, indicating an upregulation of canonical Wnt activity

(Figure 4.1C and C'). Moreover, the high level of *Axin2* expression was restricted to the odontoblast layer close to the damage region (arrows in Figure 4.1C').

In addition to the 3 signalling pathways (FGF, TGF-β and WNT) selected to explore their effect on dental pulp cell migration in chapter 3, the Sonic hedgehog signalling (SHH) pathway is also one of the major signalling pathways involved in the growth and morphogenesis of the tooth (Dassule et al., 2000) as well as regulation of stem cell niches in the mouse incisor (Seidel et al., 2004). Therefore, its possible role during the tooth injury and repair process was of interest. To detect SHH signalling, the expression of sonic ligand receptor Patched1 (Ptch1) was examined in the damaged incisors. Figure 4.1B indicates Ptch1 expression present where SHH is normally active in the mesenchyme adjacent to the labial cervical loop in the undamaged tooth. However, when wounded, in contrast to *Axin2*, there is a marked absence of Ptch1 expression close to the wound area (Figure 4.1D) and indicated at higher magnification in Figure 4.1D'.

Following examination of the canonical Wnt signalling response in wild type mice, using the *Axin2*$^{LacZ/+}$ mutant mice, the same needle damage procedure was performed. Because *Axin2* is a negative regulator of the canonical Wnt pathway that suppresses signal transduction by promoting β-catenin degradation, lacZ expression in these mice would reveal any changes to the endogenous canonical Wnt signals in the dental pulp during the tooth damage and repair process. In Figure 4.2A, lacZ expression is absent from the undamaged incisor pulp. However, one day post injury the blue β-galactosidase+ve pulp cells surrounding the wound demonstrated the activation of the Wnt/β-catenin by the dental pulp cells in response to damage (arrow Figure 4.2B). This further confirmed the upregulation of canonical Wnt activity in response to damage observed previously in the wild type mice.
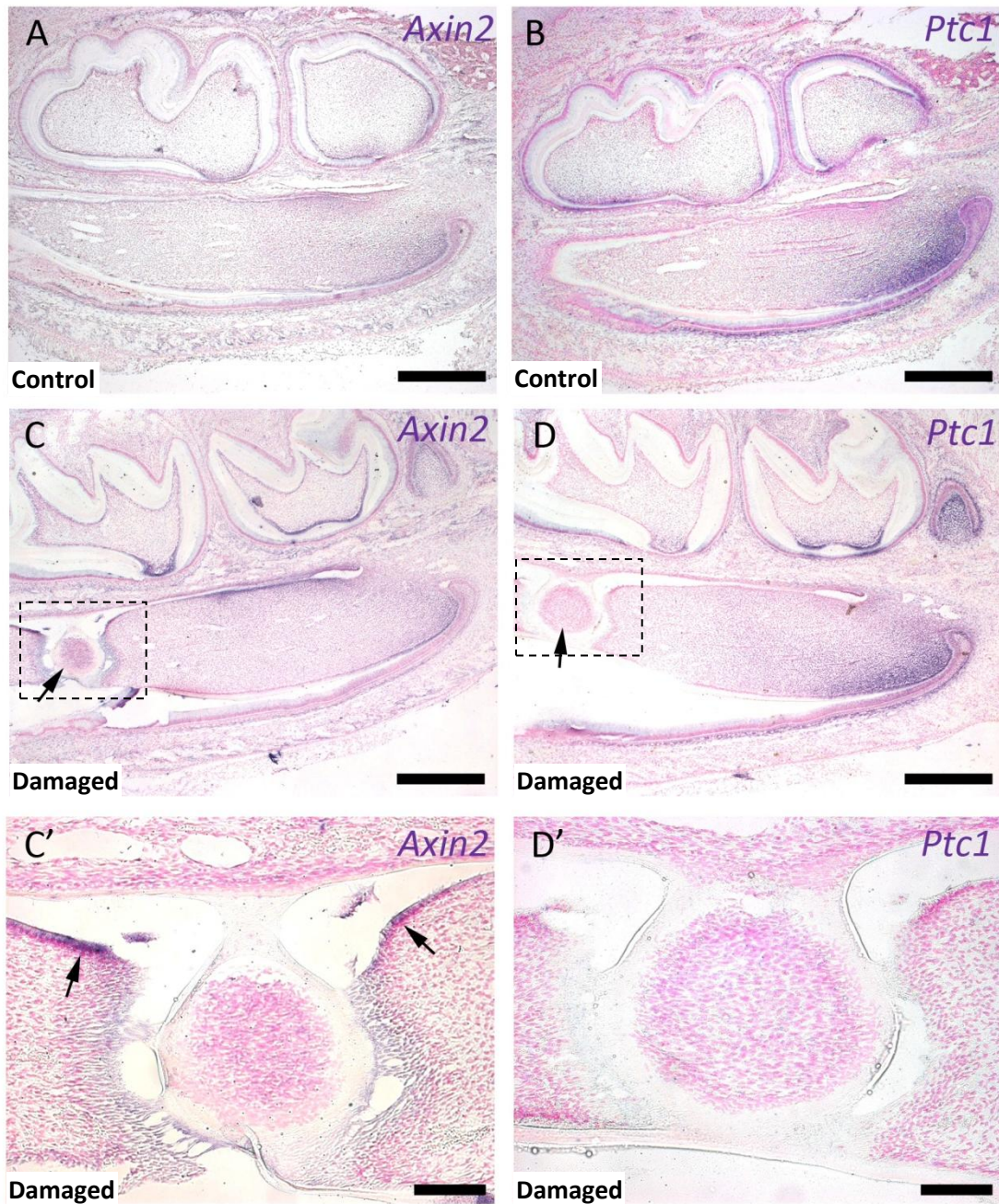
Figure 4.1 Expression of *Axin2* and Ptch1 in incisor pulp injury.
Incisor damage with a needle was performed on post natal day 5 wild type CD1 mice and collected 24 hours later. In situ hybridisation on sagittal sections of the mandibles was performed. The control mandible without damage shown in panels A and B indicate *Axin2* and Ptch1 expression close to the cervical loop mesenchyme. Incisor pulp damage is indicated by the black arrows in C and D. Increased *Axin2* expression surrounding the damaged pulp is observed (C). Furthermore, the odontoblast layer close to the injury strongly expresses *Axin2* indicated by the dark purple colour (arrows in C'). However, Ptch1 expression is absent around the injury (D and D'). Scale bars indicate 500µm (A, B, C, D), 100µm (C', D').
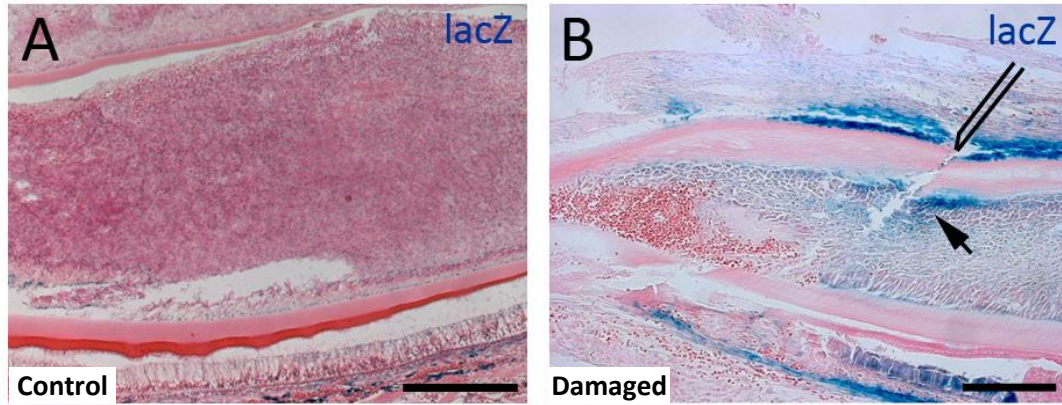
Figure 4.2 *Axin2* activation during incisor pulp damage

Incisor pulp damage was performed on *Axin2*$^{LacZ/+}$ P5 mouse incisors and collected 24 hours after injury. In the control undamaged incisor pulp, no β-galactosidase positive pulp cells were present (A). Upon damage, lacZ expression is visible in the dental pulp cells within the immediate wound site (arrow in B). Scale bars represent 150μm in A and 250μm in B.

4.2 *In vivo* molar damage

The needle damage method was found difficult to reproduce because the teeth were non-erupted and therefore the precise location of the incisor pulp region had to be estimated. In addition, local anaesthesia was used since general anaesthesia poses greater risk in neonatal death from hypothermia during the recovery period. Therefore, because the pups were able to move, generating equivalent damage in the incisors was challenging. To circumvent these inconsistencies, damage response was investigated in another tooth model, the adult mouse molar. Unlike the incisors, the mouse molar teeth possess roots and therefore do not grow continuously. Since these teeth will not contain a continuously active source of MSCs for growth, any stem cells present in the pulp would presumably become stimulated upon injury thus, the molar tooth provides a more comparable model of repair in human teeth.

In place of the needle damage method, a high speed dental drill was used for a better damage technique. The arrows in Figure 4.3A and A' illustrate the drill damage wound site created by the ball tipped diamond burr. The samples were collected 8 days after damage and H&E staining was performed on sagittal sections of the maxillary molars. Located within the injury site (shown by the arrow in Figure 4.3B), regions in the damaged pulp that resemble mineralized nodules were reflected by the intense areas of red staining (Figure 4.3B'). Also, at the top of the molar pulp wound, there appears to be the presence of red blood cells indicating the remnants of the initial inflammatory response (Figure 4.3B'). The control molar sections indicated in Figures 4.3C and 4.3C' show uniform pulp morphology with a distinctive odontoblast layer of columnar cells located adjacent to the dentine (Figure 4.3C').

Using a different soluble dye, aniline blue staining confirmed the presence of osseous tissue inside the injured molar dental pulp of CD1 adult mice (Figure 4.4). Dark patches of aniline blue staining were present in the damaged pulp (Figure 4.4B, D) in comparison to the undamaged molar pulp where staining appears paler and more uniform (Figure 4.4A, C). Similar to the H&E stain, at higher magnification, regions of disorganized matrix-like mineral is apparent within the injured pulp (arrows in Figure 4.4F), while the control pulp morphology is regular in appearance as shown by the uniform odontoblast layer of cells adjacent to the dentine (arrows in Figure 4.4E).
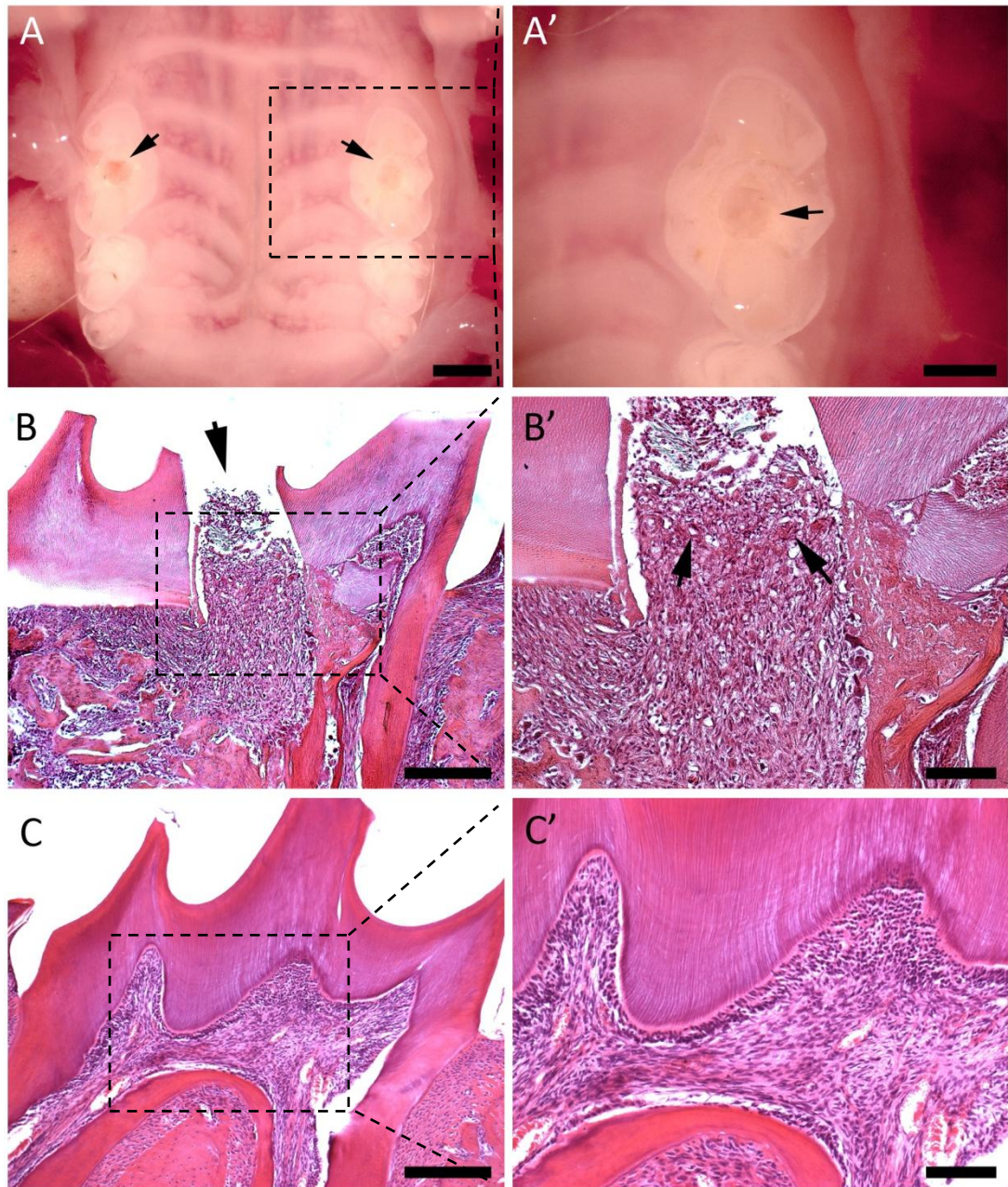
Figure 4.3 Drill damaged maxillary first molars
Maxillary first molars of adult CD1 wild type mice were drilled with a ball tipped diamond burr to achieve more controlled tooth damage in comparison to the needle damage method (arrows A and A'). Animals were culled 8 days post damage and stained with H&E. The drill pulp injury is indicated by the arrows in B and areas that resemble irregular matrix/ reparative dentine are shown in more detail by the arrows in B'. H&E stained control undamaged molar teeth are shown in C and C' demonstrating the natural morphology of the teeth. Scale bars represent 500µm (B) and 200µm (B').
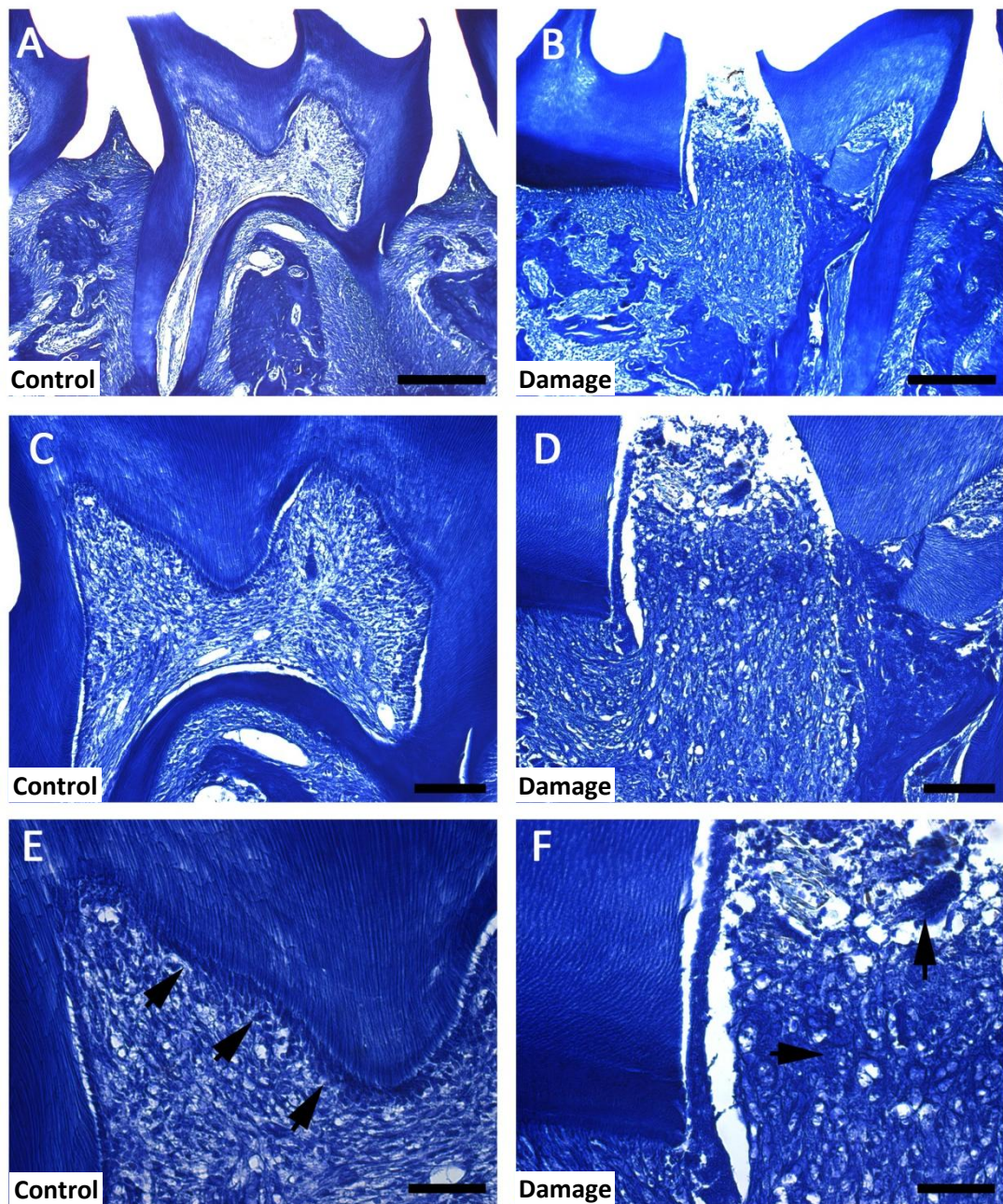
Figure 4.4 Aniline blue staining of drill damaged maxillary first molars
To detect areas of osseous tissues, sagittal sections of CD1 drill damaged and undamaged mouse molars were sectioned and stained with aniline blue. In the undamaged tooth (A), the intensity of aniline blue within the pulp chamber is weaker than the pulp region at the wound site (B). At higher magnifications (D, F), darker blue patches of staining indicate more ossified regions (arrows in F), while in the undamaged pulp the staining remains uniform (C). The morphology of the undamaged molar pulp is normal indicated by the presence of the columnar odontoblast cell layer adjacent to the dentine (arrows in E). Scale bars represent 500µm (A, B), 200µm (C,D) and 100µm (E,F).

4.3 Canonical Wnt response to molar tooth damage

To examine the Wnt/β-catenin activity response during tooth damage, using the *Axin2* lacZ mice, the same maxillary first molar drill damage procedure was performed on the *Axin2*+/- and the *Axin2*-/- mutants. Because *Axin2* is a negative regulator of the canonical Wnt pathway that suppresses signal transduction by promoting β-catenin degradation, lacZ expression in these mice will reveal any changes to the endogenous canonical Wnt signals in the dental pulp during the tooth damage and repair process.

In the heterozygous (+/-) mice, where lacZ has been knocked into a single allele, the repair response shown by osseous tissue formation is limited to small patches of aniline blue within the injured pulp chamber (arrows in Figure 4.5A). However, in the homozygous mutants (-/-), where Wnt/β-catenin signalling is upregulated, the repair response is massively enhanced indicated by the mass secretion of osseous matrix present within the entire damage pulp area (asterisk in Figure 4.5B). In contrast to the control, uninjured molar teeth, when stained with aniline blue, the pulp is uniformly pale in colour demonstrating the absence of reparative mineral formation inside the pulp (Figure 4.5C and C').
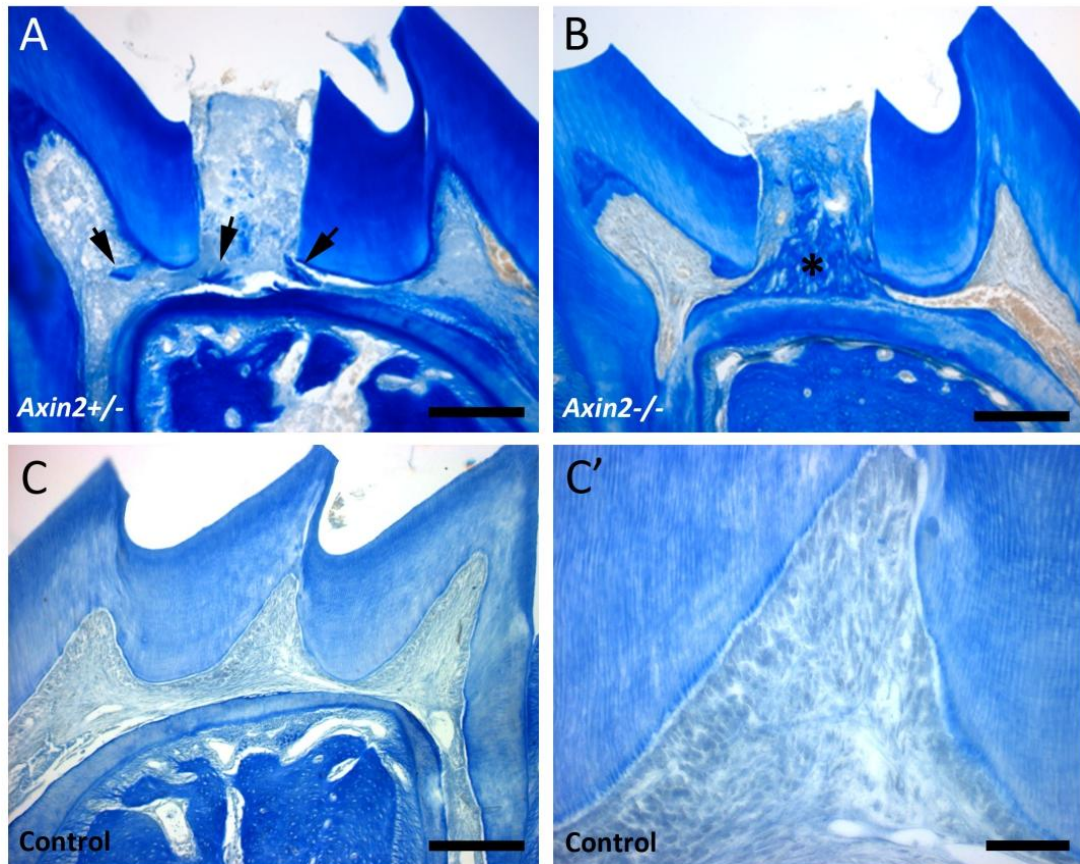
Figure 4.5 Enhanced molar pulp response in Axin2LacZ/LacZ adult mice
The drill damage procedure was performed on the first molars of *Axin2*$^{LacZ/+}$ and *Axin2*$^{LacZ/LacZ}$ mice. In the *Axin2*$^{LacZ/+}$ mutant, small regions of darker aniline blue staining is observed (arrows in A). In contrast, the wound response observed in the *Axin2*$^{LacZ/LacZ}$ mice is immensely upregulated as shown by the marked increase in dark blue staining of the pulp (asterisk in B). Scale bars represent 500µm (A,B) and 50 µm (C, C'). Data in panels A and B from collaboration with Helms group (Stanford University, USA).

4.4 Pericyte response to dental pulp damage

It is clear that canonical Wnt signalling is enhanced in the region where damage to the pulp occurs. However, it is unknown on what cells the signals are acting on. Following the initial response via inflammatory cells one such population to react to the signal could be the endogenous mesenchymal stem cells. An important source of these MSCs within the dental pulp is the pericyte population. These cells are associated with blood capillaries and under normal conditions remain in a "quiescent" state in the pulp. However, upon injury to the mouse incisor tooth, they could become mobilised as suggested by Feng et al., (2011). In contrast to the open-rooted incisors that continue to grow throughout life, mouse molars develop roots and remain constant in size after eruption. Therefore, unlike the incisors which have a readily available "pool" of MSCs responsible for growth, in the molar tooth, the MSCs present in the pulp would exclusively serve to maintain pulp homeostasis and orchestrate injury repair. We believe these stem cells belong to the pericyte population hence, to fully appreciate their contribution and involvement in tooth injury and repair, the molar tooth damage model was used as a novel approach.

In order to trace these MSCs, permanent labelling of NG2+ve pericytes within the dental pulp was achieved by crossing NG2creER mice (Zhu et al., 2011) with the Rosa26R reporter mice (Soriano, 1999) to produce tamoxifen inducible NG2creER; R26R transgenic mice. After tamoxifen induction, the NG2+ve pericytes and their derivatives are labelled indelibly and can be visualised by x-gal staining, thus, this system was used to lineage-trace the contribution of pericytes during molar tooth injury.

When the upper first molar teeth of adult NG2creER; R26R transgenic mice were drilled to mimic tooth damage, a massive pericyte response (blue lacZ+ve cells) was visible adjacent to the injury site indicated by the arrow in Figure 4.6A. At higher magnification, areas suggestive of disorganized reparative mineral close to the lacZ positive pericytes was

visible (labelled as rd in Figure 4.6B). In the same tooth, the pulp cells away from the injury site shown in Figure 4.6C indicate the presence of very few pericytes. In any section, the number of pericytes was no greater than 4 or 5. This is consistent with the study by Feng et al. (2011) where numbers of NG2+ve pericytes at the resting phase were low. Similarly, in the control undamaged tooth, very few lacZ+ve pericytes was observed (Figure 4.6D). In this image, immediately adjacent to the dentine, there is a noticeable columnar-shaped odontoblast-like pulp cell demonstrating pericyte contribution to odontoblast differentiation in a non-continuously growing tooth (Arrow in Figure 4.6D).
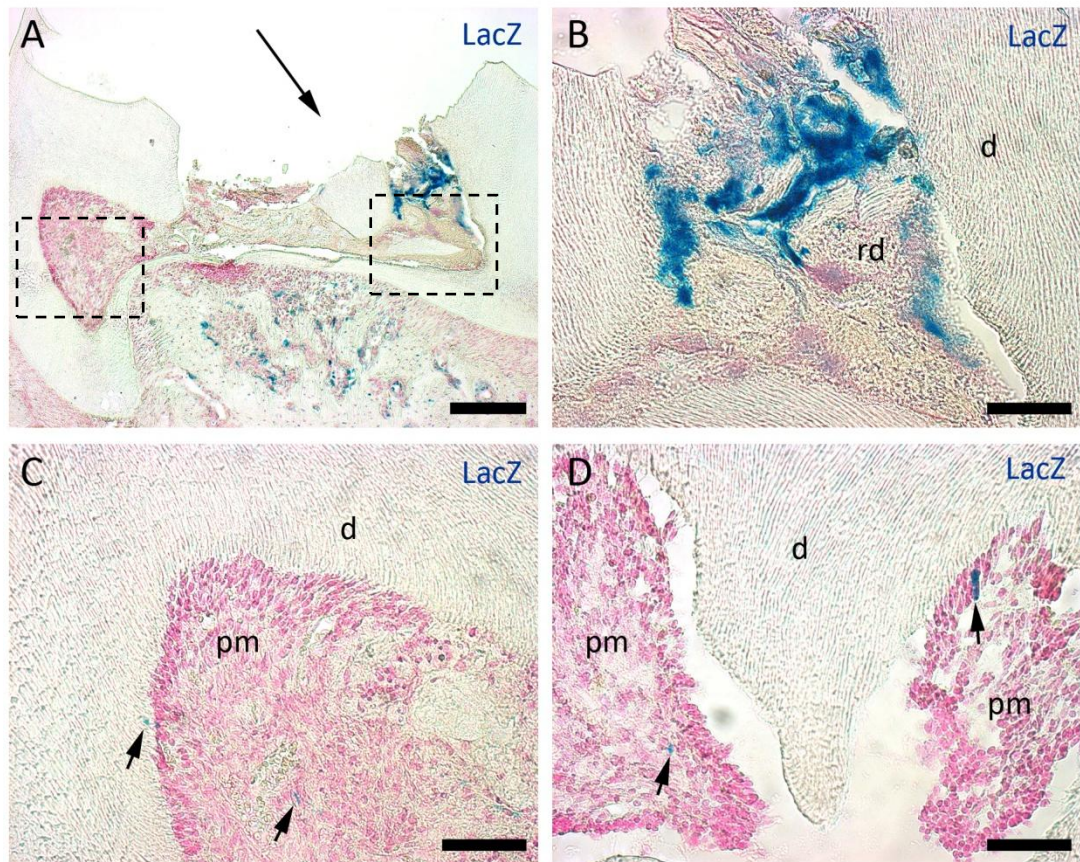
Figure 4.6 Pericyte response following *in vivo* molar tooth damage
First molars of NG2creER; R26R transgenic adult mice were drill damaged (arrow in A) and the animals were culled 4 days after. Following x-gal staining, a huge pericyte response is observed within the wound indicated by the lacZ+ve cells in A and also at higher magnification, disorganized mineral-like areas resemble reparative dentine within and surrounding the NG2-lacZ+ve cells (B). Compared to the non-injured region of the same tooth, few lacZ+ cells are present (arrows in C). Similarly, in the undamaged molar control tooth, few NG2-lacZ+ve cells are present however, notice the elongated odontoblast-like LacZ+ cell close to the dentine (arrow in D). Abbreviations d: dentine, rd: reparative dentine, pm: pulp mesenchyme. Scale bar indicates 200µm (A) and 50µm (B,C,D).

4.5 Discussion

While previous studies have focused on the role of canonical Wnt signalling in tooth development (Lin et al., 2011; Liu et al., 2008; Lohi et al., 2010; Sarkar and Sharpe, 1999), little is known about its role during tooth repair of mature adult teeth. In light of the results obtained in chapter 3 that suggest rat dental pulp cell migration in a Wnt-dependent manner, this chapter investigated the *in vivo* pulp cell properties taking advantage of the mutant mouse line *Axin2*^LacZ, to follow canonical Wnt signalling, and NG2-creER; R26R to explore the extent that pericytes contribute to postnatal tooth repair.

4.5.1 Canonical Wnt signalling in tooth injury

Wnt/β-catenin signalling plays essential roles in organogenesis and tissue homeostasis (Grigoryan et al., 2008). The importance of this pathway led to the investigation of its role in tooth repair. Using experimentally injured teeth from wild type CD1 mice and *Axin2*^LacZ mice, *in situ* hybridization and x-gal staining respectively, revealed activation of canonical Wnt signalling exclusively within close proximity to the wound. This represents a novel finding and shows that Wnt/β catenin signalling acts as a damage response mechanism during tooth injury in both the mouse incisors and molars. Similar responses upon damage have been described in other tissues in species of both vertebrate and invertebrate origins (Gurley et al., 2008; Kawakami et al., 2006; Petersen and Reddien, 2009). Common to all these studies, the Wnt/β catenin pathway is activated upon injury to the tissue, thereby indicating the relevance of the results achieved from modelling tooth injury in the mouse in this chapter. Morever, in terms of tooth development, the canonical Wnt signalling pathway has been demonstrated to be essential for the activation of the odontogenic

mesenchyme (Chen et al., 2009) and further development, including the crown and root both embryonically and postnatally (Lohi et al., 2010; Zhang et al., 2013). β-catenin-mediated canonical Wnt signaling was confirmed necessary for the activation of odontogenic potential in the developing tooth mesenchyme. Using the Catnb$^{f/f}$;Osr2-IresCre mutant mice where β-catenin is inactivated in the dental mesenchymal cells, molar tooth development failed to progress from the bud to cap stage (Chen et al., 2009). Later studies using the *Axin2*^{LacZ} reporter mice revealed for the first time the canonical Wnt expression patterns in the secondary enamel knots and also in the underlying odontoblasts that previous Wnt/ β-catenin reporter mice (TOPgal and BATgal) were unable to detect (Lohi et al., 2010). This therefore demonstrated that the *Axin2* reporter mouse represents the most accurate transgenic mouse line to identify canonical Wnt expression. This study was also the first to examine canonical Wnt signalling postnatally, where strong *Axin2* expression in the developing roots of P10 to P15 mice revealed new roles for Wnt/ β-catenin signalling in tooth root development (Lohi et al., 2010), further confirmed by a recent report showing that conditional knockout of the β-catenin gene (Ctnnb1) within developing odontoblasts and cementoblasts during the development of tooth roots results in rootless molar teeth (Zhang et al., 2013). Together, this data substantiates the important role that canonical Wnt signalling plays during the mesenchymal component of tooth development, therefore, it is not surprising that this signalling pathway was found to be upregulated during damage to the dental pulp mesenchyme both in the incisor and molars, where presumably, similar developmental signals are required to orchestrate the repair of the dentin/pulp complex by odontoblast differentiation.

One of the most striking results observed in this chapter was the huge repair response indicated by the aniline blue stained osseous areas in the *Axin2*$^{-/-}$ drill damaged molars compared to the heterozygous *Axin2*$^{+/-}$ mutants. In the homozygous mutants where both

Axin2 alleles have been replaced by the LacZ gene, nuclear β-catenin protein levels are increased because *Axin2* is a negative regulator of the canonical Wnt pathway and under normal conditions, suppresses signal transduction by promoting degradation of β-catenin (Jho et al., 2002). This has been demonstrated by *Axin2* knock out studies in bone remodelling where increased Wnt–β-catenin signalling produces enhanced bone formation (Yan et al., 2009) and in craniofacial morphogenesis where homozygous *Axin2* knockout (KO) mice were shown to have craniofacial defects and premature closure of the cranial sutures due to increased β- catenin signaling (Yu et al., 2005).

Increased canonical Wnt signalling led to increased mineral formation as part of the tooth repair response. This result is consistent with data observed from studies in bone, where damage to the tibia of TOPgal Wnt reporter mice indicated upregulation of Wnt signalling analogous to the results observed here in teeth, and causes bone-marrow derived progenitor cells to respond to the endogenous Wnt signal by differentiating into osteoblasts (Kim et al., 2007). In the case of tooth damage, the endogenous Wnt signal would signal pulp progenitor cell differentiation into odontoblasts. Further *in situ* hybridisation studies using odontoblast markers such as DSPP would confirm this.

4.5.2 Pericyte response to postnatal tooth repair

Cells with mesenchymal stem cell like properties isolated from a range of mesenchyme tissues using expression of pericyte markers followed by long term culture have provided evidence that pericytes can act as a source of MSCs *in vitro* (Crisan et al., 2008b; Shi and Gronthos, 2003). More recently, one study using genetic lineage tracing experiments has confirmed that pericytes are a source of MSCs *in vivo* (Feng et al., 2011). Using expression of the pericyte marker gene, NG2, inducible NG2-Cre expressing mice crossed with R26R

reporter mice allowed permanent labelling of NG2-expressing pericytes and their progeny with β galactosidase (LacZ[+]). The contribution of pericytes to incisor mesenchymal differentiation was then followed during growth and in response to injury. Very few LacZ+ (pericyte derived) odontoblasts were observed under normal postnatal incisor growth suggesting that an in addition to the MSCs derived from the pericyte niche, another source of MSCs must be of non-perivascular origin which contributes to the continuous renewal of odontoblasts during normal incisor growth. In contrast, incisor damage to the NG2creER;R26R double transgenic mice showed that pericytes are stimulated to proliferate and also differentiate into new reparative-dentine producing odontoblast cells (Feng et al., 2011). This was the first report to indicate dual origins of MSCs within the continuously growing mouse incisor. Interestingly, the unique properties of this continuously growing tooth is reflected in the different responses to tooth damage in that for all teeth, under injurious conditions, a generic perivascular response occurs whereas the cervical loop MSC niche response only takes place in continuously growing teeth. Therefore, the pericyte damage response in non-continuously growing mouse molar teeth was examined on the basis of it being a potential source of Wnt-responsive MSCs.

Using the NG2creER;R26R double transgenic mice under normal conditions without stimulus, consistent with results in the study conducted in incisors by Feng *et al.* (2011), there are very few pericytes in the molar pulp. In addition, pericytes appear to contribute to odontoblast differentiation in non-continuously growing teeth which has not been documented in the past. In the molar tooth damage scenario, there appears to be massive proliferation of LacZ+ pericytes situated at the injury site, alongside the appearance of mineral resembling reparative dentine, further substantiating the original hypothesis in that pericytes may be a Wnt responsive MSC population contributing to the tooth repair process.

In summary, the results presented in this chapter build upon a body of evidence suggesting that pericytes are directly involved in the tooth repair process and provide a source of MSCs for tooth homeostasis as well as repair. Furthermore, alongside the *in vitro* transwell results in Chapter 3, the *in vivo* studies here using transgenic Wnt reporter mice suggest that canonical Wnt signalling appears to be a likely candidate to drive the mobilisation of these MSCs and subsequent proliferation and differentiation as part of the healing process.

After studying the damage response mechanism by intentional drill damage to the molar tooth as a way to circumvent the difficulties in creating damage to the mouse incisor, the unique continuously growing property of this tooth led to the consideration of modelling tooth damage at their tips. Constant attrition at the incisal tips as a result of gnawing and feeding provides a unique opportunity to examine a form of natural, continuous damage and repair process which has never been studied before. This intriguing avenue will be further explored in the following chapter.

5. Results chapter III: The incisor tip niche

Tooth damage has been experimentally modelled by artificially injuring the teeth providing evidence for Wnt signalling and pericyte contribution to the tooth repair process. In rodents, incisors are continuously abraded at their tips, with tissue loss being balanced by continuous growth. In 1915, a study on the structure and growth of the rat incisors by Addison and Appleton described a region at the tip of the incisor that contains irregular structured dentine that appears to seal off the pulp chamber preventing pulp damage as the tooth is continually sheared (Addison and Appleton, 1915). The presence of both mesenchymal and epithelial stem cells located at the proximal ends of mouse incisors allows them to sustain continuous growth and renewal to counterbalance the wearing at the incisor tips (Harada et al., 1999; Seidel et al., 2004). Because the tips of the mouse incisors undergo constant functional attrition when the animal feeds and gnaws, in order to protect the pulp from damage and infection, the mouse must rapidly "seal" the exposed pulp. To test this hypothesis, tetracycline studies and histological analysis were performed on the mouse incisors under different stimulus conditions to assess the tip response to the natural damage of tooth wear.

To further understand the mineral composition of the incisor tips and compare differences between the region of normal and irregular dentine at the occlusal surface of the tips based on the morphological differences observed, micro-Raman spectroscopy was carried out. This laser based technique enables biochemical analysis of cells and tissues using the inelastic scattering of light by chemical bonds, allowing the biomolecular composition of cells or tissues to be determined by the relative intensities of characteristic molecular vibrations (Swain and Stevens, 2007).

Based on the results presented in chapter 4 suggesting a pericyte contribution to both homeostasis and repair of the tooth, a possible role of pericytes in mineralization at the incisor tips was investigated. The expression of another known pericyte marker Nestin, was studied using the double transgenic mouse (NestincreER; Rosa26R) to lineage trace Nestin+ pericyte contribution to the incisor tip region. Any Nestin-positive pericytes could then be visualised following x-gal staining. This work allows a comparison between two contrasting forms of repair: that mediated in response to intentional tooth damage (presented in chapter 4); and continuous repair from natural damage.

5.1 Mouse incisor tip features

"*Osteodentine*" was described as granular material filling the apex of the pulp chamber in the tips of the rat incisor tooth (Addison and Appleton, 1915). To begin to examine in detail how this compares with the morphology of the mouse incisor tips, gross morphology of freshly dissected teeth was assessed. Freshly dissected mouse incisors viewed under the dissecting microscope revealed that the occlusal surfaces of both the maxillary and mandibular incisors showed evidence of mineralised tissue in the exposed pulp (Figure 5.1A, 5.1B). The central region of the tip mineral appears irregular and coarse (arrows in Figure 5.1A, 5.1B), while the regular dentine is smooth in appearance (labelled as d in Figure 5.1A, 5.1B). To test the hypothesis that the irregular mineral is created to seal off and protect the pulp, tetracycline labelling was performed. Tetracycline is an antibiotic that has long been known to be incorporated into newly formed human dentine and fluoresces under UV light microscopy (Kawasaki et al., 1977). More recently, this property has been exploited to label newly formed dentine by SHED cells in mice (Sakai et al., 2010). The same method was applied to this study in search of evidence to support the hypothesis

that the patch of irregular mineral located at the occlusal surface of the incisal tips is rapidly produced to "repair" the continuous damage that takes place. After tetracycline labelling for 24 hours, areas of rapid mineral production, characterised by strong fluorescence signals, were located at the tips of both the maxillary and mandibular incisors, seen in Figure 5.1C and 5.1D respectively. Furthermore, both patches indicated by the arrows correspond to the central region containing the morphologically irregular mineral indicated by the arrows in Figure 5.1A and 5.1B. This suggests that mineral is being rapidly generated in the exposed pulp cavity at the tips of the mouse incisor teeth.
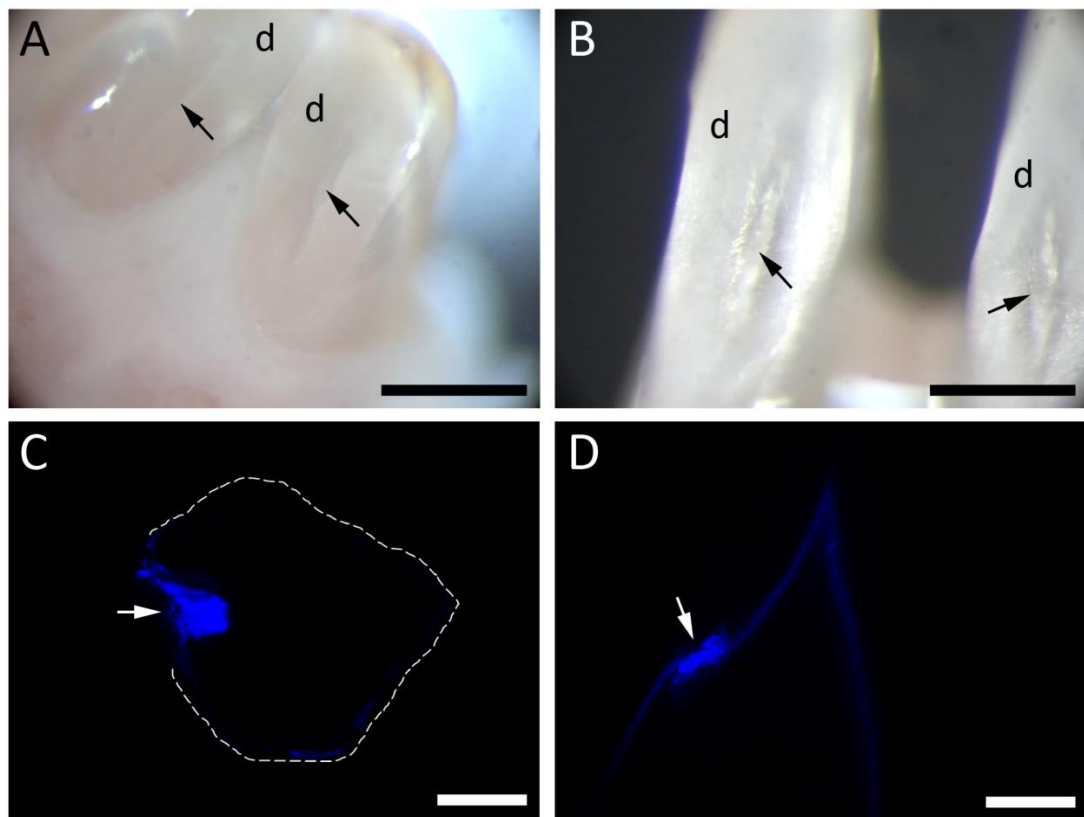
Figure 5.1 The incisor tip of CD1 adult mice

The tips of the mouse maxillary (A) and mandibular (B) incisors show a central region on the occlusal surface of the tooth that contains morphologically irregular mineral (arrows in A and B) compared to the surrounding dentine that is smooth in appearance (labelled d in A and B). A single tetracycline injection to the mice followed by a 24 hour chase period was used to locate any areas of rapid mineralisation. With UV confocal laser scanning microscopy, frontal (C) and saggital (D) cryosections of the tip reveal an intense fluorescent patch indicating newly deposited tooth mineral that corresponds to the irregular mineralised region on the tip surface (arrows in A and B). Abbreviations: d: dentine. Scale bars represent 500 μm (A, B) and 250μm (C, D).

5.2 Tip niche response to different stimulus

To analyse the role of this irregular patch of mineralised tissue capping the incisor tips, it was important to evaluate the response of this mineral under different external stimuli. The primary stimulus to influence this deposition of mineral at the incisal tips is feeding since it is a direct cause of incisal tooth abrasion. To investigate the response of the incisal tips towards this external stimulus, mice were placed onto soft "mash" diets for a period of 1 and 4 days in contrast to their normal diet that consists of hard rodent chow pellets. Mineralization at the tips was observed under all feeding regimes (arrows Figure 5.2 A,B,C,D), which was consistent with the location of the irregular occlusal surface observed in Figure 5.1. On the soft diet, the incisor pulp appeared more mineralised in comparison to the control mice on their normal hard chow (Figure 5.2B,C). The percentage area of irregular tip mineralisation compared to the whole tip in the control mice was 12.5% while the mineralisation of the tips of those on the 4 days and 1 day soft diet were 44.1% and 44.2% respectively. Interestingly, although the percentage area of tip mineralisation for both the short and longer term soft diet were similar, there was a distinct morphological difference in mineral deposition over the 4 day period resulting in a multilayered–lacunae type structure (Figure 5.2B'). In comparison, the mineralization after 1 day on the soft diet was less intricately developed and more granulated in appearance (Figure 5.2C'). Interestingly, after feeding on a soft diet for 1 day, when the mice were changed back to their regular hard pellets for 4 hours before collection, there is a prominent reduction (~52%) in the area of the irregular tip mineral (Figure 5.2D') which appears to restore the tooth closer to its original morphology under normal hard diet conditions (Figure 5.2A'). Thus, tip mineralisation appears to change based on exposure to different abrasion stimuli and overcompensation by the pulp cavity defence mechanism results in excess mineral production when under-stimulated by the soft diet.
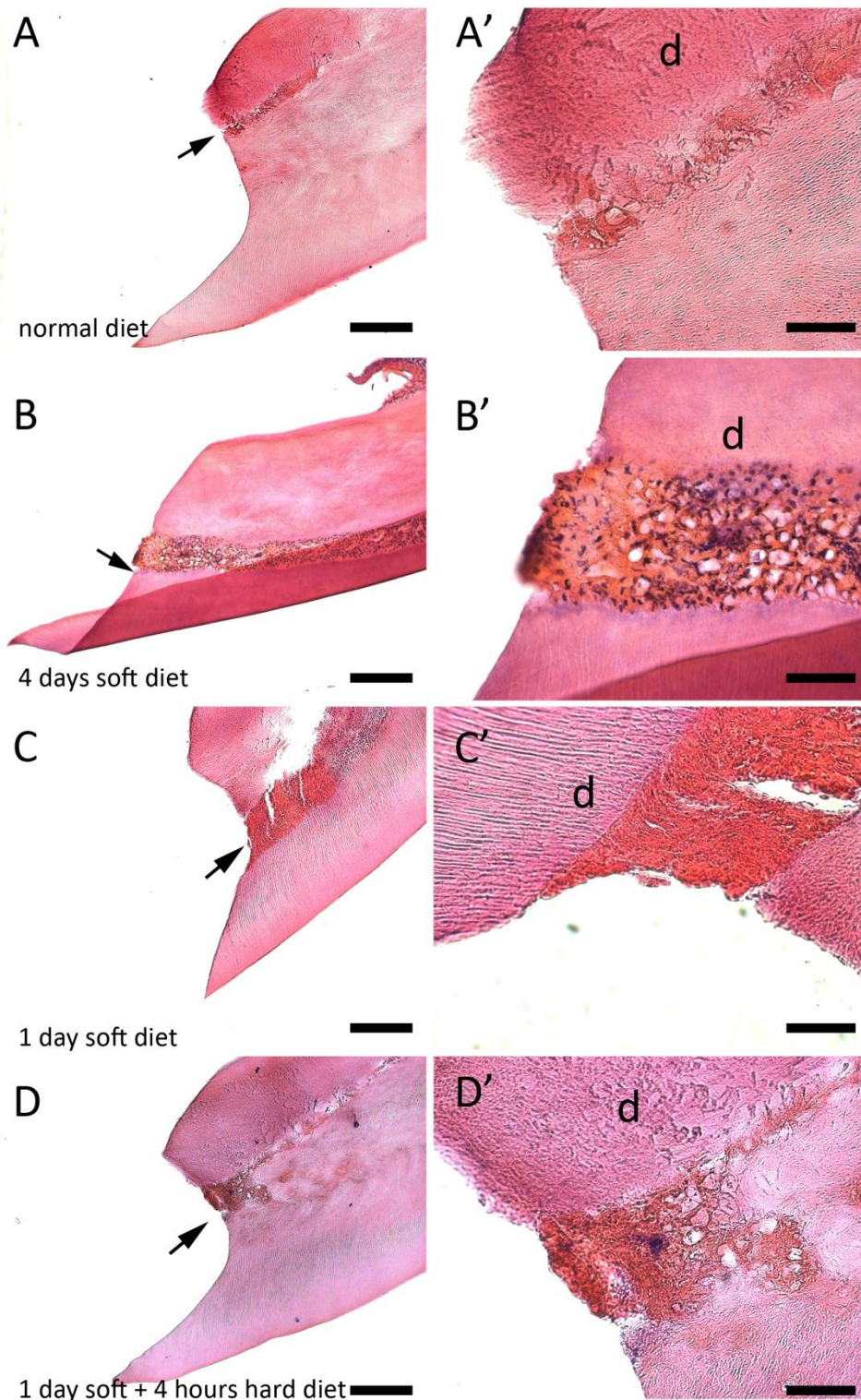
Figure 5.2 The incisal tip niche in CD1 adult mice.
CD1 mice were exposed to 4 different feeding regimes including control ordinary hard pellet diet, 4 days and 1 day on soft mash diet or 1 day soft diet followed by 4 hours ordinary hard diet. Incisor tip mineral of the mice on normal hard chow are shown in panels (A and A'). Both the incisor tips of the mice on the 4 days and 1 day soft diet had a larger region of irregular mineral indicated by the arrows in B and C in comparison to A. Upon higher magnification, the mineral produced after 4 days on the soft diet appears to contain lacunae structures and cells (B') compared to 1 day (C') where the mineral appears more granulated. Interestingly, after switching back to the hard diet for 4 hours, this chunk of mineral diminished significantly (D, D'). Scale bars indicate 200µm (A,B,C,D) and 50µm (A', B', C',D').

5.3 Pericyte contribution to incisor tip mineralisation

To evaluate whether pericyte-derived MSCs contribute to incisor tip mineralisation, Nestincre; R26R double transgenic mice were used. Following x-gal staining of cryosections, it is clear that blue lacZ+ve pericyte-derived cells were in abundance at the tip of the incisors (Figure 5.3). Again, there appears to be a mass of mineral at the tip of the incisors (asterisk in Figure 5.3A) consistent with the the morphology observed both immediately following dissection and the results obtained from the tetracycline studies. Remarkably, the LacZ+ pericyte-derived cells appear visibly embedded within the irregular tip mineral at the apex of the pulp chamber indicated at a higher magnification by the arrows in Figure 5.3A'.

In cross sections of the incisal tip just beneath the occlusal surface, the tip of the pulp mesenchyme region is visibly rich in Nestin+ve cells (Figure 5.3B). Interestingly, Nestin+ve dentine tubules resembling remnants of odontoblast processes and dentinogenesis are observed at the tips suggesting pericyte contribution towards odontoblast differentiation (arrows Figure 5.3B').
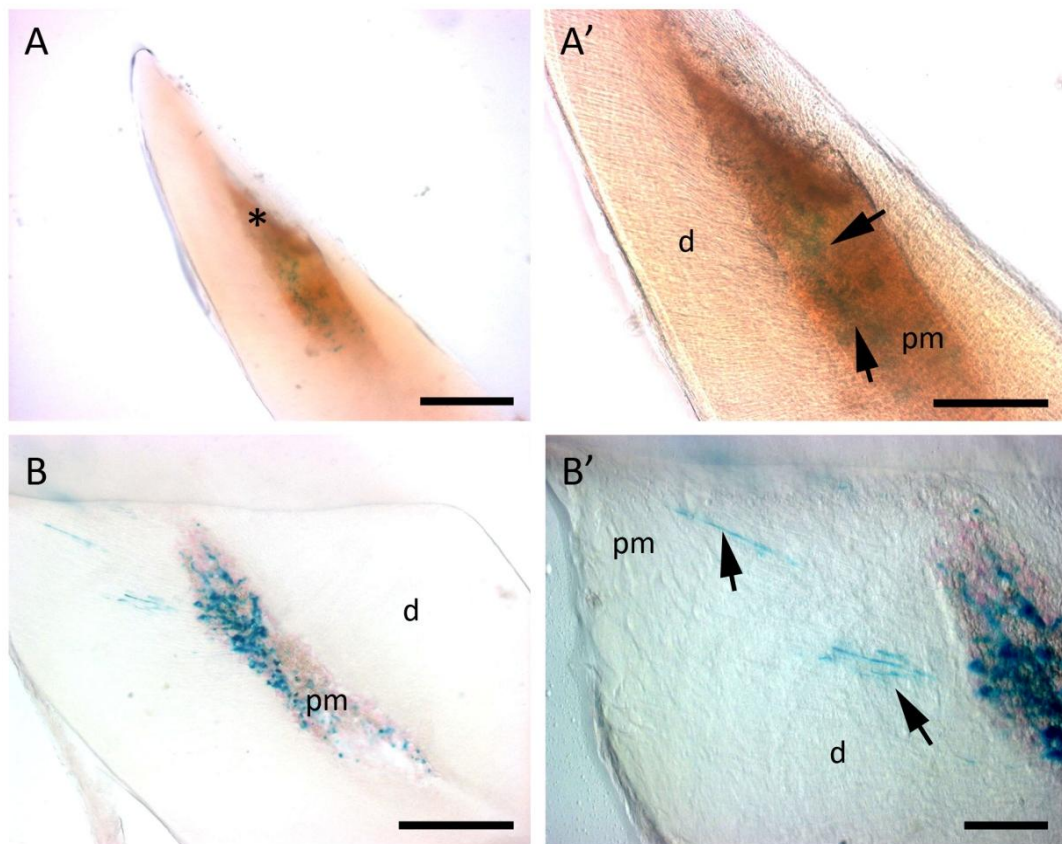
Figure 5.3 Nestin-positive pericyte contribution to the incisal tip niche
A region of irregular dentine is located at the tip of the mouse incisor indicated by the asterisk in A. At higher magnification, genetically labelled Nestin+ve pericytes appear visibly embedded beneath the irregular mineral-like structure at (arrows in A'). Panel B indicates a pool of lacZ+ve pericyte cells located in the apical end of the pulp mesenchmye. Interestingly, lacZ+ve dentinal tubules are present suggestive of pericyte contribution to odontoblast differentiation (arrows in B'). Abbreviations, d: dentine, pm: pulp mesenchyme. Scale bars represent 250µm (A), 150µm (A', B) and 50µm (B').

5.4 Incisor tip mineral composition

The standard biological techniques used thus far including morphological, histological and lineage tracing experiments have enabled the identification of observational differences between the normal dentine and irregular mineral on the incisal tip occlusal surface. However, these techniques provide limited information on the overall structural and biochemical properties of the mineralised tissue produced at the incisor tips. To better understand the structural composition and differences in the mineral properties between the normal dentine and irregular mineral, laser-based Raman microspectroscopy was used as a more materials-based analytical approach. When an intense monochromatic light source (laser) is fired at a sample, the majority of the light is scattered elastically and this is known as the Raleigh effect. A small quantity of light scatters inelastically, which is the Raman effect. Small shifts in the wavelengths of the inelastically scattered light occur as a result of energy exchange between the excitation light and the molecules within the tissue. These Raman shifts yields a spectrum that indicates the type of bonds present in the sample that caused the particular shifts, thus providing a "biochemical fingerprint" of the tissue. Moreover because Raman microspectroscopy was used, this enabled the analysis of micro-scale features of the mineral providing molecular-level information about the biochemical composition and structure of the incisor tips (Figure 5.4).
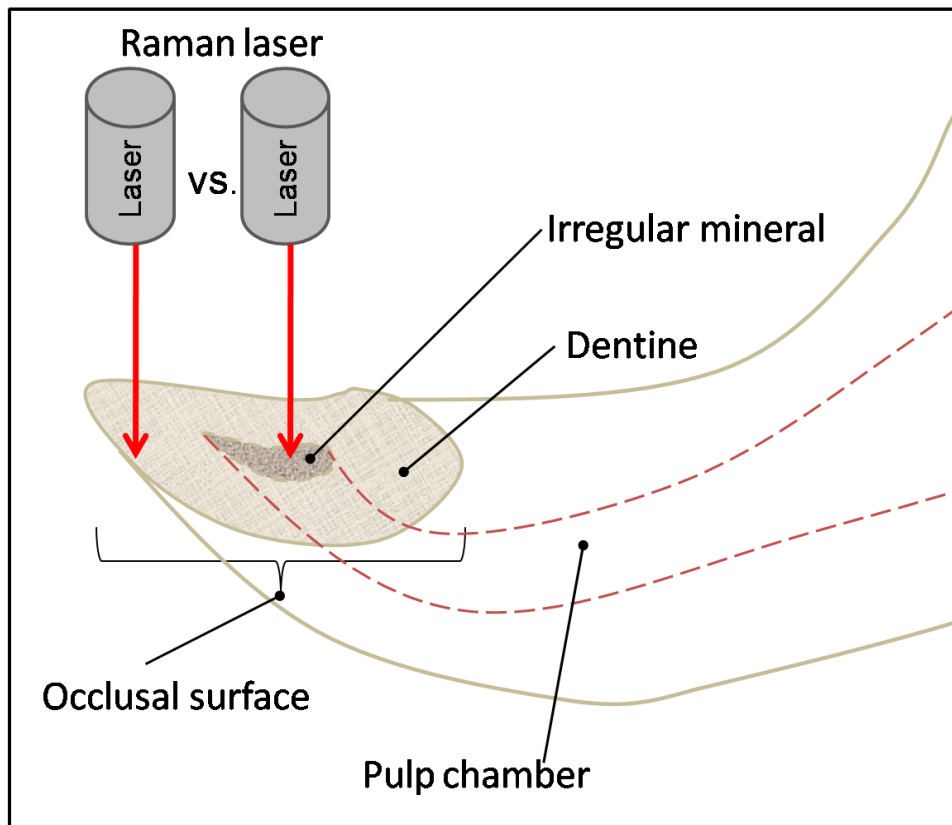
Figure 5.4 Schematic of Raman spectra collection
The occlusal surface of the mouse incisor tip is illustrated in the schematic above. Raman spectra were collected from two different regions of the occlusal surface to compare structural and compositional mineral differences between the morphologically normal dentine located towards the outer region of the occlusal surface, and the central region of irregular hard matrix where the presumptive pulp chamber seal is situated.

Raman spectra obtained from the irregular and normal dentine revealed strong peaks indicative of inorganic phosphate ($PO_4^{3-}v_1$) near wavenumber 960cm^{-1} and weaker peaks associated with substituted $CO_3^{2-}v_1$ near 1070cm^{-1} (Figure 5.5 C,D). In contrast to the normal dentine, prominent protein bands corresponding to amide I (1,595-1,720cm^{-1}) and amide III (1,243-1,269cm^{-1}) in the Raman spectra of the irregular pulp mineral, reflected a proteinaceous component suggestive of less mineralisation and the presence of more collagen/protein in this region. Further evidence from the microspectroscopic mapping of the spectra displayed as heatmaps of the occlusal surface suggests high mineral content compared to collagen/proteins for areas containing normal dentine shown as red in the 960/amide I ratio heatmap and less mineral in the black regions which correspond to the central occlusal surface containing irregular pulp mineral (Figure 5.5E). The Figure 5.5F heatmap indicating the CO_3 intensity enables information on the presence of hydroxyapatite ($Ca_{10}(PO_4)_6(OH)_2$), a mineral component of bones and teeth where OH^- ions or PO_4^{3-} groups can be substituted with carbonate (CO_3^{2-}). Therefore, the difference in carbonate intensity on the occlusal surface suggests more crystallised/solid mineral in the normal dentine (red areas) in comparison to the irregular mineral containing less carbonate substitution indicated in black (Figure 5.5F). The final heat map (Figure 5.5G) indicates the full width at half maximum (FWHM) of the peak corresponding to amide I where the presence of the strong red region along the centre of the irregular mineral suggests many amide bonds and collagen whereas the outer areas are darker and therefore suggests more mineralization and less protein (Figure 5.5G).

The Raman spectra analyses thus reveal that the mineral covering the tip pulp tissue is less mineralised than regular dentine and contains more protein/collagen bonds and is therefore structurally weaker. This would correlate with the tetracycline result as rapidly generated mineral would be "immature" and less structurally complex and consequently "softer".
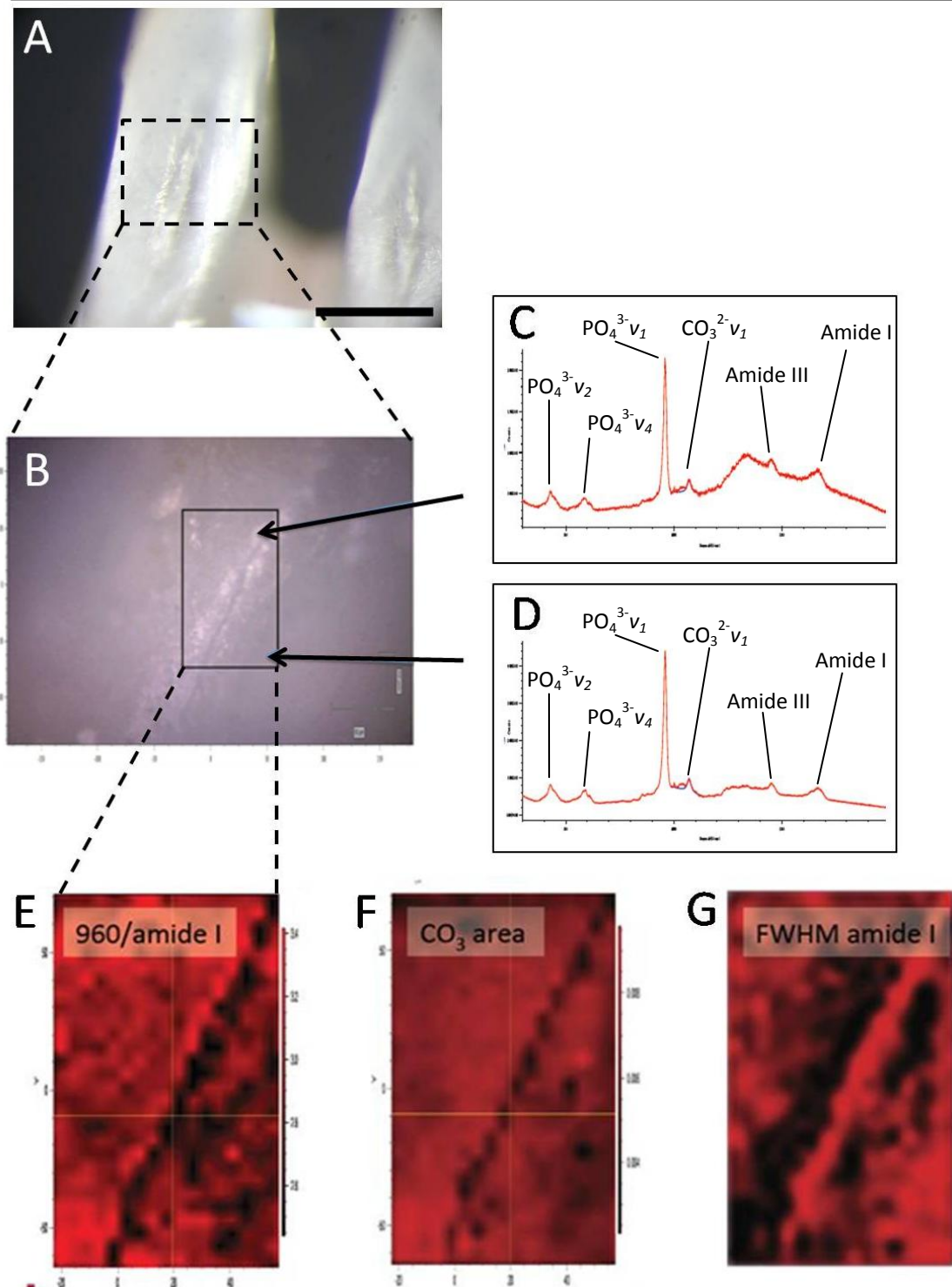
Figure 5.5 Raman spectroscopy conducted on the incisor occlusal surface
Image A illustrates the incisor occlusal surface and the region where Raman spectra were obtained is indicated in image B. Raman spectra of the irregular pulp mineral and normal dentine on the occlusal surface are shown in C and D respectively. Both Raman spectra reveal a strong characteristic $PO_4^{3-}v_1$ peak at 960cm^{-1} in addition, peaks associated with substituted $CO_3^{2-}v_1$ appear near 1,070cm^{-1}, further towards the right of the phosphate peak, lower intensity protein bands are evident including amide I and III at (1,595-1,720cm^{-1}) and (1,243-1,269cm^{-1}) respectively (C,D). E, F and G represent high spatial resolution mapping of the occlusal surface region indicated by the box in B and correspond to the phosphate/amide I ratio, CO_3 area and full width at half max (FWHM)/amide I. The red and black colour denotes high and low intensity respectively.

5.5 Discussion

The rationale behind studying the incisor tip was based on the assumption that continuous wear must involve "repair" of exposed pulp, i.e. a continuous, natural form of tooth repair. Thus, this could provide more insight into reparative dentine formation. The interest in the continuously growing mouse incisor tips stems from a study conducted over almost a century ago where the authors observed a region of irregular hard matrix on the occlusal surfaces of both the maxillary and mandibular incisors of the adult rat (Addison and Appleton, 1915). The results presented are consistent with those observed by Addison and Appleton in the mouse incisor tips where the exposed pulp cavity contained a narrow strip of coarse and irregular structured mineral. The similarities between the results presented here and those observed in the 1915 study are illustrated in the Figure 5.6.

After distinguishing a clear morphological difference between the regular dentine and the irregular hard matrix at the occlusal surface, to enable a more detailed analysis of the mineral properties, tetracycline labelling technique (Skinner and Nalbandian, 1975) was employed to detect any regions of rapidly produced mineral. Since protection of the pulp chamber is necessary to prevent pulp damage and infection from the constant wearing at the tips, the hypothesis was that constant mineral turnover would provide a "plug" to seal off the pulp cavity and prevent infection to the most vital component of the tooth. The strong UV fluorescence indicated remarkably rapid production of fresh mineral corresponding to the region that displayed irregular mineral morphology, thereby confirming this hypothesis. Furthermore, histological analysis of the tips using H&E staining provided further evidence to indicate the presence of the distinctive pulp-mineral "plug". Interestingly, the varied morphological response achieved by subjecting the teeth to hard and soft diets reflected the stem-cell niche-like nature of the incisal tips.

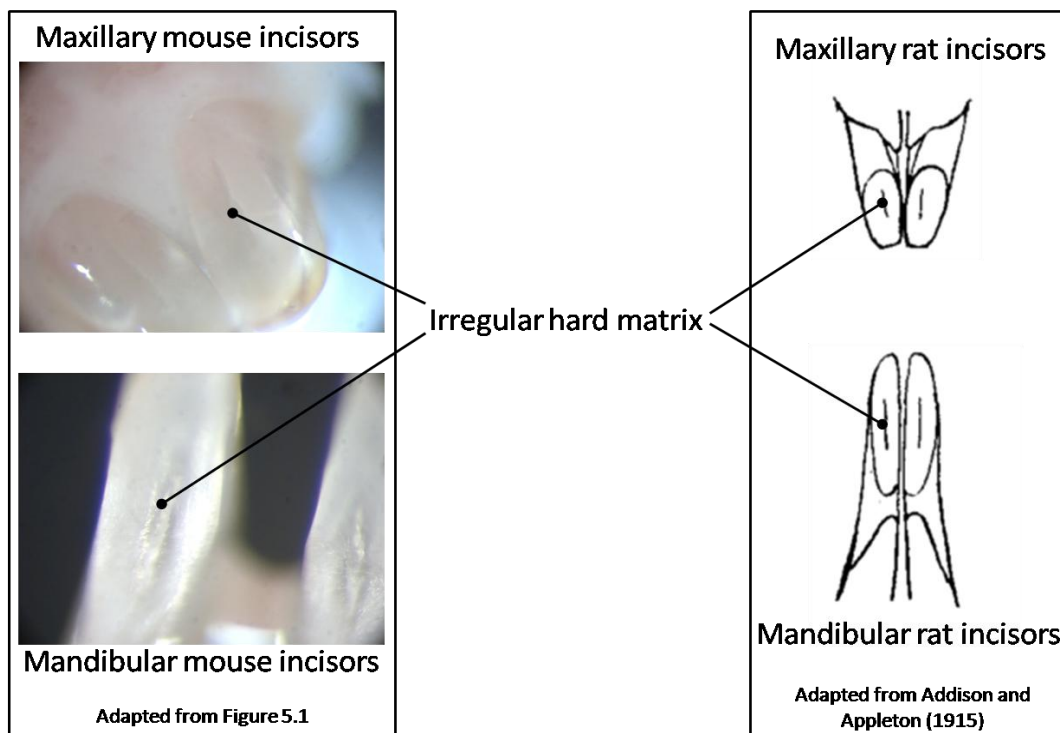**Figure 5.6 Schematic comparison between rat and mouse incisal tip morphology**
In the left panel, photographic images presented in Figure 5.1 demonstrate the similarities between the mouse and rat incisor occlusal surfaces. The location of the lines on the occlusal surfaces in the hand drawn figure (right panel) indicates the region of irregular dentine or "filled in pulp chamber" as described by Addison and Appleton (1915).

Stem cell niches are not static in function, rather, they are highly dynamic since their role is to participate in the regulation of tissue generation, maintenance and repair (Scadden, 2006). Given that the incisor tips are continuously subjected to different external stimuli whether that is changes in the diet or gnawing pattern, the incisal tips provided an ideal opportunity to explore all three roles of the stem cell niche as it undergoes constant damage, repair and therefore maintenance of the tissue. On the longer term 4 day soft diet, a thicker mineral-plug containing a complex lacunae-type structure was observed. In comparison, the mineral produced after 1 day on the soft diet appeared more granulated in morphology. These results could be attributed to the lack of abrasion to offset continuous mineral production under normal feeding conditions where the tooth is worn down more destructively. As a result, the long term soft diet appears to lead to an overproduction of complex, denser mineral illustrated by the lacunae formation. Intriguingly, when the mice were returned to their normal hard diet for 4 hours after 1 day on the soft mash diet, the accumulated mineral appears to have been sheared off, resulting in the mineral returning closer to the original size and morphology as observed in the normal diet samples.

Raman spectroscopy was employed to compare differences in mineral composition between the regular dentine and irregular pulp mineral observed on the occlusal surface of the mouse incisor tips. Interestingly, the Raman spectra suggested that the central irregular dentine region was more proteinaceous in comparison to the outer normal dentine shown by the stronger amide I and III peaks, and less mineralised reflected by less carbonate substitution within hydroxyapetite (the main mineral component of teeth). This substantiates the hypothesis of continuous filling or "restoration" of the apex of the pulp chamber as the Raman spectra suggests rapidly produced, structurally weaker, more immature mineral that is therefore more easily abraded. In 1915, Addison and Appleton referred to the region at the apex of the rat incisor as "osteodentine". However, after the

combination of histological analysis and Raman spectroscopy, a more appropriate term should be allocated to this specialised product of the incisal tip niche. Previous terms including reactionary and reparative dentine are both variants of tertiary dentine and seem unsuitable because they do not reflect the specific function of this mineral production at the tip of the mouse incisor. Reactionary dentine is produced upon irritation or damage to the post-mitotic odontoblasts causing them to upregulate extracellular matrix secretion and by definition do not require pulp cell involvement other than the surviving odontoblasts (Goldberg and Smith, 2004). In contrast, with tooth injury that is more severe resulting in odontoblast death and pulp damage, reparative dentine is formed from a new generation of odontoblast-like cells differentiated from pulp progenitor cells (Smith et al., 1995b). At the incisal tips the mineral formed must be a form of reparative dentine because the pulp cells are involved in the generation of the mineral shown by the results of the lineage tracing experiment where Nestin positive cells were located close to the tip of the pulp chamber. This suggests that the source of progenitor cells likely to give rise to the "secondary odontoblast-like" cells belong to the vascular-derived pericytes which is perhaps unsurprising given that compelling evidence suggests that pericytes act not only as generic sources of MSCs (Crisan et al., 2008b) but they have also been demonstrated more specifically to contribute to both tooth growth and repair (Feng et al., 2011).

The nature of the signalling processes that mediate MSCs within the incisal tip niche warrants further investigation. However, the combination of morphological, histological, Raman microspectroscopy as well as lineage tracing data so far suggests that the incisal tip represents a specialised niche devoted to constant restoration of the "mineral plug" to defend the pulp from damage and infection. This continuous replenishment or restoration of rapidly abraded mineral therefore requires a novel, more appropriate term to highlight its unique function, which we propose as "restorative" dentine.

6. General discussion and future considerations

Rodent teeth provide excellent models for the *in vivo* study of MSC characteristics. Not only do they have non-continuously growing sets of molar teeth that are equivalent to the non-continuous growth of the human dentition, mice possess incisors with the unique ability to grow continuously throughout life and harbour MSCs that reside in a niche at the cervical end of the tooth. In the last few years, exciting research on the rodent incisor has enabled it to emerge as a model for the study of MSC biology by providing new insights for their roles in tissue homeostasis and injury repair (Feng et al., 2011; Zhao et al., 2014) and discovery of new MSC origins (Kaukua et al., 2014).

Human dental pulp stem cells have been isolated in the past decade yet already show great clinical potentials in tissue engineering and immunoregulation applications. These MSCs are heterogeneous populations identified based on their *in vitro* MSC characteristics and to date, their *in vivo* identities remain contentious as specific markers for their isolation are lacking. Interestingly, in rodents, several lines of evidence indicate that the continuous growth of mouse incisors is sustained by the undifferentiated epithelial stem/progenitor cells located in the most apical end (Harada et al., 1999; Harada et al., 2002; Juuri et al., 2012; Seidel et al., 2004) . We reasoned that the presence of an MSC niche must also exist to support the homeostasis of the mesenchymal counterpart and therefore hypothesised that pulp cells within the rodent incisor have varying stemness based on their anatomical location. *In vitro* characterization of pulp mesenchymal cells isolated from two specific regions of the rat incisor enabled the identification of a MSC-like population from the cervical end, while those at the incisor body end lacked MSC features including tri-lineage potential and colony forming capacity. In agreement with previous *in*

vitro reports of rat dental pulp cells demonstrating MSC criteria (Alge et al., 2010; Yang et al., 2007a), our results support and augment these findings by showing that stemness is not uniformly distributed among the whole pulp tissue. Despite numerous *in vitro* studies on the pulp mesenchyme of rat incisors, their isolation has previously been derived from the whole pulp and/or sorting with MSC markers (Yang et al., 2007a; Yu et al., 2010; Zhang et al., 2005a). Our data reveals that similar to mice, rat incisors may house a MSC niche at the cervical end of the tooth and shows that isolation based upon anatomical location certainly provides novel supporting *in vitro* evidence for the presumptive MSC niche recently identified *in vivo* (Feng et al., 2011; Lapthanasupkul et al., 2012).

6.1 Molecular mechanisms regulating MSC response during injury repair *in vivo* and *in vitro*

During the *in vitro* characterization of the dental pulp cells, our novel *in vitro* cell homing assay enabled the observation of rat cervical loop pulp cell migration towards damaged dentine which corroborates with findings observed by Feng and colleagues in their mouse incisor pulp damage culture (Feng et al., 2011) and suggests the release of chemotatic molecules upon injury, that under normal conditions are sequestered within the dentine matrix, in agreement with previous studies demonstrated in rat incisor tooth slice cultures by Sloan and Smith (Sloan et al., 2000; Sloan and Smith, 1999). The qualitative nature of the assay used in this thesis is a limitation, however, subsequent transwell assays together with various growth factors implicated during tooth development provided quantitative assessment of cell migration and Wnt3a was found to promote greatest pulp cell migration, consistent with a similar study where Wnt3a promoted rat BMMSC migration (Shang et al., 2007). Growing evidence has implicated Wnt signalling as a key regulator of stem cells and

in tissue injury and repair where it is known to be elevated soon after damage (reviewed by (Whyte et al., 2012). Our *in vitro* results are suggestive of pulp stem/progenitor cell migratory response towards the upregulation of canonical Wnt signalling that could possibly be associated with the injury response mechanism. Interestingly, a recent report showed that the common dental restorative material 2-Hydroxyethyl methacrylate has an inhibitive effect on the migration of dental pulp stem cells suggestive of poor wound healing (Williams et al., 2013), this highlights that common dental procedures are yet to be fully compatible restorative processes and natural repair methods are still unmet in the clinical setting. Our results demonstrating the involvement of the Wnt/β-catenin pathway supports the idea of utilizing chemical genetics where small molecules are employed to perturb biological processes, in this case, tooth repair. This alternative strategy of controlling Wnt signalling by enhancing it with the addition of small molecules/recombinant protein to guide tooth repair could represent a more feasible approach of activating resident dental pulp stem cells to proliferate and differentiate for *in situ* regeneration of a damaged tooth.

To evaluate Wnt signaling in regulating MSC behaviour during injury repair *in vivo*, we utilised an *in vivo* transgenic mouse model tooth damage experiment. We hypothesised that canonical Wnt signalling is implicated during tooth injury and possibly guides the repair process. Our work demonstrates for the first time, that canonical Wnt signalling is upregulated in the tooth after damage, more specifically within the pulp mesenchyme which corresponds to our *in vitro* data and the hypothesis that dental pulp mesenchymal cells can respond to injury through Wnt signalling. Further to the candidate signalling pathways such as BMPs, TGFβ and Notch signalling that have been suggested to mediate dental pulp stem cells during tooth repair previously (Mitsiadis et al., 2011), our *in vivo* data suggests the addition of Wnt signalling to this list can be applicable. We showed that both incisor and molar tooth damage exhibit increased Axin2 activity indicating increased

β-catenin signalling. In addition, *in vivo* analysis of the Axin2^{LacZ} Wnt reporter mice provided further support that Wnt signalling contributes to the repair process since enhanced Wnt signalling in the Axin2$^{-/-}$ animals results in amplified secretion of mineral-like matrix reminiscent of increased odontoblast secretory activity during reparative dentinogenesis (Smith and Lesot, 2001). These results are not only in line with a diverse range of literature regarding enhanced Wnt signalling during injury, Wnt associated repair seems related to a mineralization response in the tooth reflecting pulp cell contribution to repair. Using the NG2creER;R26R transgenic mouse line, that labels pericytes and their progeny we demonstrated limited pericyte response under homeostasis conditions of mouse molar teeth, which upon damage stimulation underwent a considerable proliferative response. These *in vivo* results support those observed by Feng et al, 2011 in the continuously growing mouse incisor. Here, we complement their findings demonstrating for the first time a pericyte contribution to odontoblast differentiation in a non-continuously growing tooth, which is a more comparable model for human teeth. It is tempting to speculate that these pericytes are Wnt-responsive, to accurately demonstrate this it would in theory be possible to cross our Axin2LacZ mice with the NG2 cre mice. However, both readouts of pericyte lineage and Wnt activity are through lacZ activity rendering this option unfeasible. Instead, an Axin2LacZ; NG2^{ERT2}Cre; mT/mG triple transgenic mouse line could be generated allowing β-galactosidase activity as the readout for Wnt and GFP expression for the NG2 lineage tracing of the pericytes. Future time course experiments will also give a clearer picture of the extent Wnt signalling participates during tooth repair which was a limitation in this study. Interestingly a recent study has shown using lineage tracing in a mouse incisor model a neurovascular bundle MSC niche where Gli1$^+$ derived NG2$^+$ pericytes were shown to be actively involved in injury repair but provide limited contribution to homeostasis of the organ (Zhao et al., 2014). In common with this study, our NG2creER;R26R molar tooth injury experiments also demonstrated

analogous findings. Another interesting role for pericytes is their ability to regulate the extracellular matrix microenvironment which has been implicated in human skin tissue regeneration (Paquet-Fifield et al., 2009) it would therefore be interesting to further investigate their role in a tooth repair context given that extracellular matrix produced by the pulp cells and their interactions are important regulators of the reparative processes.

6.2 The incisal tip model to study perivascular MSCs in injury repair

In this thesis I have also used the mouse incisor model from a different perspective by studying the incisor tip as an injury repair model "designed by nature". The lifelong growth of these unique teeth is compensated by continuous functional attrition at the incisal tips during occlusion of the upper and lower incisors and feeding. We hypothesised that the persistent abrasion at the tips must be counterbalanced with continuous sealing of the pulp chamber to prevent infection. Tetracycline labelling studies confirmed this idea, as freshly deposited mineral located at the apex of the tooth was visually distinct from regular dentine, in agreement with a study that first reported this morphological feature of rodent incisor teeth (Addison and Appleton, 1915). By giving different feeding regimes to the mice, we also demonstrated that this tip "niche" appeared to respond to environmental stimulus where tip mineralisation altered based upon exposure to hard or soft feed. Further work with longer periods of soft and hard diet regimes will provide more in depth understanding of the tip niche response. Importantly we found the proposed incisal tip niche contained a pericyte contribution demonstrated by a resident Nestin positive population. This novel finding supports the notion that pericytes mainly function in injury repair as we argue that the tip of the incisors undergo a form of natural, consistent "injury" through abrasion. This work provides an innovative perspective to investigating different injury repair processes

and highlights the diverse applications of the mouse incisor model in studying different MSC populations. Raman microspectroscopy is a useful tool to analyse the biochemical and structural composition of mineralised tissue such as bone differentiated from MSCs to produce a material that is capable of replicating the natural function of healthy native tissue (Gentleman et al., 2009). The use of Raman microspectroscopy on mouse incisors has never previously been performed and from the tetracycline results we hypothesised that the composition of the mineral produced as a defence mechanism at the tips would be distinct from normal dentine. As expected this tip mineral was unique and appeared more proteinaceous with a higher collagen content than regular dentine, which could be justified based on its rapid production thus, a distinctive, immature mineral that is structural weaker is present here. Future work to investigate the underlying signalling pathways that regulate the tip niche are necessary. Initially, whether canonical Wnt signalling is also implicated in this tip niche that undergoes constant "natural" injury/repair in comparison to the experimental damage response detailed in Chapter 4 should be examined. In addition, Raman spectra of reactionary, reparative and our new proposed term of the incisal tip niche mineral, "restorative" dentine would provide new insights into the biochemical composition of these minerals to enable the production of tissue that better replicates native dentine for therapeutic applications in dental care.

7. Concluding remarks

This work has demonstrated that dental pulp cells from different anatomical locations have different behaviours. We have demonstrated that those associated with the MSC niche at the cervical end demonstrate key properties required for successful injury repair which includes the capacity to proliferate, migrate and differentiate. We have also began to shed light on Wnt signalling involvement in the tooth repair process demonstrated from our *in vivo* tooth injury experiments. This begins to address the deeper question of what mechanisms underlie the MSC response to injury *in vivo*, which is undoubtedly a key element in supporting the development of future stem cell therapies not limited dental MSCs but to all other MSC populations. Finally, we have identified a novel specialised region of the incisor, the "incisal tip niche" which has never been studied before and provides an exciting new concept of "restorative dentine" and a totally different perspective to assessing a continuous, natural injury repair system. To provide a biological basis for tooth repair the combination of new tissue engineering approaches together with greater biological understanding of MSCS will enable the development of novel treatments in clinical dentistry.

8. References

About, I., Laurent-Maquin, D., Lendahl, U., and Mitsiadis, T.A. (2000). Nestin expression in embryonic and adult human teeth under normal and pathological conditions. American Journal of Pathology *157*, 287-295.

Addison, W.H.F., and Appleton, J.L. (1915). The structure and growth of the incisor teeth of the albino rat. Journal of Morphology *26*, 43-96.

Aisagbonhi, O., Rai, M., Ryzhov, S., Atria, N., Feoktistov, I., and Hatzopoulos, A.K. (2011). Experimental myocardial infarction triggers canonical Wnt signaling and endothelial-to-mesenchymal transition. Dis Model Mech *4*, 469-483.

Al Alam, D., Green, M., Tabatabai Irani, R., Parsa, S., Danopoulos, S., Sala, F.G., Branch, J., El Agha, E., Tiozzo, C., Voswinckel, R.*, et al.* (2011). Contrasting expression of canonical Wnt signaling reporters TOPGAL, BATGAL and Axin2(LacZ) during murine lung development and repair. PLoS One *6*, e23139.

Alge, D.L., Zhou, D., Adams, L.L., Wyss, B.K., Shadday, M.D., Woods, E.J., Gabriel Chu, T.M., and Goebel, W.S. (2010). Donor-matched comparison of dental pulp stem cells and bone marrow-derived mesenchymal stem cells in a rat model. J Tissue Eng Regen Med *4*, 73-81.

Allt, G., and Lawrenson, J.G. (2001). Pericytes: cell biology and pathology. Cells Tissues Organs *169*, 1-11.

Alonso, L., and Fuchs, E. (2003). Stem cells in the skin: waste not, Wnt not. Genes Dev *17*, 1189-1200.

Arana-Chavez, V.E., and Massa, L.F. (2004). Odontoblasts: the cells forming and maintaining dentine. Int J Biochem Cell Biol *36*, 1367-1373.

Armulik, A., Abramsson, A., and Betsholtz, C. (2005). Endothelial/pericyte interactions. Circ Res *97*, 512-523.

Arthur, A., Koblar, S., Shi, S., and Gronthos, S. (2009). Eph/ephrinB mediate dental pulp stem cell mobilization and function. J Dent Res *88*, 829-834.

Augello, A., Kurth, T.B., and De Bari, C. (2010). Mesenchymal stem cells: a perspective from in vitro cultures to in vivo migration and niches. Eur Cell Mater *20*, 121-133.

Avery, J. (2001). Oral Development and Histology 3rd Edition *Stuttgart: Thieme*.

Barker, N. (2014). Adult intestinal stem cells: critical drivers of epithelial homeostasis and regeneration. Nat Rev Mol Cell Biol *15*, 19-33.

Barolo, S. (2006). Transgenic Wnt/TCF pathway reporters: all you need is Lef? Oncogene *25*, 7505-7511.

Bartholomew, A., Sturgeon, C., Siatskas, M., Ferrer, K., McIntosh, K., Patil, S., Hardy, W., Devine, S., Ucker, D., Deans, R.*, et al.* (2002). Mesenchymal stem cells suppress lymphocyte proliferation in vitro and prolong skin graft survival in vivo. Exp Hematol *30*, 42-48.

Becerra, J., Santos-Ruiz, L., Andrades, J.A., and Mari-Beffa, M. (2011). The stem cell niche should be a key issue for cell therapy in regenerative medicine. Stem Cell Rev *7*, 248-255.

Belema-Bedada, F., Uchida, S., Martire, A., Kostin, S., and Braun, T. (2008). Efficient homing of multipotent adult mesenchymal stem cells depends on FROUNT-mediated clustering of CCR2. Cell Stem Cell *2*, 566-575.

Bergers, G., and Song, S. (2005). The role of pericytes in blood-vessel formation and maintenance. Neuro Oncol *7*, 452-464.

Boland, G.M., Perkins, G., Hall, D.J., and Tuan, R.S. (2004). Wnt 3a promotes proliferation and suppresses osteogenic differentiation of adult human mesenchymal stem cells. J Cell Biochem *93*, 1210-1230.

Cadigan, K.M., and Nusse, R. (1997). Wnt signaling: a common theme in animal development. Genes Dev *11*, 3286-3305.

Caplan, A. (2009). Why are MSCs therapeutic? New data: new insight. The Journal of Pathology *217*, 318-324.

Cassidy, N., Fahey, M., Prime, S.S., and Smith, A.J. (1997). Comparative analysis of transforming growth factor-beta isoforms 1-3 in human and rabbit dentine matrices. Arch Oral Biol *42*, 219-223.

Chai, Y., Jiang, X., Ito, Y., Bringas, P., Jr., Han, J., Rowitch, D.H., Soriano, P., McMahon, A.P., and Sucov, H.M. (2000). Fate of the mammalian cranial neural crest during tooth and mandibular morphogenesis. Development *127*, 1671-1679.

Chan, R.W., and Gargett, C.E. (2006). Identification of label-retaining cells in mouse endometrium. Stem Cells *24*, 1529-1538.

Chang, H.Y., Chi, J.T., Dudoit, S., Bondre, C., van de Rijn, M., Botstein, D., and Brown, P.O. (2002). Diversity, topographic differentiation, and positional memory in human fibroblasts. Proc Natl Acad Sci U S A *99*, 12877-12882.

Chen, C.W., Okada, M., Proto, J.D., Gao, X., Sekiya, N., Beckman, S.A., Corselli, M., Crisan, M., Saparov, A., Tobita, K.*, et al.* (2013). Human pericytes for ischemic heart repair. Stem Cells *31*, 305-316.

Chen, F.M., Wu, L.A., Zhang, M., Zhang, R., and Sun, H.H. (2011). Homing of endogenous stem/progenitor cells for in situ tissue regeneration: Promises, strategies, and translational perspectives. Biomaterials *32*, 3189-3209.

Chen, H.C. (2005). Boyden chamber assay. Methods Mol Biol *294*, 15-22.

Chen, H.C., Yeh, L.K., Tsai, Y.J., Lai, C.H., Chen, C.C., Lai, J.Y., Sun, C.C., Chang, G., Hwang, T.L., Chen, J.K.*, et al.* (2012). Expression of angiogenesis-related factors in human corneas after cultivated oral mucosal epithelial transplantation. Invest Ophthalmol Vis Sci *53*, 5615-5623.

Chen, J., Lan, Y., Baek, J.A., Gao, Y., and Jiang, R. (2009). Wnt/beta-catenin signaling plays an essential role in activation of odontogenic mesenchyme during early tooth development. Dev Biol *334*, 174-185.

Chen, L., Wu, Q., Guo, F., Xia, B., and Zuo, J. (2004). Expression of Dishevelled-1 in wound healing after acute myocardial infarction: possible involvement in myofibroblast proliferation and migration. J Cell Mol Med *8*, 257-264.

Chen, Y., Whetstone, H.C., Lin, A.C., Nadesan, P., Wei, Q., Poon, R., and Alman, B.A. (2007). Beta-catenin signaling plays a disparate role in different phases of fracture repair: implications for therapy to improve bone healing. PLoS Med *4*, e249.

Chen, Y., Xiang, L.X., Shao, J.Z., Pan, R.L., Wang, Y.X., Dong, X.J., and Zhang, G.R. (2010). Recruitment of endogenous bone marrow mesenchymal stem cells towards injured liver. J Cell Mol Med *14*, 1494-1508.

Cheon, S.S., Wei, Q., Gurung, A., Youn, A., Bright, T., Poon, R., Whetstone, H., Guha, A., and Alman, B.A. (2006). Beta-catenin regulates wound size and mediates the effect of TGF-beta in cutaneous healing. FASEB J *20*, 692-701.

Corselli, M., Chen, C.W., Crisan, M., Lazzari, L., and Peault, B. (2010). Perivascular ancestors of adult multipotent stem cells. Arterioscler Thromb Vasc Biol *30*, 1104-1109.

Cotsarelis, G., Sun, T.T., and Lavker, R.M. (1990). Label-retaining cells reside in the bulge area of pilosebaceous unit: implications for follicular stem cells, hair cycle, and skin carcinogenesis. Cell *61*, 1329-1337.

Crisan, M., Chen, C.W., Corselli, M., Andriolo, G., Lazzari, L., and Peault, B. (2009). Perivascular multipotent progenitor cells in human organs. Ann N Y Acad Sci *1176*, 118-123.

Crisan, M., Yap, S., Casteilla, L., Chen, C.-W., Corselli, M., Park, T.S., Andriolo, G., Sun, B., Zheng, B., Zhang, L*., et al.* (2008a). A Perivascular Origin for Mesenchymal Stem Cells in Multiple Human Organs. *3*, 301-313.

Crisan, M., Yap, S., Casteilla, L., Chen, C.W., Corselli, M., Park, T.S., Andriolo, G., Sun, B., Zheng, B., Zhang, L*., et al.* (2008b). A perivascular origin for mesenchymal stem cells in multiple human organs. Cell Stem Cell *3*, 301-313.

d'Aquino, R., Graziano, A., Sampaolesi, M., Laino, G., Pirozzi, G., De Rosa, A., and Papaccio, G. (2007). Human postnatal dental pulp cells co-differentiate into osteoblasts and endotheliocytes: a pivotal synergy leading to adult bone tissue formation. Cell Death Differ *14*, 1162-1171.

da Silva Meirelles, L., Caplan, A.I., and Nardi, N.B. (2008). In search of the in vivo identity of mesenchymal stem cells. Stem Cells *26*, 2287-2299.

da Silva Meirelles, L., Sand, T.T., Harman, R.J., Lennon, D.P., and Caplan, A.I. (2009). MSC frequency correlates with blood vessel density in equine adipose tissue. Tissue Eng Part A *15*, 221-229.

Das, A.V., Bhattacharya, S., Zhao, X., Hegde, G., Mallya, K., Eudy, J.D., and Ahmad, I. (2008). The canonical Wnt pathway regulates retinal stem cells/progenitors in concert with Notch signaling. Dev Neurosci *30*, 389-409.

DasGupta, R., and Fuchs, E. (1999). Multiple roles for activated LEF/TCF transcription complexes during hair follicle development and differentiation. Development *126*, 4557-4568.

Dassule, H.R., Lewis, P., Bei, M., Maas, R., and McMahon, A.P. (2000). Sonic hedgehog regulates growth and morphogenesis of the tooth. Development *127*, 4775-4785.

Dell'Accio, F., De Bari, C., El Tawil, N.M., Barone, F., Mitsiadis, T.A., O'Dowd, J., and Pitzalis, C. (2006). Activation of WNT and BMP signaling in adult human articular cartilage following mechanical injury. Arthritis Res Ther *8*, R139.

Denayer, T., Locker, M., Borday, C., Deroo, T., Janssens, S., Hecht, A., van Roy, F., Perron, M., and Vleminckx, K. (2008). Canonical Wnt signaling controls proliferation of retinal stem/progenitor cells in postembryonic Xenopus eyes. Stem Cells *26*, 2063-2074.

DeStefano, F., Anda, R.F., Kahn, H.S., Williamson, D.F., and Russell, C.M. (1993). Dental disease and risk of coronary heart disease and mortality. BMJ *306*, 688-691.

Devine, S.M., Bartholomew, A.M., Mahmud, N., Nelson, M., Patil, S., Hardy, W., Sturgeon, C., Hewett, T., Chung, T., Stock, W*., et al.* (2001). Mesenchymal stem cells are capable of homing to the bone marrow of non-human primates following systemic infusion. Exp Hematol *29*, 244-255.

Diaz-Flores, L., Gutierrez, R., Lopez-Alonso, A., Gonzalez, R., and Varela, H. (1992a). Pericytes as a supplementary source of osteoblasts in periosteal osteogenesis. Clin Orthop Relat Res, 280-286.

Diaz-Flores, L., Gutierrez, R., and Varela, H. (1992b). Behavior of postcapillary venule pericytes during postnatal angiogenesis. J Morphol *213*, 33-45.

Diekwisch, T.G. (2001). The developmental biology of cementum. Int J Dev Biol *45*, 695-706.

Dominici, M., Le Blanc, K., Mueller, I., Slaper-Cortenbach, I., Marini, F., Krause, D., Deans, R., Keating, A., Prockop, D., and Horwitz, E. (2006). Minimal criteria for defining multipotent mesenchymal stromal cells. The International Society for Cellular Therapy position statement. Cytotherapy *8*, 315-317.

Dore-Duffy, P., Katychev, A., Wang, X., and Van Buren, E. (2006). CNS microvascular pericytes exhibit multipotential stem cell activity. J Cereb Blood Flow Metab *26*, 613-624.

Esch, F., Baird, A., Ling, N., Ueno, N., Hill, F., Denoroy, L., Klepper, R., Gospodarowicz, D., Bohlen, P., and Guillemin, R. (1985). Primary structure of bovine pituitary basic fibroblast growth factor (FGF) and comparison with the amino-terminal sequence of bovine brain acidic FGF. Proc Natl Acad Sci U S A *82*, 6507-6511.

Evans, M.J., and Kaufman, M.H. (1981). Establishment in culture of pluripotential cells from mouse embryos. Nature *292*, 154-156.

Feng, J., Mantesso, A., De Bari, C., Nishiyama, A., and Sharpe, P.T. (2011). Dual origin of mesenchymal stem cells contributing to organ growth and repair. Proc Natl Acad Sci U S A *108*, 6503-6508.

Finkelman, R.D., Mohan, S., Jennings, J.C., Taylor, A.K., Jepsen, S., and Baylink, D.J. (1990). Quantitation of growth factors IGF-I, SGF/IGF-II, and TGF-beta in human dentin. J Bone Miner Res *5*, 717-723.

Fitzgerald, M., Chiego, D.J., Jr., and Heys, D.R. (1990). Autoradiographic analysis of odontoblast replacement following pulp exposure in primate teeth. Arch Oral Biol *35*, 707-715.

Fournier, B.P., Ferre, F.C., Couty, L., Lataillade, J.J., Gourven, M., Naveau, A., Coulomb, B., Lafont, A., and Gogly, B. (2010). Multipotent progenitor cells in gingival connective tissue. Tissue Eng Part A *16*, 2891-2899.

Francois, S., Bensidhoum, M., Mouiseddine, M., Mazurier, C., Allenet, B., Semont, A., Frick, J., Sache, A., Bouchet, S., Thierry, D*., et al.* (2006). Local irradiation not only induces homing of human mesenchymal stem cells at exposed sites but promotes their widespread engraftment to multiple organs: a study of their quantitative distribution after irradiation damage. Stem Cells *24*, 1020-1029.

Friedenstein, A.J., Chailakhjan, R.K., and Lalykina, K.S. (1970). The development of fibroblast colonies in monolayer cultures of guinea-pig bone marrow and spleen cells. Cell Tissue Kinet *3*, 393-403.

Fuchs, E., Tumbar, T., and Guasch, G. (2004). Socializing with the neighbors: stem cells and their niche. Cell *116*, 769-778.

Funk, R.T., and Alexanian, A.R. (2013). Enhanced dopamine release by mesenchymal stem cells reprogrammed neuronally by the modulators of SMAD signaling, chromatin modifying enzymes, and cyclic adenosine monophosphate levels. Transl Res *162*, 317-323.

Gentleman, E., Swain, R.J., Evans, N.D., Boonrungsiman, S., Jell, G., Ball, M.D., Shean, T.A., Oyen, M.L., Porter, A., and Stevens, M.M. (2009). Comparative materials differences revealed in engineered bone as a function of cell-specific differentiation. Nat Mater *8*, 763-770.

Ghadge, S.K., Muhlstedt, S., Ozcelik, C., and Bader, M. (2011). SDF-1alpha as a therapeutic stem cell homing factor in myocardial infarction. Pharmacol Ther *129*, 97-108.

Ghannam, S., Bouffi, C., Djouad, F., Jorgensen, C., and Noel, D. (2010). Immunosuppression by mesenchymal stem cells: mechanisms and clinical applications. Stem Cell Res Ther *1*, 2.

Goldberg, M., and Smith, A.J. (2004). Cells and Extracellular Matrices of Dentin and Pulp: A Biological Basis for Repair and Tissue Engineering. Crit Rev Oral Biol Med *15*, 13-27.

Grigoryan, T., Wend, P., Klaus, A., and Birchmeier, W. (2008). Deciphering the function of canonical Wnt signals in development and disease: conditional loss- and gain-of-function mutations of beta-catenin in mice. Genes Dev *22*, 2308-2341.

Gronthos, S., Brahim, J., Li, W., Fisher, L.W., Cherman, N., Boyde, A., DenBesten, P., Robey, P.G., and Shi, S. (2002). Stem cell properties of human dental pulp stem cells. Journal of Dental Research *81*, 531-535.

Gronthos, S., Mankani, M., Brahim, J., Robey, P.G., and Shi, S. (2000). Postnatal human dental pulp stem cells (DPSCs) in vitro and in vivo. Proc Natl Acad Sci U S A *97*, 13625-13630.

Gronthos, S., Mrozik, K., Shi, S., and Bartold, P.M. (2006). Ovine periodontal ligament stem cells: Isolation, characterization, and differentiation potential. Calcified Tissue International *79*, 310-317.

Gronthos, S., Zannettino, A.C., Hay, S.J., Shi, S., Graves, S.E., Kortesidis, A., and Simmons, P.J. (2003). Molecular and cellular characterisation of highly purified stromal stem cells derived from human bone marrow. J Cell Sci *116*, 1827-1835.

Gurley, K.A., Rink, J.C., and Sanchez Alvarado, A. (2008). Beta-catenin defines head versus tail identity during planarian regeneration and homeostasis. Science *319*, 323-327.

Han, X.L., Liu, M., Voisey, A., Ren, Y.S., Kurimoto, P., Gao, T., Tefera, L., Dechow, P., Ke, H.Z., and Feng, J.Q. (2011). Post-natal effect of overexpressed DKK1 on mandibular molar formation. J Dent Res *90*, 1312-1317.

Handa, K., Saito, M., Tsunoda, A., Yamauchi, M., Hattori, S., Sato, S., Toyoda, M., Teranaka, T., and Narayanan, A.S. (2002a). Progenitor cells from dental follicle are able to form cementum matrix in vivo. Connective Tissue Research *43*, 406-408.

Handa, K., Saito, M., Yamauchi, M., Kiyono, T., Sato, S., Teranaka, T., and Sampath Narayanan, A. (2002b). Cementum matrix formation in vivo by cultured dental follicle cells. Bone *31*, 606-611.

Hao, L., Wang, J., Zou, Z., Yan, G., Dong, S., Deng, J., Ran, X., Feng, Y., Luo, C., Wang, Y.*, et al.* (2009). Transplantation of BMSCs expressing hPDGF-A/hBD2 promotes wound healing in rats with combined radiation-wound injury. Gene Ther *16*, 34-42.

Harada, H., Kettunen, P., Jung, H.S., Mustonen, T., Wang, Y.A., and Thesleff, I. (1999). Localization of putative stem cells in dental epithelium and their association with notch and FGF signaling. Journal of Cell Biology *147*, 105-120.

Harada, H., and Ohshima, H. (2004). New perspectives on tooth development and the dental stem cell niche. Archives of Histology and Cytology *67*, 1-11.

Harada, H., Toyono, T., Toyoshima, K., Yamasaki, M., Itoh, N., Kato, S., Sekine, K., and Ohuchi, H. (2002). FGF10 maintains stem cell compartment in developing mouse incisors. Development *129*, 1533-1541.

Hare, J.M., Fishman, J.E., Gerstenblith, G., DiFede Velazquez, D.L., Zambrano, J.P., Suncion, V.Y., Tracy, M., Ghersin, E., Johnston, P.V., Brinker, J.A.*, et al.* (2012). Comparison of allogeneic vs autologous bone marrow-derived mesenchymal stem cells delivered by transendocardial injection in patients with ischemic cardiomyopathy: the POSEIDON randomized trial. JAMA *308*, 2369-2379.

Hsu, S.H., Huang, G.S., and Feng, F. (2012). Isolation of the multipotent MSC subpopulation from human gingival fibroblasts by culturing on chitosan membranes. Biomaterials *33*, 2642-2655.

Hsu, Y.C., and Fuchs, E. (2012). A family business: stem cell progeny join the niche to regulate homeostasis. Nat Rev Mol Cell Biol *13*, 103-114.

Huang, G.T.J. (2009). Pulp and dentin tissue engineering and regeneration: current progress. Regenerative Medicine *4*, 697-707.

Huang, G.T.J., Sonoyama, W., Liu, Y., Liu, H., Wang, S.L., and Shi, S.T. (2008). The hidden treasure in apical papilla: The potential role in pulp/dentin regeneration and bioroot engineering. Journal of Endodontics *34*, 645-651.

Huang, X.F., and Chai, Y. (2012). Molecular regulatory mechanism of tooth root development. Int J Oral Sci *4*, 177-181.

Ikeda, E., Yagi, K., Kojima, M., Yagyuu, T., Ohshima, A., Sobajima, S., Tadokoro, M., Katsube, Y., Isoda, K., Kondoh, M.*, et al.* (2008). Multipotent cells from the human third molar: feasibility of cell-based therapy for liver disease. Differentiation *76*, 495-505.

Ito, M., Yang, Z., Andl, T., Cui, C., Kim, N., Millar, S.E., and Cotsarelis, G. (2007). Wnt-dependent de novo hair follicle regeneration in adult mouse skin after wounding. Nature *447*, 316-320.

Jensen, K.B., and Watt, F.M. (2006). Single-cell expression profiling of human epidermal stem and transit-amplifying cells: Lrig1 is a regulator of stem cell quiescence. Proc Natl Acad Sci U S A *103*, 11958-11963.

Jho, E.H., Zhang, T., Domon, C., Joo, C.K., Freund, J.N., and Costantini, F. (2002). Wnt/beta-catenin/Tcf signaling induces the transcription of Axin2, a negative regulator of the signaling pathway. Mol Cell Biol *22*, 1172-1183.

Jiang, Y., Jahagirdar, B.N., Reinhardt, R.L., Schwartz, R.E., Keene, C.D., Ortiz-Gonzalez, X.R., Reyes, M., Lenvik, T., Lund, T., Blackstad, M.*, et al.* (2002). Pluripotency of mesenchymal stem cells derived from adult marrow. Nature *418*, 41-49.

Jones, P.H., and Watt, F.M. (1993). Separation of human epidermal stem cells from transit amplifying cells on the basis of differences in integrin function and expression. Cell *73*, 713-724.

Juuri, E., Saito, K., Ahtiainen, L., Seidel, K., Tummers, M., Hochedlinger, K., Klein, O.D., Thesleff, I., and Michon, F. (2012). Sox2+ stem cells contribute to all epithelial lineages of the tooth via Sfrp5+ progenitors. Dev Cell *23*, 317-328.

Kaukua, N., Shahidi, M.K., Konstantinidou, C., Dyachuk, V., Kaucka, M., Furlan, A., An, Z., Wang, L., Hultman, I., Ahrlund-Richter, L.*, et al.* (2014). Glial origin of mesenchymal stem cells in a tooth model system. Nature.

Kawakami, Y., Rodriguez Esteban, C., Raya, M., Kawakami, H., Marti, M., Dubova, I., and Izpisua Belmonte, J.C. (2006). Wnt/beta-catenin signaling regulates vertebrate limb regeneration. Genes Dev *20*, 3232-3237.

Kawasaki, K., Tanaka, S., and Ishikawa, T. (1977). On the incremental lines in human dentine as revealed by tetracycline labeling. J Anat *123*, 427-436.

Kim, J.B., Leucht, P., Lam, K., Luppen, C., Ten Berge, D., Nusse, R., and Helms, J.A. (2007). Bone regeneration is regulated by wnt signaling. J Bone Miner Res *22*, 1913-1923.

Kim, J.Y., Xin, X., Moioli, E.K., Chung, J., Lee, C.H., Chen, M., Fu, S.Y., Koch, P.D., and Mao, J.J. (2010). Regeneration of dental-pulp-like tissue by chemotaxis-induced cell homing. Tissue Eng Part A *16*, 3023-3031.

Kolf, C.M., Cho, E., and Tuan, R.S. (2007). Mesenchymal stromal cells. Biology of adult mesenchymal stem cells: regulation of niche, self-renewal and differentiation. Arthritis Res Ther *9*, 204.

Kratochwil, K., Galceran, J., Tontsch, S., Roth, W., and Grosschedl, R. (2002). FGF4, a direct target of LEF1 and Wnt signaling, can rescue the arrest of tooth organogenesis in Lef1(-/-) mice. Genes Dev *16*, 3173-3185.

Laird, D.J., von Andrian, U.H., and Wagers, A.J. (2008). Stem cell trafficking in tissue development, growth, and disease. Cell *132*, 612-630.

Lajtha, L.G. (1979). Stem cell concepts. Differentiation *14*, 23-34.

Lamster, I.B., Lalla, E., Borgnakke, W.S., and Taylor, G.W. (2008). The relationship between oral health and diabetes mellitus. J Am Dent Assoc *139 Suppl*, 19S-24S.

Lapthanasupkul, P., Feng, J., Mantesso, A., Takada-Horisawa, Y., Vidal, M., Koseki, H., Wang, L., An, Z., Miletich, I., and Sharpe, P.T. (2012). Ring1a/b polycomb proteins regulate the mesenchymal stem cell niche in continuously growing incisors. Dev Biol *367*, 140-153.

Le Blanc, K., Rasmusson, I., Sundberg, B., Gˆtherstrˆm, C., Hassan, M., Uzunel, M., and RingdÈn, O. (2004). Treatment of severe acute graft-versus-host disease with third party haploidentical mesenchymal stem cells. The Lancet *363*, 1439-1441.

Liang, C.C., Park, A.Y., and Guan, J.L. (2007). In vitro scratch assay: a convenient and inexpensive method for analysis of cell migration in vitro. Nat Protoc *2*, 329-333.

Lin, M., Li, L., Liu, C., Liu, H., He, F., Yan, F., Zhang, Y., and Chen, Y. (2011). Wnt5a regulates growth, patterning, and odontoblast differentiation of developing mouse tooth. Dev Dyn *240*, 432-440.

Liu, F., Chu, E.Y., Watt, B., Zhang, Y., Gallant, N.M., Andl, T., Yang, S.H., Lu, M.M., Piccolo, S., Schmidt-Ullrich, R., *et al.* (2008). Wnt/beta-catenin signaling directs multiple stages of tooth morphogenesis. Dev Biol *313*, 210-224.

Liu, F., and Millar, S.E. (2010). Wnt/beta-catenin signaling in oral tissue development and disease. J Dent Res *89*, 318-330.

Liu, H., Xu, S., Wang, Y., Mazerolle, C., Thurig, S., Coles, B.L., Ren, J.C., Taketo, M.M., van der Kooy, D., and Wallace, V.A. (2007). Ciliary margin transdifferentiation from neural retina is controlled by canonical Wnt signaling. Dev Biol *308*, 54-67.

Logan, C.Y., and Nusse, R. (2004). The Wnt signaling pathway in development and disease. Annu Rev Cell Dev Biol *20*, 781-810.

Lohi, M., Tucker, A.S., and Sharpe, P.T. (2010). Expression of Axin2 indicates a role for canonical Wnt signaling in development of the crown and root during pre- and postnatal tooth development. Dev Dyn *239*, 160-167.

Lovschall, H., Tummers, M., Thesleff, I., Fuchtbauer, E.M., and Poulsen, K. (2005). Activation of the Notch signaling pathway in response to pulp capping of rat molars. Eur J Oral Sci *113*, 312-317.

Luan, X., Ito, Y., and Diekwisch, T.G. (2006a). Evolution and development of Hertwig's epithelial root sheath. Dev Dyn *235*, 1167-1180.

Luan, X.G., Ito, Y., Dangaria, S., and Diekwisch, T.G.H. (2006b). Dental follicle progenitor cell heterogeneity in the developing mouse periodontium. Stem Cells and Development *15*, 595-608.

Lustig, B., Jerchow, B., Sachs, M., Weiler, S., Pietsch, T., Karsten, U., van de Wetering, M., Clevers, H., Schlag, P.M., Birchmeier, W.*, et al.* (2002). Negative feedback loop of Wnt signaling through upregulation of conductin/axin2 in colorectal and liver tumors. Mol Cell Biol *22*, 1184-1193.

Mantesso, A., and Sharpe, P. (2009). Dental stem cells for tooth regeneration and repair. Expert Opinion on Biological Therapy *9*, 1143-1154.

Maretto, S., Cordenonsi, M., Dupont, S., Braghetta, P., Broccoli, V., Hassan, A.B., Volpin, D., Bressan, G.M., and Piccolo, S. (2003). Mapping Wnt/beta-catenin signaling during mouse development and in colorectal tumors. Proc Natl Acad Sci U S A *100*, 3299-3304.

McCulloch, C.A. (1985). Progenitor cell populations in the periodontal ligament of mice. Anat Rec *211*, 258-262.

Meyrick, B., and Reid, L. (1978). The effect of continued hypoxia on rat pulmonary arterial circulation. An ultrastructural study. Lab Invest *38*, 188-200.

Midwood, K.S., Williams, L.V., and Schwarzbauer, J.E. (2004). Tissue repair and the dynamics of the extracellular matrix. Int J Biochem Cell Biol *36*, 1031-1037.

Miletich, I., and Sharpe, P.T. (2003). Normal and abnormal dental development. Hum Mol Genet *12 Spec No 1*, R69-73.

Minear, S., Leucht, P., Jiang, J., Liu, B., Zeng, A., Fuerer, C., Nusse, R., and Helms, J.A. (2010). Wnt proteins promote bone regeneration. Sci Transl Med *2*, 29ra30.

Mitrano, T.I., Grob, M.S., Carrion, F., Nova-Lamperti, E., Luz, P.A., Fierro, F.S., Quintero, A., Chaparro, A., and Sanz, A. (2010). Culture and characterization of mesenchymal stem cells from human gingival tissue. J Periodontol *81*, 917-925.

Mitsiadis, T.A., Feki, A., Papaccio, G., and Caton, J. (2011). Dental pulp stem cells, niches, and notch signaling in tooth injury. Adv Dent Res *23*, 275-279.

Miura, M., Gronthos, S., Zhao, M., Lu, B., Fisher, L.W., Robey, P.G., and Shi, S. (2003). SHED: stem cells from human exfoliated deciduous teeth. Proc Natl Acad Sci U S A *100*, 5807-5812.

Moon, R.T., Kohn, A.D., De Ferrari, G.V., and Kaykas, A. (2004). WNT and beta-catenin signalling: diseases and therapies. Nat Rev Genet *5*, 691-701.

Morikawa, S., Mabuchi, Y., Kubota, Y., Nagai, Y., Niibe, K., Hiratsu, E., Suzuki, S., Miyauchi-Hara, C., Nagoshi, N., Sunabori, T.*, et al.* (2009). Prospective identification, isolation, and systemic transplantation of multipotent mesenchymal stem cells in murine bone marrow. J Exp Med *206*, 2483-2496.

Morrison, S.J., Shah, N.M., and Anderson, D.J. (1997). Regulatory mechanisms in stem cell biology. Cell *88*, 287-298.

Morsczeck, C., Gotz, W., Schierholz, J., Zellhofer, F., Kuhn, U., Mohl, C., Sippel, C., and Hoffmann, K.H. (2005). Isolation of precursor cells (PCs) from human dental follicle of wisdom teeth. Matrix Biology *24*, 155-165.

Mutsaers, S.E., Bishop, J.E., McGrouther, G., and Laurent, G.J. (1997). Mechanisms of tissue repair: from wound healing to fibrosis. Int J Biochem Cell Biol *29*, 5-17.

Nakamura, T., Inatomi, T., Sotozono, C., Amemiya, T., Kanamura, N., and Kinoshita, S. (2004). Transplantation of cultivated autologous oral mucosal epithelial cells in patients with severe ocular surface disorders. Br J Ophthalmol *88*, 1280-1284.

Nakamura, T., Koizumi, N., Tsuzuki, M., Inoki, K., Sano, Y., Sotozono, C., and Kinoshita, S. (2003). Successful regrafting of cultivated corneal epithelium using amniotic membrane as a carrier in severe ocular surface disease. Cornea *22*, 70-71.

Nakashima, M. (1994). Induction of dentin formation on canine amputated pulp by recombinant human bone morphogenetic proteins (BMP)-2 and -4. J Dent Res *73*, 1515-1522.

Nanci, A. (2008). Ten Cate's Oral Histology: Development, Structure, and Function. St Louis, Missouri, *Mosby*.

Neubuser, A., Peters, H., Balling, R., and Martin, G.R. (1997). Antagonistic interactions between FGF and BMP signaling pathways: a mechanism for positioning the sites of tooth formation. Cell *90*, 247-255.

Neubüser, A., Peters, H., Balling, R., and Martin, G.R. (1997). Antagonistic interactions between FGF and BMP signaling pathways: a mechanism for positioning the sites of tooth formation. Cell *90*, 247-255.

Nusse, R. (2008). Wnt signaling and stem cell control. Cell Res *18*, 523-527.

Ohshima, H., Nakasone, N., Hashimoto, E., Sakai, H., Nakakura-Ohshima, K., and Harada, H. (2005). The eternal tooth germ is formed at the apical end of continuously growing teeth. Archives of Oral Biology *50*, 153-157.

Paquet-Fifield, S., Schluter, H., Li, A., Aitken, T., Gangatirkar, P., Blashki, D., Koelmeyer, R., Pouliot, N., Palatsides, M., Ellis, S., *et al.* (2009). A role for pericytes as microenvironmental regulators of human skin tissue regeneration. J Clin Invest *119*, 2795-2806.

Petersen, C.P., and Reddien, P.W. (2009). A wound-induced Wnt expression program controls planarian regeneration polarity. Proc Natl Acad Sci U S A *106*, 17061-17066.

Phipps, R.P., Borrello, M.A., and Blieden, T.M. (1997). Fibroblast heterogeneity in the periodontium and other tissues. J Periodontal Res *32*, 159-165.

Pispa, J., and Thesleff, I. (2003). Mechanisms of ectodermal organogenesis. Developmental Biology *262*, 195-205.

Pittenger, M.F., Mackay, A.M., Beck, S.C., Jaiswal, R.K., Douglas, R., Mosca, J.D., Moorman, M.A., Simonetti, D.W., Craig, S., and Marshak, D.R. (1999). Multilineage potential of adult human mesenchymal stem cells. Science *284*, 143-147.

Potten, C.S., Owen, G., and Booth, D. (2002). Intestinal stem cells protect their genome by selective segregation of template DNA strands. J Cell Sci *115*, 2381-2388.

Potten, C.S., Schofield, R., and Lajtha, L.G. (1979). A comparison of cell replacement in bone marrow, testis and three regions of surface epithelium. Biochim Biophys Acta *560*, 281-299.

Ramachandran, R., Zhao, X.F., and Goldman, D. (2011). Ascl1a/Dkk/beta-catenin signaling pathway is necessary and glycogen synthase kinase-3beta inhibition is sufficient for zebrafish retina regeneration. Proc Natl Acad Sci U S A *108*, 15858-15863.

Reya, T., and Clevers, H. (2005). Wnt signalling in stem cells and cancer. Nature *434*, 843-850.

Richardson, R.L., Hausman, G.J., and Campion, D.R. (1982). Response of pericytes to thermal lesion in the inguinal fat pad of 10-day-old rats. Acta Anat (Basel) *114*, 41-57.

Ringden, O., Uzunel, M., Rasmusson, I., Remberger, M., Sundberg, B., Lonnies, H., Marschall, H.-U., Dlugosz, A., Szakos, A., Hassan, Z., *et al.* (2006). Mesenchymal Stem Cells

for Treatment of Therapy-Resistant Graft-versus-Host Disease. [Article]. Transplantation May *81*, 1390-1397.

Robertson, A., Lundgren, T., Andreasen, J.O., Dietz, W., Hoyer, I., and Noren, J.G. (1997). Pulp calcifications in traumatized primary incisors. A morphological and inductive analysis study. Eur J Oral Sci *105*, 196-206.

Sackstein, R., Merzaban, J.S., Cain, D.W., Dagia, N.M., Spencer, J.A., Lin, C.P., and Wohlgemuth, R. (2008). Ex vivo glycan engineering of CD44 programs human multipotent mesenchymal stromal cell trafficking to bone. Nat Med *14*, 181-187.

Saito, M., Iwase, M., Maslan, S., Nozaki, N., Yamauchi, M., Handa, K., Takahashi, O., Sato, S., Kawase, T., Teranaka, T.*, et al.* (2001). Expression of cementum-derived attachment protein in bovine tooth germ during cementogenesis. Bone *29*, 242-248.

Sakai, V.T., Zhang, Z., Dong, Z., Neiva, K.G., Machado, M.A., Shi, S., Santos, C.F., and Nor, J.E. (2010). SHED differentiate into functional odontoblasts and endothelium. J Dent Res *89*, 791-796.

Sarkar, L., and Sharpe, P.T. (1999). Expression of Wnt signalling pathway genes during tooth development. Mechanisms of Development *85*, 197-200.

Sasaki, T., Ito, Y., Xu, X., Han, J., Bringas, P., Jr., Maeda, T., Slavkin, H.C., Grosschedl, R., and Chai, Y. (2005). LEF1 is a critical epithelial survival factor during tooth morphogenesis. Dev Biol *278*, 130-143.

Scadden, D.T. (2006). The stem-cell niche as an entity of action. Nature *441*, 1075-1079.

Schofield, R. (1978). The relationship between the spleen colony-forming cell and the haemopoietic stem cell. Blood Cells *4*, 7-25.

Schor, S.L., Ellis, I., Irwin, C.R., Banyard, J., Seneviratne, K., Dolman, C., Gilbert, A.D., and Chisholm, D.M. (1996). Subpopulations of fetal-like gingival fibroblasts: characterisation and potential significance for wound healing and the progression of periodontal disease. Oral Dis *2*, 155-166.

Schwab, K.E., and Gargett, C.E. (2007). Co-expression of two perivascular cell markers isolates mesenchymal stem-like cells from human endometrium. Hum Reprod *22*, 2903-2911.

Seidel, K., Ahn, C.P., Lyons, D., Nee, A., Ting, K., Brownell, I., Cao, T., Carano, R.A., Curran, T., Schober, M.*, et al.* (2004). Hedgehog signaling regulates the generation of ameloblast progenitors in the continuously growing mouse incisor. Development *137*, 3753-3761.

Seltzer, S. (1999). Long-term radiographic and histological observations of endodontically treated teeth. J Endod *25*, 818-822.

Seo, B.M., Miura, M., Gronthos, S., Bartold, P.M., Batouli, S., Brahim, J., Young, M., Robey, P.G., Wang, C.Y., and Shi, S.T. (2004). Investigation of multipotent postnatal stem cells from human periodontal ligament. Lancet *364*, 149-155.

Seo, B.M., Miura, M., Sonoyama, W., Coppe, C., Stanyon, R., and Shi, S. (2005). Recovery of stem cells from cryopreserved periodontal ligament. Journal of Dental Research *84*, 907-912.

Shang, Y.C., Wang, S.H., Xiong, F., Zhao, C.P., Peng, F.N., Feng, S.W., Li, M.S., Li, Y., and Zhang, C. (2007). Wnt3a signaling promotes proliferation, myogenic differentiation, and migration of rat bone marrow mesenchymal stem cells. Acta Pharmacol Sin *28*, 1761-1774.

Shi, M., Li, J., Liao, L., Chen, B., Li, B., Chen, L., Jia, H., and Zhao, R.C. (2007). Regulation of CXCR4 expression in human mesenchymal stem cells by cytokine treatment: role in homing efficiency in NOD/SCID mice. Haematologica *92*, 897-904.

Shi, S., Bartold, P.M., Miura, M., Seo, B.M., Robey, P.G., and Gronthos, S. (2005). The efficacy of mesenchymal stem cells to regenerate and repair dental structures. Orthod Craniofac Res *8*, 191-199.

Shi, S., and Gronthos, S. (2003). Perivascular niche of postnatal mesenchymal stem cells in human bone marrow and dental pulp. J Bone Miner Res *18*, 696-704.

Shi, S., Gronthos, S., Chen, S., Reddi, A., Counter, C.M., Robey, P.G., and Wang, C.Y. (2002). Bone formation by human postnatal bone marrow stromal stem cells is enhanced by telomerase expression. Nat Biotechnol *20*, 587-591.

Simmons, P.J., and Torok-Storb, B. (1991). Identification of stromal cell precursors in human bone marrow by a novel monoclonal antibody, STRO-1. Blood *78*, 55-62.

Skinner, H.C., and Nalbandian, J. (1975). Tetracyclines and mineralized tissues: review and perspectives. Yale J Biol Med *48*, 377-397.

Sloan, A.J., Rutherford, R.B., and Smith, A.J. (2000). Stimulation of the rat dentine-pulp complex by bone morphogenetic protein-7 in vitro. Arch Oral Biol *45*, 173-177.

Sloan, A.J., and Smith, A.J. (1999). Stimulation of the dentine-pulp complex of rat incisor teeth by transforming growth factor-beta isoforms 1-3 in vitro. Arch Oral Biol *44*, 149-156.

Sloan, A.J., and Smith, A.J. (2007). Stem cells and the dental pulp: potential roles in dentine regeneration and repair. Oral Dis *13*, 151-157.

Sloan, A.J., and Waddington, R.J. (2009). Dental pulp stem cells: what, where, how? Int J Paediatr Dent *19*, 61-70.

Smith, A.J., Cassidy, N., Perry, H., Begue-Kirn, C., Ruch, J.V., and Lesot, H. (1995a). Reactionary dentinogenesis. Int J Dev Biol *39*, 273-280.

Smith, A.J., Cassidy, N., Perry, H., Beguekirn, C., Ruch, J.V., and Lesot, H. (1995b). Reactionary Dentinogenesis. International Journal of Developmental Biology *39*, 273-280.

Smith, A.J., and Lesot, H. (2001). Induction and regulation of crown dentinogenesis: embryonic events as a template for dental tissue repair? Crit Rev Oral Biol Med *12*, 425-437.

Smith, A.J., Tobias, R.S., Cassidy, N., Plant, C.G., Browne, R.M., Begue-Kirn, C., Ruch, J.V., and Lesot, H. (1994). Odontoblast stimulation in ferrets by dentine matrix components. Arch Oral Biol *39*, 13-22.

Smith, A.N., Willis, E., Chan, V.T., Muffley, L.A., Isik, F.F., Gibran, N.S., and Hocking, A.M. (2010). Mesenchymal stem cells induce dermal fibroblast responses to injury. Exp Cell Res *316*, 48-54.

Son, B.R., Marquez-Curtis, L.A., Kucia, M., Wysoczynski, M., Turner, A.R., Ratajczak, J., Ratajczak, M.Z., and Janowska-Wieczorek, A. (2006). Migration of bone marrow and cord blood mesenchymal stem cells in vitro is regulated by stromal-derived factor-1-CXCR4 and hepatocyte growth factor-c-met axes and involves matrix metalloproteinases. Stem Cells *24*, 1254-1264.

Sonoyama, W., Liu, Y., Fang, D., Yamaza, T., Seo, B.M., Zhang, C., Liu, H., Gronthos, S., Wang, C.Y., Wang, S.*, et al.* (2006). Mesenchymal stem cell-mediated functional tooth regeneration in swine. PLoS One *1*, e79.

Soriano, P. (1999). Generalized lacZ expression with the ROSA26 Cre reporter strain. Nat Genet *21*, 70-71.

Spaggiari, G.M., Capobianco, A., Becchetti, S., Mingari, M.C., and Moretta, L. (2006). Mesenchymal stem cell-natural killer cell interactions: evidence that activated NK cells are capable of killing MSCs, whereas MSCs can inhibit IL-2-induced NK-cell proliferation. Blood *107*, 1484-1490.

Stokowski, A., Shi, S., Sun, T., Bartold, P.M., Koblar, S.A., and Gronthos, S. (2007). EphB/ephrin-B interaction mediates adult stem cell attachment, spreading, and migration: implications for dental tissue repair. Stem Cells *25*, 156-164.

Suzuki, T., Lee, C.H., Chen, M., Zhao, W., Fu, S.Y., Qi, J.J., Chotkowski, G., Eisig, S.B., Wong, A., and Mao, J.J. (2011). Induced migration of dental pulp stem cells for in vivo pulp regeneration. J Dent Res *90*, 1013-1018.

Swain, R.J., and Stevens, M.M. (2007). Raman microspectroscopy for non-invasive biochemical analysis of single cells. Biochem Soc Trans *35*, 544-549.

Takahashi, K., and Yamanaka, S. (2006). Induction of pluripotent stem cells from mouse embryonic and adult fibroblast cultures by defined factors. Cell *126*, 663-676.

Tecles, O., Laurent, P., Zygouritsas, S., Burger, A.S., Camps, J., Dejou, J., and About, I. (2005). Activation of human dental pulp progenitor/stem cells in response to odontoblast injury. Archives of Oral Biology *50*, 103-108.

Thesleff, I. (2003). Epithelial-mesenchymal signalling regulating tooth morphogenesis. J Cell Sci *116*, 1647-1648.

Thesleff, I., and Nieminen, P. (1996). Tooth morphogenesis and cell differentiation. Curr Opin Cell Biol *8*, 844-850.

Thesleff, I., and Tummers, M. (2008). Tooth organogenesis and regeneration.

Thesleff, I., and Tummers, M. (2009). Tooth organogenesis and regeneration. StemBook, ed The Stem Cell Research Community, StemBook, doi/103824/stembook1371, http://wwwstembookorg.

Tsuchiya, S., Honda, M.J., Shinohara, Y., Saito, M., and Ueda, M. (2008). Collagen type I matrix affects molecular and cellular behavior of purified porcine dental follicle cells. Cell and Tissue Research *331*, 447-459.

Tsutsumi, S., Shimazu, A., Miyazaki, K., Pan, H., Koike, C., Yoshida, E., Takagishi, K., and Kato, Y. (2001). Retention of multilineage differentiation potential of mesenchymal cells during proliferation in response to FGF. Biochem Biophys Res Commun *288*, 413-419.

Tucker, A., and Sharpe, P. (2004). The cutting-edge of mammalian development; How the embryo makes teeth. Nature Reviews Genetics *5*, 499-508.

Tumbar, T., Guasch, G., Greco, V., Blanpain, C., Lowry, W.E., Rendl, M., and Fuchs, E. (2004). Defining the epithelial stem cell niche in skin. Science *303*, 359-363.

Tummers, M., and Thesleff, I. (2003). Root or crown: a developmental choice orchestrated by the differential regulation of the epithelial stem cell niche in the tooth of two rodent species. Development *130*, 1049-1057.

Tziafas, D. (1995). Basic Mechanisms of Cytodifferentiation and Dentinogenesis During Dental-Pulp Repair. International Journal of Developmental Biology *39*, 281-290.

van Genderen, C., Okamura, R.M., Farinas, I., Quo, R.G., Parslow, T.G., Bruhn, L., and Grosschedl, R. (1994). Development of several organs that require inductive epithelial-mesenchymal interactions is impaired in LEF-1-deficient mice. Genes Dev *8*, 2691-2703.

Villar, J., Cabrera, N.E., Valladares, F., Casula, M., Flores, C., Blanch, L., Quilez, M.E., Santana-Rodriguez, N., Kacmarek, R.M., and Slutsky, A.S. (2011). Activation of the Wnt/beta-catenin signaling pathway by mechanical ventilation is associated with ventilator-induced pulmonary fibrosis in healthy lungs. PLoS One *6*, e23914.

Volponi, A.A., Pang, Y., and Sharpe, P.T. (2010). Stem cell-based biological tooth repair and regeneration. Trends Cell Biol *20*, 715-722.

Voog, J., and Jones, D.L. (2010). Stem cells and the niche: a dynamic duo. Cell Stem Cell *6*, 103-115.

Wada, N., Wang, B., Lin, N.H., Laslett, A.L., Gronthos, S., and Bartold, P.M. (2011). Induced pluripotent stem cell lines derived from human gingival fibroblasts and periodontal ligament fibroblasts. J Periodontal Res *46*, 438-447.

Wall, I.B., Moseley, R., Baird, D.M., Kipling, D., Giles, P., Laffafian, I., Price, P.E., Thomas, D.W., and Stephens, P. (2008). Fibroblast dysfunction is a key factor in the non-healing of chronic venous leg ulcers. J Invest Dermatol *128*, 2526-2540.

Wang, X., Sha, X.J., Li, G.H., Yang, F.S., Ji, K., Wen, L.Y., Liu, S.Y., Chen, L., Ding, Y., and Xuan, K. (2012). Comparative characterization of stem cells from human exfoliated deciduous teeth and dental pulp stem cells. Arch Oral Biol *57*, 1231-1240.

Wang, X.P., Suomalainen, M., Felszeghy, S., Zelarayan, L.C., Alonso, M.T., Plikus, M.V., Maas, R.L., Chuong, C.M., Schimmang, T., and Thesleff, I. (2007). An integrated gene regulatory network controls stem cell proliferation in teeth. PLoS Biol *5*, e159.

Whyte, J.L., Smith, A.A., and Helms, J.A. (2012). Wnt signaling and injury repair. Cold Spring Harb Perspect Biol *4*, a008078.

Williams, D.W., Wu, H., Oh, J.E., Fakhar, C., Kang, M.K., Shin, K.H., Park, N.H., and Kim, R.H. (2013). 2-Hydroxyethyl methacrylate inhibits migration of dental pulp stem cells. J Endod *39*, 1156-1160.

Wislet-Gendebien, S., Leprince, P., Moonen, G., and Rogister, B. (2003). Regulation of neural markers nestin and GFAP expression by cultivated bone marrow stromal cells. J Cell Sci *116*, 3295-3302.

Yamashiro, T., Zheng, L., Shitaku, Y., Saito, M., Tsubakimoto, T., Takada, K., Takano-Yamamoto, T., and Thesleff, I. (2007). Wnt10a regulates dentin sialophosphoprotein mRNA expression and possibly links odontoblast differentiation and tooth morphogenesis. Differentiation *75*, 452-462.

Yan, Y., Tang, D., Chen, M., Huang, J., Xie, R., Jonason, J.H., Tan, X., Hou, W., Reynolds, D., Hsu, W.*, et al.* (2009). Axin2 controls bone remodeling through the beta-catenin-BMP signaling pathway in adult mice. J Cell Sci *122*, 3566-3578.

Yang, X., Van der Kraan, P.M., Van den Dolder, J., Walboomers, X.F., Bian, Z., Fan, M.W., and Jansen, J.A. (2007a). STRO-1 selected rat dental pulp stem cells transfected with adenoviral-mediated human bone morphogenetic protein 2 gene show enhanced odontogenic differentiation. Tissue Engineering *13*, 2803-2812.

Yang, X., Zhang, W., van den Dolder, J., Walboomers, X.F., Bian, Z., Fan, M., and Jansen, J.A. (2007b). Multilineage potential of STRO-1+ rat dental pulp cells in vitro. J Tissue Eng Regen Med *1*, 128-135.

Young, B. (2006). Wheater's Functional Histology. 5th ed. London: Elsevier Health Sciences. 252.

Yu, J., He, H., Tang, C., Zhang, G., Li, Y., Wang, R., Shi, J., and Jin, Y. (2010). Differentiation potential of STRO-1+ dental pulp stem cells changes during cell passaging. BMC Cell Biol *11*, 32.

Zeichner-David, M., Oishi, K., Su, Z., Zakartchenko, V., Chen, L.S., Arzate, H., and Bringas, P., Jr. (2003). Role of Hertwig's epithelial root sheath cells in tooth root development. Dev Dyn *228*, 651-663.

Zhang, Q., Shi, S., Liu, Y., Uyanne, J., Shi, Y., and Le, A.D. (2009). Mesenchymal stem cells derived from human gingiva are capable of immunomodulatory functions and ameliorate inflammation-related tissue destruction in experimental colitis. J Immunol *183*, 7787-7798.

Zhang, R., Yang, G., Wu, X., Xie, J., Yang, X., and Li, T. (2013). Disruption of Wnt/beta-catenin signaling in odontoblasts and cementoblasts arrests tooth root development in postnatal mouse teeth. Int J Biol Sci *9*, 228-236.

Zhang, W., Walboomers, X.F., Wolke, J.G., Bian, Z., Fan, M.W., and Jansen, J.A. (2005a). Differentiation ability of rat postnatal dental pulp cells in vitro. Tissue Eng *11*, 357-368.

Zhang, Y.D., Chen, Z., Song, Y.Q., Liu, C., and Chen, Y.P. (2005b). Making a tooth: growth factors, transcription factors, and stem cells. Cell Res *15*, 301-316.

Zhao, H., Feng, J., Seidel, K., Shi, S., Klein, O., Sharpe, P., and Chai, Y. (2014). Secretion of shh by a neurovascular bundle niche supports mesenchymal stem cell homeostasis in the adult mouse incisor. Cell Stem Cell *14*, 160-173.

Zhu, X., Hill, R.A., Dietrich, D., Komitova, M., Suzuki, R., and Nishiyama, A. (2011). Age-dependent fate and lineage restriction of single NG2 cells. Development *138*, 745-753.

9. Publications

Volponi, A.A., Pang, Y., and Sharpe, P.T. (2010) Stem cell-based biological tooth repair and regeneration. Trends Cell Biology 20, 715-722.